Walter L. Pohl

Economic Geology

Principles and Practice

2nd revised edition

Schweizerbart
Science
Publishers

Economic Geology
Principles and Practice

Walter L. Pohl

2nd revised ed.

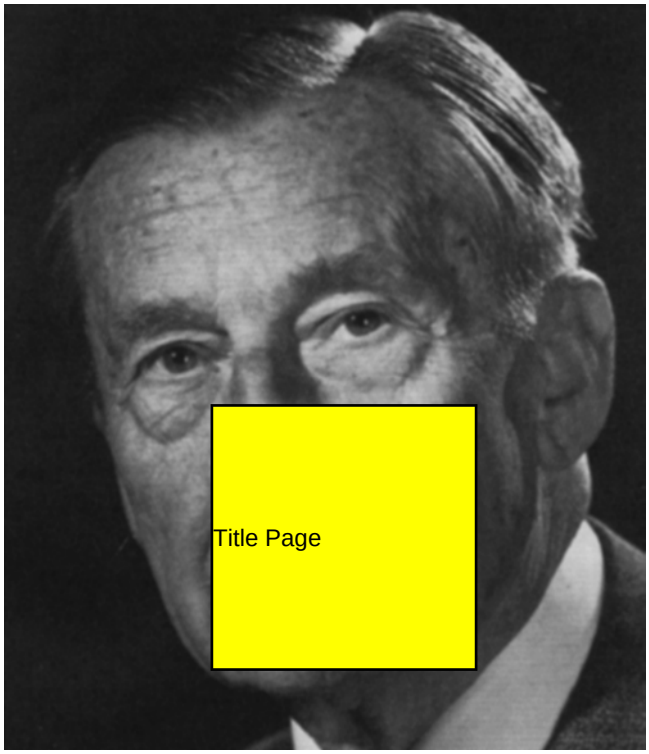

Photograph by Fayer Wien; Courtesy Austrian Academy of Sciences

To the Memory of Walther E. Petrascheck (1906–1991)

Inspiring Geologist and Academic Teacher

Economic Geology

Principles and Practice

Metals, Minerals, Coal and Hydrocarbons – Introduction to Formation and Sustainable Exploitation of Mineral Deposits

Walter L. Pohl

2nd revised edition

Schweizbart Science Publishers · Stuttgart 2020

W.L. Pohl: Economic Geology. Principles and Practice

Author's address: Walter L. Pohl, Austrian Academy of Sciences, Dr. Ignaz Seipel-Platz 2, 1010 Vienna, Austria
e-mail: ecogeo13@gmail.com website: https://www.walter-pohl.com/

We would be pleased to receive your comments on the content of this book:
editors@schweizerbart.de

Front cover: Natural outcrops of massive magnetite bodies (black) at Pliocene-Pleistocene suprasubduction El Laco volcano, Chile. On the flanks of El Laco volcano (5325 m a.s.l.), there are seven large deposits of high-grade iron ore within an area of 30 km^2, with total resources exceeding 1500 million tonnes. Black iron ore is composed of magnetite and minor amounts of hematite, anhydrite, apatite and pyroxene. Set in the Chilean iron ore belt among over 50 related deposits, those at El Laco recently yielded astounding scientific findings and are now recognized as the best preserved examples of iron oxide apatite (IOA) ore of Kiruna type in the world. Iron-oxide liquid segregated at 12–22 km depth by mingling between juvenile mafic and crustally derived felsic melt. Erupted as a hot volcanic magmatic gas plume saturated in iron, magnetite crystallized to form orthomagmatic-extrusive and pyroclastic iron ore at El Laco ("the surface venting of an IOA system"). Equally surprising is the recent recognition that in some magmatic columns, iron oxide apatite systems evolve upwards into magmatic-hydrothermal IOCG (iron oxide copper gold) systems. Read more inside this book ... Photo credit Matthias Benz
(Germany, https://world-of-crystals.com/).

1st edition Wiley-Blackwell 2011

2nd revised edition 2020

ISBN 978-3-510-65435-2 (softcover)
Information on this title: www.schweizerbart.de/9783510654352

ISBN 978-3-510-65441-3 (hardcover)
Information on this title: www.schweizerbart.de/9783510654413

ISBN 978-3-510-65436-9 ebook (pdf)

Publisher: Schweizerbart Science Publishers, Johannesstraße 3A, 70176 Stuttgart, Germany
mail@schweizerbart.de/www.schweizerbart.de
∞ Printed on permanent paper conforming to ISO 9706-1994
Printed in Germany by Nothhaft Druck, 93080 Pentling

Preface (2nd revised edition)

The new age of economic geology

A new age? Yes, I do believe that we witness an exciting growth of geological research and its application in economic geology, even though building on knowledge created by generations of earlier scientists. Foundation of this revolution – some call it disruption – are new geological understanding and concepts. One of the great advances is Lid Tectonics that have dominated Earth systems in the first half of our planet's history. Tremendous new tools and methods at all scales are available, from Earth observing satellites to tomography of crust and mantle, drones mapping alteration minerals in open pits, handheld XRF and SWIR spectrometers, laser Raman spectroscopy, laser ablation ICP-MS, and electron probe microanalyzers (EPMA). Add the unlimited potential of the digital transformation, of big data artificial intelligence, mineral systems research, and, of course, the professionals who drive the pace.

Is it possible to catch a screenshot of this movement? Not fully. I admit that some parts of the image provided in this book may be fuzzy, where science advances at too quick a pace. Yet, this book (Economic Geology 2nd revised edition or EG2) aspires to provide a systematic overview across the state of science and practice in economic geology. EG2 offers a panorama of the whole field of geology applied to the realm of mineral resources. Its range is global, reflecting the spread of mining and exploration activity, and of the actors out there. It is based on over a thousand recent papers selected from first class journals. Readers may expect to find access to present-day knowledge in order to explore the great new ideas, discoveries, methods and technologies as well as much detail!

EG2 addresses professionals, earth science students and graduates, academic teachers and scientists; undergraduates are invited to practice selective reading. Some authors of introductory ore geology books strip science of contradictions, avoiding the discussion of different interpretations and minimizing references to published papers. True, this may facilitate learning for beginners, but in my opinion, is wrong. We should not hide complexity, but accept a world of many unknowns and fuzziness. Like most natural sciences, economic geology seeks ever better comprehension and builds models, parts of which are uncertain and in flux. The book proposes to improve the current haphazard subdivision and denomination of ore deposits by merging them into a systematic petrogenetic-tectonic classification.

How to use EG2? – I suggest to initially quick-read Chapter One, which provides the foundation for the rest of the book. Only then should you follow your specific interests.

Do not hesitate to refer frequently to the Subject and Location Indexes because information is often spread through the book, concerning themes, ore deposit classes and mines such as, for example, the Olympic Dam iron oxide copper gold (IOCG) deposit. Jumping back and forth to different pages is an absolute must.

Soon, the world population will reach the number of 10 billion. The supply of minerals for humanity requires exploration, development and extraction, from mines on land to floating platforms on the high seas or to submarine robots. Metallogenetic-minerogenetic (source – transport – trap) models of Earth processes that contribute to the formation of ore and mineral deposits are the foundation for many of these activities. And let us not forget that as a profession, we always have to strive for precautionary mitigation of any negative environmental and socio-economic impact of our work, guided by an enlightened environmentalism.

Many people have supported me in preparing this second edition of my Economic Geology. Outstandingly helpful was Dr. Bernd Lehmann, Professor at Clausthal University and Chief Editor of Mineralium Deposita. Thank you Bernd, thank you all.

January 2020 *Walter L. Pohl*

Preface (1st edition)

Wisely used, mineral resources create wealth, employment, a vital social and natural environment, and peace. If the reverse of these conditions occurs only too often, illustrating the so-called "resource curse", this should be attributed to the true perpetrators, namely irresponsible, weak or selfish leaders. This book, however, does not intend to provide rules for good governance. I wrote it as a broad overview on geoscientific aspects of mineral deposits, including their origin and geological characteristics, the principles of the search for ores and minerals, and the investigation of newly found deposits. In addition, practical and environmental aspects are addressed that arise during the life cycle of a mine and after its closure. I am convinced that in our time, economic geology cannot be taught, studied or practiced without an understanding of environmental issues. The scientific core of the book is the attempt to present the extraordinary genetic variability of mineral deposits in the frame of fundamental geological process systems. The comprehensive approach – covering materials from metal ores to minerals and hydrocarbons – is both an advantage and a loss. The second concerns the sacrifice of much detail but I chose the first for its benefit of a panoramic view over the whole field of economic geology. Being aware that the specialist level of subjects presented in this book fills whole libraries, I do hope that even experienced practicians, academic teachers and advanced students of particular subjects will find the synopsis useful.

Over more than 50 years, five editions of this title were published in German. Since the first edition (Wilhelm & Walther E. Petrascheck 1950), the book was intended to provide a concise introduction to the geology of mineral deposits, including its applications to exploration and mining. The target readership has changed, however. Originally, it was written for students of mining engineering. Today, it is mainly directed to aspiring and practicing geologists. Each of the seven chapters of the book was developed with my own students as a university course and should be useful to fellow academic teachers. After initially working in industry I never lost contact with applications of economic geology, which is my motive for the constant interweaving of practical aspects in the text and for dedicating one of the chapters to the practice of economic geology. For professional reference purposes, practitioners in geology and mining should appreciate this melange of science and application. Frequent explanations and references to environmental and health aspects of extraction and processing of ores and minerals should assist users involved in environmental work. To those with no background in geology, I recommend to acquire an introductory geoscience text for looking up terms that are employed but cannot be explained in the available space.

Compared with the last German edition (Pohl 2005), this book has been rewritten for an international public. Although it retains a moderate European penchant by referring to examples from this region, important deposits worldwide are preferentially chosen to explain genetic types and practical aspects. I trust that this will be useful to both scholars and practitioners, wherever they work. Generally, it was my ambition to present the state of the art in economic geology, by referring to and citing recent publications as well as earlier fundamental concepts. This should assist and motivate students to pursue topics to greater depth.

Many people have supported me in my life-long pursuit of theory and practice of economic geology, and helped with this book, especially by donating photographs. I cannot name them all but in captions, donors are acknowledged. Here, just let me say thank you.

Walter L. Pohl

Contents

This book has a companion website: www.schweizerbart.de

Introduction

Human societies need sufficient water, productive soil, food, energy in different forms, and organic and mineral raw materials as a base for their physical existence. Of high importance is a healthy natural and socio-economic environment.

Economic Geology is a subdiscipline of the geosciences; according to Lindgren (1933) it is "the application of geology". Today, we might call it the scientific study of the Earth's sources of mineral raw materials and the practical application of the acquired knowledge. Considering the life cycle of a mine, economic geology leads in the search for new mineral deposits and in their detailed investigation. It contributes to economic and technical evaluations, which confirm the feasibility of a project and result in the physical establishment of a new mine. While mining goes on, economic geology provides many services that assist rational exploitation, foremost by continuously extending mineable reserves and by limiting effects on the mine's environment to a minimum. Possibly negative impacts of mining include surface subsidence, lowering the water table, various emissions and mechanically unstable or environmentally doubtful waste rock dumps. In the phase of mine closure, economic geology helps to avoid insufficient or outright wrong measures of physical and chemical stabilization, recultivation and renaturalization.

In recent years, the economic progress of industrial and of rapidly developing countries caused incisive changes in supply and consumption of mineral raw materials. China rather than Europe or North America provides world markets with essential metals and minerals, although at the same time importing large quantities of needed feedstock for its expanding industry and for improving her people's quality of life. The future supply with petroleum appears to be secure because of new sources and technologies; its role as the main source of liquid fuels for transport is hardly dented by biofuels and other developments. Wind, solar and geothermal energy are increasingly contributing to electricity production, yet without coal, nuclear power and natural gas, industrial economies would soon break down and developing nations would be locked in poverty. Ours is a time of transition but we cannot yet discern the outcome. Whatever it will be, metals, minerals and energy are certain to remain a precondition of progress and human well-being.

What are ore deposits?

Ore and mineral deposits are natural concentrations of useful metals, minerals or rocks, which can be economically exploited. Concentrations that are too small or too low-grade for mining are called occurrences or mineralizations. It is very important to understand the economic implications of the difference between these terms. Unfortunately, their wrong application is common and leads to fundamentally misleading deductions. Therefore, the denomination "economic ore deposit" may be used when a clear attribution to this class is to be emphasized. Note that not all ores are strictly natural – it is very common that waste of a former miners' generation is today's profitable ore, such as tailings of earlier gold, copper and diamond mining.

Mineral deposits are basically valuable rock bodies.. Their formation is compared with processes that have produced ordinary rocks and is investigated with petrological methods. Mineral deposits can also be thought of as a geochemical enrichment of elements or of compounds in the Earth's crust that is determined by their chemical properties (Railsback 2003; Lehmann et al. 2000b). The ratio between the content of a valued element in an ore deposit and its crustal average ('Clarke values', Wedepohl 1995) is called the "concentration factor". Formation of iron ore with today's typical grade of 60 wt.% Fe relative to an average crustal iron concentration of ~5% requires 12-fold concentration. Copper ore that has 1% Cu compared to the average of 0.007% Cu in the crust exhibits a 140-fold enrichment. Gold ore with 10 grams/tonne "distilled" from ordinary rocks with 0.002 g/t Au attests to a 5000-fold concentration.

Manifold are the processes and factors leading to the concentration of elements and minerals, including the formation of mineral deposits (Robb 2004). Final causes are the dynamic interactions between the Earth's core, mantle and crust, and of the hydro-, bio- and atmosphere. Cooling and devolatilization of the Earth and unmixing of the system in the geological-geochemical cycle and during the transfer of elements have important roles (Lehmann et al. 2000b). With reference to the origin, endogenous and exogenous process systems are distinguished. The first are those resulting from the dynamics of the Earth's interior that are ultimately driven by the Earth's heat. At present, the total heat flow at the Earth's surface is 0.1 W m^{-2}, resulting from heat entering the mantle from the core, of mantle cooling, radiogenic heating of mantle and crust by the decay of radioactive elements and of various minor processes (Lay et al. 2008). Exogenous processes take place at the Earth's surface and are mainly due to the flow of energy from the sun (solar irradiance of 240 W m^{-2} (Feulner 2012). In rare cases, extraterrestrial processes have contributed to the formation of mineral deposits by impacting meteorites and asteroids.

The origin of mineral deposits is often due to a complex combination of several processes, boundary conditions and modifying factors, collectively making up metallogenetic, or minerogenetic systems. Evidence for such systems that operated in the geological past is always fragmentary. Some questions can possibly be answered by studying presently active ore-forming systems (e.g. black smokers in the deep oceans), but this method ("actualism") has limitations. Because of the unknown factors there is often room for different interpretations (hypotheses) of the scientific facts. Economic geology strives to continuously improve the genetic models of ore formation, i.e. complete schemes of these systems. This effort is assisted by progress in many other sciences (from biology to physics) but the reverse is also true. Economic geology provides a fascinating insight into geological systems that are rare and can only be illuminated by studying mineral deposits. The practical mission of economic geology is the provision of metals and minerals that society requires. Of course, this implies cooperation with other scientific, technical and financial professionals.

Mining in the stress field between society and environment

> *Cum semper fuerit inter homines de metallis dissensio, quod alii eis praeconium tribuerent, alii ea graviter vituperarent* (the original text in Latin by Agricola 1556).
> In English: "People were always divided in their opinion about mining, as some praised it highly while others condemned it fiercely."

Agricola reports that enemies of mining in his time deplored not only harmful effects on the immediate environs but even moral aspects - they accused mining of advancing greed. Today, this remains one motive of opposition to the industry, but fundamental rejection of any extraction of minerals is more common. The main reasons given are that mining visibly uses the land and often leaves a profound and enduring change.

Undoubtedly, mining adds to the pressure exerted on natural systems by growing human populations. Yet, well managed and responsible mining provides a net-positive, long-term contribution to human society and to ecosystem well being (ICMM 2016). Its overall balance of benefits, costs and risks is positive. True, there often are sound arguments against mining at a specific location. Compromises should be sought, however, because mineral deposits cannot be installed at arbitrary places. Their locations are predetermined by nature. An example are sand and gravel deposits in river plains. Today, these raw materials are so scarce in many regions that they have to be protected against other claims (e.g. housing developments). Yet, everyone consumes minerals and mineral-derived products for homes, heating, transport, computers, medicinal use and numerous articles of daily life. Mining provides these minerals. Recycling replaces only part of primary production.

Ours is a time when the impact of humanity on the Earth is fully revealed (Steffen et al. 2018). By farming, industry, traffic infrastructure, building giant cities, and simply by being

alive, humans exert a strong imprint on the face of the Earth. Their huge energy consumption may even influence weather and climate. This has provoked ecologists and media to call for a new name for the current geological epoch – the *Anthropocene*. Among practicing geologists, the response appears to be negative (Klein 2015), because the term lacks any geological utility. While the formal judgement of the International Commission on Stratigraphy is pending, the profession of economic geology should not delay recognizing its responsibility and act accordingly, guided by an *enlightened environmentalism* (Pinker 2018).

Land use by mining is very small (~0.3% of the global ice-free area: Hooke et al. 2012) and only locally visible. Biofuel agriculture, solar and wind energy plants require much more land. Indeed, they create additional demand for minerals (e.g. fertilizer, metals for machines and processing plants, transport). Toxic elements such as arsenic and cadmium are essential for sustainable energy production, for example in photovoltaics. In many cases, even low foot-print technologies like geothermal power plants have serious problems with waste such as brines, salt, toxic and heavy metals (most notably arsenic, mercury and radionuclides). This demonstrates that there are no simple solutions for a sustainable economy without mining. On the contrary, it is undeniable that conservation of our quality of life and development for the major part of humans who still lack the most basic necessities for a life in dignity require both, mineral raw materials and an intact environment.

Mining without an impact on the environment is impossible (Fig. 1.1), but the industry strives to minimize negative effects (Fig. 1.2) and to improve the welfare of affected communities ("green mining"). The natural capital and its ecosystem services needs to be incorporated into decision-making; "natural capital" refers to the living and nonliving components of ecosystems – other than people and what they manufacture – that contribute to the generation of goods and services of value for people; "ecosystem services" are the conditions and processes of ecosystems that generate benefits for people (Guerry et al. 2015). Green mining operations create an enriched landscape of (re-) constructed ecosystems, which provide humans with a variety of services (e.g. food, timber, flood and erosion control, areas for recreation and aesthetics, and clean water). Examples include lignite and clay pits, which bequeath beautiful new lakes. Hard rock mines and quarries may grow into rare islands of nature in a sea of human occupation. Many of these sites support rare and threatened species from archea and bacteria to plants and animals, helping to preserve biodiversity.

Reversing mineral extraction, mines also have an extremely important role as deep disposal sites for the safe storage of society's unavoidable toxic and radioactive waste. Chemically dangerous waste is stored in worked sections of suitable underground mines. For highly toxic and radioactive waste, the construction of dedicated underground disposal mines is the best solution for protecting the biosphere. Underground disposal takes lessons from nature that has preserved high concentrations of hazardous solid, liquid and gaseous substances in the form of mineral deposits over many millions of years (e.g. sulfide metal ores, natural gas, petroleum, uranium and even the remains of natural nuclear reactors).

In 1987, the World Commission on Environment and Development ("*Brundtland-Report*") extended the concept of sustainable development to non-renewable resources. Clearly, few mineral resources fit into the concept of sustainability as it was formulated 300 years ago for the management of forests, "that the amount of wood cut should not exceed the growth rate" (Carlowitz 1713). Such exceptions may be salt, magnesium and potassium harvested from seawater. Most metals and minerals are non-renewable and their use should be managed according to the following rules: i) Consume as little as possible; ii) optimize the recycling rate; and iii) increase the efficiency of using natural resources, especially of energy. The original concept of sustainability considered mainly the interests of later generations. In the Rio Declaration (UN Conference on Environment and Development 1992) the concept of intrageneration fairness was added, to allow for the interests of the living generation of mankind.

In fact, the world population's rapid growth and demands for a better life enforce a continuing expansion of raw materials production. Yet, every individual extractive operation

must have the acceptance of public opinion. To reach that aim, all stakeholders must profit and the mine's social as well as the natural environment needs to be improved. The radical call that sustainability requires immediate termination of any extraction of minerals is, of course, social and economic nonsense (Gilpin 2000). Humanity cannot return to Stone-Age hunting and gathering. Let us use needed resources in the interest of living humans, and let us trust in technical and economic inventiveness and ingenuity to provide for later generations.

The mineral resources conundrum

But is there a sufficient mass of minerals for an ever-increasing consumption? Because of the limited size of our planet it is true that geological resources are principally finite, although very large indeed. The search for most minerals has hardly gone deeper than a few hundred metres below the surface, and only land, shallow seas and margins of the vast oceans are fully explored for conventional petroleum and gas deposits. Giant unconventional oil and gas resources opened up in America by technological innovation are fundamentally altering geopolitics of global energy supply. *In situ* leaching of metals may provide new resources and an alternative to conventional mining (Seredkin et al. 2016).

In contrast to *resources*, *reserves* that can be exploited at present economic and technological conditions are a small part only of the total geological endowment, because searching and defining reserves is a capital investment that must be paid back with interest. Due to the rules of depreciation of a future income, reserves are typically defined for the next 10–30 years. The result is that at any time, a division of total reserves by the yearly consumption (the R/C ratio or "life-index") will predict that in ten (or twenty, or thirty) year's time "the world will run out of the respective mineral". This fundamental error was famously made by the *Club of Rome* when it predicted this dire fate for the years 1990–2000 (Meadows et al. 1974). Because predictions of impending catastrophes are always popular this gave the Club of Rome's hypothesis a sweeping impact. Actually, the imminent scarcity of important minerals was announced many times in the past but never arrived. The term "life-index" is misleading, and the figure is rather an indication of specific conditions that dictate financing, production and marketing of individual metals and minerals. With few exceptions, R/C ratios change little over time-scales of several decades.

In the future, just as in the past, science and technology will continue to provide the mineral raw materials needed by innovation, by finding new deposits, by recycling and by providing natural or synthetic functional replacement (Wellmer & Dalheimer 2012). The recycling rate of metals is increasing. End-of-life recycling of metals such as iron, copper and zinc has reached >50% and nearly 90% for toxic lead whereas many high-technology metals (lithium, indium, rare earth elements) are hardly ever recycled, mainly because of unfavourable economics. With complex alloys, separation is virtually impossible. Often, temporary scarceness of certain *critical raw materials* is caused by political constraints that distort markets. Furthermore, exploiting lower-grade ores, producing functional replacements for certain minerals and metals, and recycling of materials all need energy. Accordingly, energy is the most important natural resource of all.

Undeniably, there are physical limits to the availability of certain quality classes of raw materials. Severe problems arising from this fact are not expected as long as the unlimited resource of human creativity is given the freedom and incentives to search for solutions. The continuously expanding reserve base for practically all minerals, roughly in parallel to increasing consumption, is the best proof of this principle in the mining industry. Finding solutions is our strength.

Part I

Metalliferous Ore Deposits

Economic geology defines ore as a natural material ("ore rock"), from which metals or minerals can be profitably extracted. Mining professionals use the word in an identical connotation. Note that metals and minerals can also be recovered from quite exotic materials that are not ore *sensu stricto*, for example, saline brines (lithium, magnesium), geothermal waters (zinc), metal-accumulating plants (nickel; "phytomining"), acid mine water (copper) and of course, recycled scrap (iron). The term ore is also applied to metalliferous minerals in a rock, for example chromite in dunite, or magnetite in gabbro ("ore minerals"). Ore rock, commonly just called ore, is typically an intergrowth of useless minerals ("gangue") with ore minerals. Massive ore consists of ore minerals with little gangue, for example high-grade hematite iron ore.

Ore deposits are economically relevant accumulations of ore. They form by geological process systems that can be viewed as a large petrogenetic cycle of constructive (e.g. magmatism) and destructive processes (e.g. weathering). Within this cycling of earth materials, individual metals have specific enrichment sites that depend on chemical and physical properties of the element or its compounds. Additionally, it is very important to remember that biogeochemical fluxes mediated by life (Falkowski et al. 2008) contribute to many ore forming processes.

Part I of this book is divided into two chapters. In chapter 1, general observations, characteristics and interpretations of ore deposit formation processes, process systems and associated outstanding deposit types are presented. In chapter 2, the economic geology of metals is systematically presented and illustrated by reference to specific mining districts and deposits.

Chapter 1

Geological ore formation process systems (metallogenesis)

Synopsis

Energy flow from the Earth's interior and from the sun drives geological process systems. The concentration of ore and minerals is part of these systems, which comprise intrusive and extrusive magmatism, weathering, erosion, transport and sedimentation, followed by diagenesis and metamorphism. Life interacts with several of the abiotic processes. In this chapter, we shall aim to acquire an overview of these systems in respect of the principles that govern the generation of ore deposits. Finally, the inspection of the different major systems is brought together in a synthetic view of global dynamics and metallogeny (i.e. the science of ore deposit formation). This chapter lays the ground for the rest of the book.

For a long time in the past, processes associated with differentiation and cooling of magmatic bodies were thought to be the main agents of ore deposit formation. Starting with mafic melt, ore minerals may form upon cooling or metal-rich melts can segregate from the silicate liquid. Because mafic silicate minerals crystallize at higher temperature, intermediate and felsic residual melts are formed with their own suite of ore deposits. Late-stage magmatic fluids collect metals and produce hydrothermal mineralization. Lindgren (1933), Niggli (1948), Schneiderhöhn (1962), Stanton (1972) and many others developed this concept of igneous ore formation. In addition, the role of weathering, erosion and sedimentation in concentrating metals was recognized. Metamorphic processes were seen to transform previously existing ore but without appreciable mass transfer.

More recently, these (here very simplified) earlier views on ore deposit formation were fundamentally expanded (Decrée & Robb 2019 Robb 2005). First of all, the discovery of plate tectonics caused a revolution in understanding the dynamic interaction of the Earth's crust and mantle. Plate tectonics determine the origin and distribution of many ore deposits. Present time ore-forming processes were investigated. Outstanding impulses brought the exploration of ocean floor hydrothermal venting that produces metal concentrations, which closely resemble long-known ore deposits (e.g. copper on Cyprus Island).

The application of new technologies of the geosciences (e.g. geochemical trace element and isotope analyses, fluid inclusions investigations, mathematical modelling and simulation) guided by old and new hypotheses, led to changes in metallogenetic thinking and to the recognition of additional ore forming systems. One example is the dehydration of sedimentary basins during diagenesis: Expelled fluids cause appreciable geochemical mass-transport and formation of numerous metallic and mineral concentrations, without involvement of igneous processes. Furthermore, the role of dissolved salt, hydrocarbons, reefs and karst cavities in diagenetic ore formation was illuminated. Long after the first hypothetical considerations, metamorphism was finally proven to cause migration of aqueous fluids that transport and precipitate ore.

Fig. 1.1 (Plate 1.1). Bauxite extraction at Huntley mine, southwestern Australia. On the Darling Plateau, bauxite is part of a mature soil profile developed over Archean gneiss and granite. The area is covered by woodland (the jarrah, or *Eucalyptus marginata* forest). Mining depends on the availability of land. Its social acceptance requires rapid re-establishment of the native ecosystem. Reproduced by permission of Alcoa Inc.

Fig. 1.2 (Plate 1.2). Rehabilitated jarrah forest covers former extraction panels of Huntley bauxite mine in front of the lake. Part of the remarkable success is due to skilful use of the natural soil seed bank. Reproduced by permission of Alcoa Inc.

The Earth's mantle is the ultimate source of many ore forming systems. According to present-day understanding, the Earth was formed at ~4.5 Ga by accretion of smaller bodies (planetesimals) formed in the solar nebula, although perhaps "the meteorites in our collection are not particularly good examples of Earth's building blocks" (Carlson 2017). The "magma ocean" stage facilitated differentiation of the metallic core that collected the siderophile elements (Table 1.1) producing the "primitive" mantle composition (Allègre 2008). The Moon originated when a giant, solid impactor hit the proto-Earth while it was in the magma ocean state (Hosono et al. 2019). For the following ~2 billion years, the early Earth was covered by a thin, stagnant lithosphere with a komatiite-basalt crust (the lid) that enclosed the convecting interior. Heat accumulation was released by mantle overturn events that produced giant ourpourings and the first patches of continental crust ("lid tectonics", Bédard

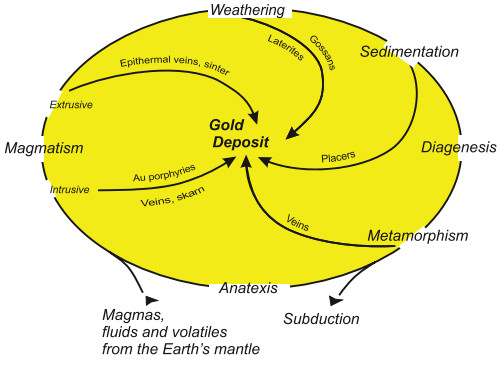

Fig. 1.3. The origin of gold deposits in relation to major geological and petrogenetic process systems within the Earth's crust and upper mantle, demonstrating the variety of ore-forming systems.

2018). At about 2.5 Ga, plate tectonics seems to have been established (Condie 2016). Later partial mantle melting throughout geological

Table 1.1 Elements grouped by general geochemical association in meteorites and in the Earth (Goldschmidt 1958).

siderophile (in iron meteorites and the core of the Earth) such as Au, Co, Fe, Ge, Ir, Mo, Ni, Os, Pd, Pt, Re, Rh, Ru
chalcophile ("sulfur-loving") Ag, As, Bi, Cd, Cu, Ga, Hg, In, Pb, S, Sb, Se, Te, Tl, Zn
lithophile (in chondrites, or mantle and crust of the Earth) Al, B, Ba, Be, Br, C, Ca, Cl, Cr, Cs, F, I, Hf, K, Li, Mg, Na, Nb, O, P, Rb, Sc, Si, Sn, Sr, Ta, Th, Ti, U, V, W, Y, Zr, Mn, and all rare earth elements (lanthanides)
atmophile (in the Earth's atmosphere) N, H and the noble gases.

Note that apart from the main attribution, many elements have additional geochemical tendencies that may dominate in ore formation processes; cf. Chapter 2.

Table 1.2 Common metallogenetic (or metallogenic*) terms.

- *Metallogeny* – the science of origin and distribution of ore deposits in geological space and time
- Metallogenesis – the process of ore deposit formation
- *Syngenetic* – denotes ores and minerals that formed at the same time as their host rocks (most often applied to sedimentary rocks and ore)
- *Epigenetic* – ores were emplaced into pre-existing rocks of any origin (e.g. veins, metasomatic ore)
- *Hypogene* – ores that were formed by ascending solutions (e.g. Mississippi Valley type lead-zinc)
- *Supergene* – ore formation by descending solutions (meteoric water interacting with rocks during surficial weathering processes)
- *Lateral secretion* – concentration of metals by abstraction from surrounding rock
- *Endogenetic* (*or endogenic**) – concentration caused by processes in the Earth's interior (magmatism or metamorphism)
- *Exogenetic* (*or exogenic**) - concentration caused by processes at the Earth's surface (sedimentation, weathering).

The British or *American variant is both used in first class scientific journals. This book is not a linguistic guide.

history preferentially extracted granitophile elements (e.g. tantalum) from the primitive/depleted mantle mix into the crust. Common transport agents from mantle to crust are mafic melts (Philpotts & Ague 2009) that drive major ore-forming process systems (Maier & Groves 2011). Mantle plumes lift nickel and blue diamonds from near the core to the upper mantle where they are transferred into carrier melts (Smith et al. 2018). The affected mantle is depleted ("residual") whereas other parts may still have a composition near the original primitive mantle (Jackson & Carlson 2011) or are re-enriched ("fertilized") in trace-elements such as Cu and Au, and in heat-producing refractory lithophile nuclides (REE, U, Th, Nb, Pb, Hf and He), mainly by subduction. Also, the latter delivered a large mass of matter, H_2O and CO_2 as evidenced by kimberlites and diamonds (Stern et al. 2016).

In principle, the classification of ore deposits by major earth process systems is simple. Complications arise because of the extreme variability of individual deposits due to manifold combinations of different individual processes and factors. In this Economic Geology book, fundamental geological cycles (Fig. 1.3), petrogenetic and ore-forming systems are to guide the reader through metallogeny.

The terms of Table 1.2 provide the basic vocabulary of metallogeny. The non-genetic descriptors stratiform (layer-shaped) and stratabound (restricted to certain strata) only denote shape and position of an orebody in relation to sedimentary features, not its origin. Comprehensive explanations of geological and

mining terms can be found in the *Dictionary of Mining* (AGI 1999) and the *Glossary of Geology* by Neuendorf et al. (2005). Geological time nomenclature in this book follows the International Stratigraphic Commission (ISC) (2018).

1.1 Magmatic ore formation systems

A very large and diverse group of ore deposits originated by various processes during formation, evolution, emplacement, cooling and crystallization of silicate melts (magmas) in the upper mantle and in the Earth's crust.

Most post-Archean magmatic rocks can be classified according to their plate-tectonic environment. Rocks of the ophiolite association (basalt, gabbro, ultramafic rocks) are remnants of former mid-ocean ridges, fore-arc and back arc basins, and of early and primitive parts of immature oceanic island arcs. Mature island arcs and active continental margins are distinguished by profuse amounts of orogenic andesites and equivalent intrusive magmatic rocks. Continental collision causes melting of sialic crust and voluminous granitic magmatism. Continental rifts are associated with bimodal alkalic volcanism (basalt and rhyolite). Extensional deformation of continents and mantle melting or mantle plumes result in emplacement of layered mafic intrusions, flood basalt and alkaline magmatic provinces. Notable are subvolcanic ring complexes with mineralized carbonatites, and kimberlite diatremes that lift diamonds from 200 km depth to the surface.

The association of certain igneous rocks with specific metal ores was established long ago. Ultramafic rocks host ores of nickel, chromium and platinum, gabbro and norite copper, cobalt, nickel, iron, titanium and vanadium, andesite and intermediate intrusive rocks bring copper and gold, and granites are related to beryllium, lithium, molybdenum, tantalum, tin and tungsten concentrations. Essentially, this distribution was understood as a result of the geochemical fate of different metals during *in situ* fractional crystallization (solid-liquid fractionation) of silicate melt bodies (Goldschmidt 1958). Meanwhile, magmatic petrogenesis is very well understood (Philpotts & Ague 2009) and rocks can be geochemically differentiated according to plate-tectonic setting, source rock composition, degree of partial melting, role of volatiles and many other genetic variables. Examples are the various basalt types (N- and E-MORB, intraplate, island arc: Dilek & Furnes 2014, Pearce 2008, Pearce et al. 1984, Pearce 1982, Winchester & Floyd 1977), or the S-, I-, and A-granitoids. We shall see later in this chapter that some of these rock classes are related to specific ore deposits.

Impact magmas result from heat and high pressure caused by collision of extraterrestrial bodies with the Earth. Melting affects part of the crust and in rare cases even the upper mantle. Impact magmas differ chemically from other melts because whole volumes of crust are liquefied, whereas normally, partial melting is the rule. In addition, the impacting body may induce geochemical anomalies, especially regarding siderophile elements (e.g. gold, platinum, iridium, cobalt and nickel). Hadean bombardment of the Earth with numerous large asteroids resulting in spherule-beds is believed to have delivered metals (the late-veneer hypothesis), which were cycled in crust and mantle and eventually reconcentrated in ore deposits (Maier et al. 2009). Post-impact cooling can induce hydrothermal systems that are able to redistribute matter and provoke ore formation.

In conclusion, the geodynamic environment controls the formation of ores from silicate melts in several ways. At the scale of ore-forming processes caused by single magmatic bodies, the following major genetic stages are distinguished:

- Orthomagmatic ore deposits are formed before the melt freezes to solidification, or in other terms, in the liquidus stage before reaching solidus.
- Pegmatitic ore deposits are the result of the segregation of small residual melt batches from a large crystallizing magma body approaching the solid state; fertile pegmatite liquid forms ore of rare elements.
- Magmatic-hydrothermal ore deposits are produced by super- or subcritical fluids, solutions and gases that are segregated by all magmas, which had more dissolved volatiles (H_2O, CO_2, S, B, F, Cl etc.) than the amount that could be accommodated in silicates during crystallization; because of this connection, the time of fluid phase expulsion is commonly coeval with the crystallization of solid phases (minerals) from the melt; a significant part of the geochemical signature of magmatic-hydrothermal ore deposits is determined by processes at the magmatic stage (Audétat et al. 2008).

1.1.1 Orthomagmatic ore formation

Oxide (magnetite, ilmenite, chromite), base metal sulfide (Ni, Cu), and ore of precious metals (Pt, Pd, Au) is often found in ultramafic and mafic igneous rocks. More rarely, magnetite occurs in intermediate and felsic silicate rocks. Textural (and many other) observations show that these ores were formed at magmatic temperatures while the melt was essentially liquid, clearly before total solidification (Naldrett 2004). Therefore, this petrogenetic class of ore deposits is called "orthomagmatic".

Numerous observations suggest that enrichment processes concentrate ("extract") low metal traces from a large mass of silicate melt into small volumes. Typically, the parent melt evolves by *in situ* fractional crystallization toward saturation so that either a solid (e.g. chromite) or an immiscible liquid (e.g. sulfide melt) accumulates the metal in question. At some stage, residual supercritical liquids and fluids may intervene. Many parameters influence these processes, including the depth of intrusion, tectonic activities, the temperature gradient in space and time, fractional crystallization, dynamics of the melt body (e.g. convective flow), repeated injection of fresh melt, assimilation of country rocks, sulfur or external fluids, liquid immiscibility of ore and silicate melts, and mixing or redissolution (Kerr & Leitch 2005). Flow dynamics of sulfide and silicate xenomelts, xenoliths, xenocrysts and xenovolatiles have crucial roles in the genesis of, for example, magmatic Ni-Cu-PGE (platinum group elements) and magmatic Cr deposits (Lesher 2017).

Because of their higher density compared to silicate liquids, ore melt droplets or solid ore phases typically accumulate above or within floor rocks, which may be cumulates below still liquid magma (gravitational accumulation; Sparks et al. 1993). Consolidation of cumulate mush can lead to expulsion of intercumulus liquid ("filter pressing"). Liquid-rich cumulates can slump down the sloping floor of a magma chamber (Maier et al. 2013). As the system cools, ore melts themselves may then separate into cumulates (e.g. Fe-sulfides) and residual liquids (Cu-rich sulfide melt). Supercritical liquids and fluids may assist in ore formation. Recently, upward segregation of dense phases (magnetite) by flotation similar to the industrial process, as opposed to downward gravitational segregation, was recognized in natural systems (Edmonds et al. 2015).

Various mathematical models have been proposed that describe the orthomagmatic enrichment process. Concentration of metals such as PGE (platinum group elements), Au, Ni, and Cu in sulfide melt is controlled by the Nernst partition coefficient (D) between sulfide and silicate liquids, and by kinetic factors. An essential variable is the silicate/sulfide liquid mass ratio ("R-factor"; Robb 2004, eq. 1.1) because a larger mass of metals can be extracted from a larger volume of fertile melt. A zone refining model is appropriate when, for example, Fe-sulfide droplets sink through a magma chamber and collect chalcophile metals.

Calculating the "R-factor" for orthomagmatic concentration of platinum elements and Au in newly discovered mineralization at the Skaergaard intrusion, East Greenland (Andersen et al. 2017):

$$R = T_{PGE+Au}/C^{CM}{}_{PGE+Au} \quad (1.1)$$

R is the silicate-sulfide mass ratio, T_{PGE+Au} is the combined tenor of PGE and Au (in ppb), and $C^{CM}{}_{PGE+Au}$ is the concentration of PGE and Au in the Skaergaard chilled margin that is assumed to represent the primary magma.

Most orthomagmatic ore deposits are found in intrusive rocks. Eruptive settings include the Ni-Cu-Fe sulfides in komatiitic lava flows of Archean greenstone belts, or the magnetite and hematite lavas or tuffs of andesitic-rhyolitic volcanoes in Chile, Mexico and Pakistan. However, the majority of orthomagmatic ores occur in mafic and ultramafic igneous rocks, due to the low viscosity of these liquids, which promotes rapid movement and easy separation of sulfide from silicate melt. Their high temperature facilitates host rock assimilation and high contents of chalcophile and siderophile ore elements. Mafic and ultramafic liquids form by mantle melting, for example in ascending plumes, in "incubated" (heated) mantle beneath a supercontinent and from upwelling asthenosphere after delamination of lithosphere (Maier & Groves 2011, Begg et al. 2010). In the Archean, most basaltic and komatiitic magmas would have formed during

overturns from upwelling primitive mantle melts (Bédard 2018).

Basic shapes (styles) of orthomagmatic orebodies are layers in stratified magmatic rocks (often formed as cumulates), lenses, or cross-cutting dykes and veins. This depends on the morphology of the segregation (sedimentation) surface and on dynamic factors. Massive ore is the product of highly efficient unmixing of ore particles or melt droplets from silicates, whereas disseminated mineralization reflects lower efficiency. Highly complex orebody shapes can be found in flow channels and pipes of lavas and subvolcanic intrusions, for example where widening or curvature of flow tubes induced lower flow velocity of silicate melt carrying chromite crystals or sulfide melt droplets (Naldrett 2004; e.g. Voisey's Bay, Canada). Textbook examples of orthomagmatic deposits are sulfide Fe-Ni-(Cu-PGE) ores hosted by Archean komatiitic lavas of the Yilgarn Craton in Western Australia (Box 1.1).

Box 1.1 Orthomagmatic ore in komatiites: rivers of nickel-iron sulfide

Komatiites are ultramafic volcanic rocks with melt temperatures of ~1700°C containing >18 wt. % MgO (Arndt et al. 2008). Prendergast (2003) describes the nickel-bearing komatiites of Zimbabwe as proximal and basal parts of submarine volcanoes that were flat and extended over hundreds of kilometres. Global tectonics in the Archean are modelled as a periodically-destabilized stagnant-lid system; most Archean basaltic and komatiitic magmas would have formed during cracking of the lid and upwelling of mantle (Bédard 2018). Komatiite formation is the consequence of mantle temperatures ~150–250°C higher than today (Herzberg et al. 2010). Komatiitic melts originated by 30–50% partial melting of mantle (co-genetic basalts ~35% compared with ~10% today: Keller & Schoene 2012). Normally, these melts remained sulfide-undersaturated from extraction through ascent and eruption to emplacement. Liquid komatiite lavas had a very low viscosity (similar to water) resulting in high flow velocities. The lavas were capable of eroding and melting most volcanic and sedimentary footwall rocks ("ground melting" or "thermochemical erosion": Staude et al. 2017). The flows formed or followed troughs on the sea floor or produced flow tubes similar to submarine basalts. Komatiites were typically charged with suspended olivine crystals. During cooling, cumulates and vesicular textures formed. Because of the extreme temperature difference between ocean water and Mg-rich melts, flow tops are characterized by skeletal growth of olivine and pyroxene ("spinifex textures", Shore & Fowler 1999).

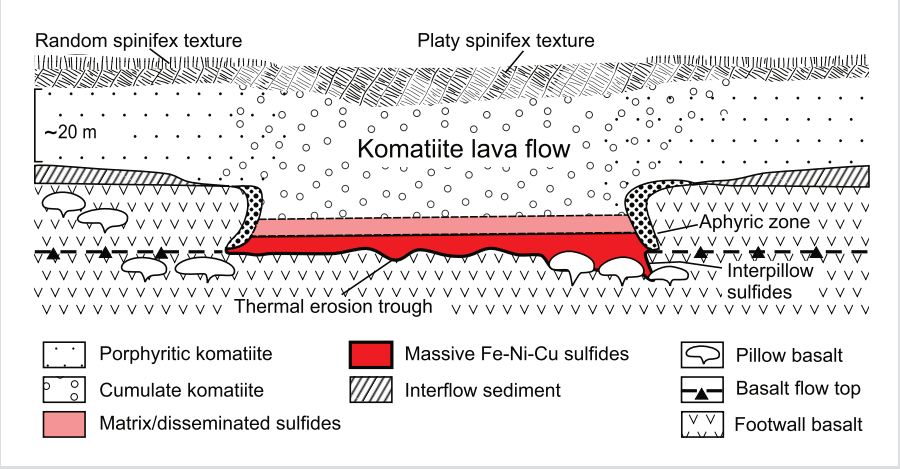

Fig. 1.4. Massive and disseminated nickeliferous pyrrhotite orebodies (Lunnon shoot, Kambalda, Western Australia) at the base of an Archean komatiite lava flow (adapted after Groves et al. 1986).

Most of the Yilgarn Craton komatiite-hosted iron-nickel-cobalt-copper-Au-PGE sulfide ores occur in elongated massive sulfide bodies, which were clearly formed from liquid sulfide melt, at the floor of flow tubes (Barnes et al. 2017). Upwards, massive ore grades into disseminated (matrix or net-textured) ore (Fig. 1.4). Ore textures reflect gravitational settling in the liquid phase. Sulfide melts can only form upon sulfur saturation implying high sulfur contents. The common association of sulfide mineralization with the presence of sulfur-rich interflow sediments derived from felsic volcanics, and the isotopic compositions of sulfur (Barnes et al. 2012) are strong arguments that assimilation of crustal sulfur is the main difference between fertile and barren komatiites. Sulfur-saturation of the melt led to unmixing of liquid iron sulfide droplets and stringers. The availability of nickel (and elements such as platinum) for partitioning into iron sulfide melt is favoured by low redox conditions. In that case, nickel is dissolved in the silicate liquid as uncharged Ni^0 and is not available for incorporation into olivine. Apart from the redox constraints, nickel contents of magmatic sulfide liquids are largely controlled by partitioning equilibria and the mass balance between silicate and sulfide melt (the "R-factor", including dynamic factors such as mixing, redissolution and turbulence. Therefore, sulfide droplets ("blebby ores") often have the highest chalcophile metal tenors, whereas massive ores may have lower grade. The ore minerals of komatiite nickel deposits typically comprise pyrrhotite, pentlandite, chalcopyrite and pyrite with nickel concentrations in ore reaching 20 wt.%. The low-T phases exsolve after freezing of the sulfide melt from intermittent solid solutions (Vaughan & Corkhill 2017).

The Neoarchean komatiites of Western Australia (2.7–2.9 Ga) host the world's third largest Ni sulfide province and the majority of the world's komatiite-associated Ni-Cu-PGE deposits. Earlier, basalts and the komatiites were interpreted as mantle plume-derived (Said et al. 2010) but a system of giant fertile mantle overturn upwelling zones breaking through a stagnant lid are the more likely model (Bédard 2018). Margins of microplates, terranes or domains are mapped by Hf-isotopes in zircon (Barnes et al. 2017). The breaks control linear komatiite belts and their geochemistry, volcanology and ore potential (Mole et al. 2014). Bimodal komatiite-dacite sequences are prospective. Paleo-Archean komatiites are depleted in platinum group elements (PGE) because during the magma ocean stage, siderophile elements of primordial Earth had been abstracted into the core. Only the younger komatiites display enrichment after a second cosmic matter bombardment hit the Earth during the Hadean from 4.5 to 3.8 Ga (the late-veneer) and was mixed into the mantle, which thereby became a fertile source (Maier et al. 2009). In contrast to Western Australia, the closely comparable Abitibi Greenstone Belt in Canada is richly endowed with volcanogenic massive sulfide deposits (e.g. Kidd Creek, Noranda). It is assumed that the disparity is due to a different lithospheric structure (Barnes et al. 2007). Both provinces display abundant orogenic gold deposits.

Gravitational settling can explain many features of ore formation in *layered mafic intrusions* (Maier et al. 2013, Naldrett 2004, Cawthorn 1996, Irvine 1982). Other processes invoked include flowage differentiation and convective scavenging (Rice & Von Gruenewaldt 1994), *in-situ* crystallization on the floor of the melt body, mixing of two different melts, and uptake of material from outside (e.g. by melting siliceous or sulfur-rich host rocks). The formation and segregation of a sulfide melt is the key to enrichment of exploitable metals (Barnes et al. 2009). Layered melt bodies (in respect of composition, temperature and density) undergo thermal and chemical "double-diffusive convection" that can concentrate ore metals. Although much less obvious than in many felsic intrusions, mafic melt bodies may also experience unmixing and expulsion of magmatic fluids that can form ore. The largest preserved layered intrusion in the world is the Bushveld Complex of South Africa, hosting an exceptional variety and mass of metal ores (Box 1.2; Vermaak & Von Gruenewaldt 1986, Eales & Cawthorn 1996).

Box 1.2 Orthomagmatic ore in the Bushveld Complex, hosting gigantic treasures

The Bushveld Intrusive Complex in South Africa comprises the Rustenburg Layered Suite and granites (the Rashoop granophyres and the Lebowa granites). The first term designates the giant layered mafic-ultramafic intrusion, which was formed in the Paleoproterozoic at ~2054 Ma (Scoates & Friedman 2008). The granites have nearly the same age and host minor fluorite and tin deposits. The roof of the Bushveld complex and the granites consists of thick precursor basaltic andesites to rhyolites (the "Rooiberg Group" volcanics). All together form a Large Igneous Province (LIP). Rooiberg volcanics and the intruding granites are the product of lower crustal melting caused by a giant mass of hot mafic melt. The ultimate cause of the igneous event was most probably a mantle plume. Country rocks of the lopolithic Bushveld intrusion are Paleoproterozoic sediments and volcanics of the Transvaal Supergroup and Archean basement. The Rustenburg Layered Suite reaches a thickness of 9000 metres. It is strongly layered at all scales. The major units from bottom to top comprise (Fig. 1.5/Plate 1.5 and 1.6):

- The Lower Zone with dunite, bronzitite, and harzburgite;
- the conspicuously banded Critical Zone with a lower part of orthopyroxenite, chromitite bands and some harzburgite, and a higher part marked by the first cumulus plagioclase and by cyclic layering of economically significant platiniferous chromitite, harzburgite, bronzitite, norite and anorthosite in this order (cyclic units); its upper boundary is marked by the Merensky Reef (PGE, Au, Ni, Cu);

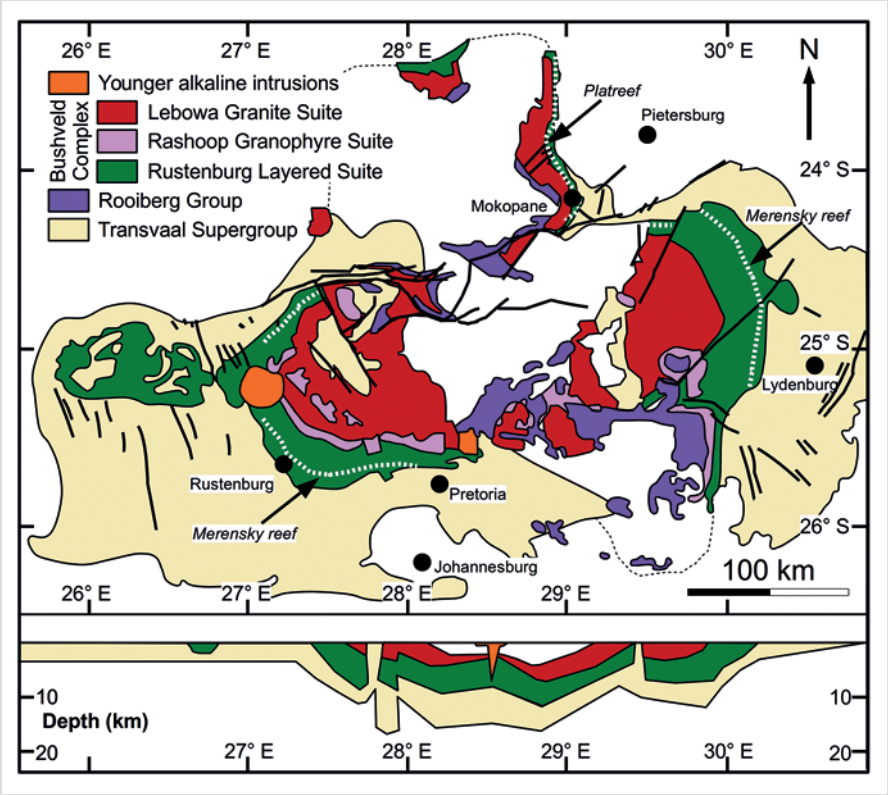

Fig. 1.5 (Plate 1.5). a) Generalized geological map of the Bushveld Complex (BC) showing the position of the Merensky reef (white dashed line). **b)** Cross section of the Bushveld Complex based on gravity modeling. Modified from Scoates & Friedman (2008).

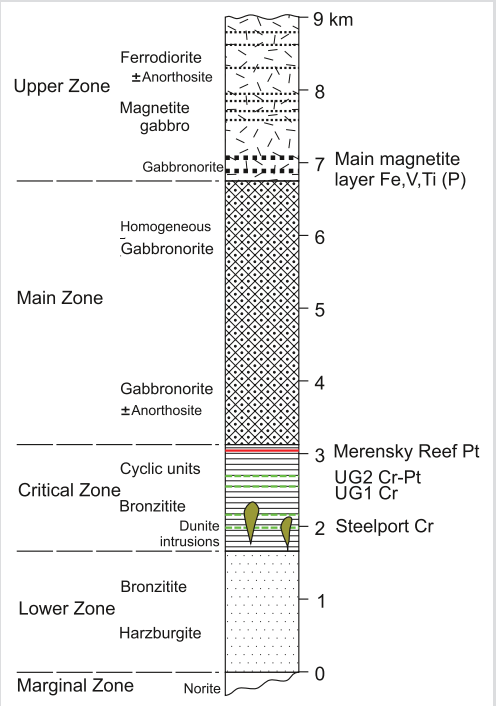

Fig. 1.6. Generalized lithostratigraphic column of the mafic Rustenburg Layered Suite in the Eastern Bushveld, South Africa, with major ore horizons.

- the Main Zone with gabbronorite and minor layering;
- the Upper Zone with magnetite (ferro) gabbro and ferrodiorite, which contains many titanomagnetite (V-Ti) layers.

A detailed lithostratigraphic scheme has been established for most parts ("lobes") of the intrusion (Vermaak & Gruenewaldt 1986, Eales & Cawthorn 1996). Strontium isotope stratigraphy suggests that the intrusion formed from many feeder zones by numerous pulses of magma of contrasting isotopic composition with concomitant mixing, crystallization and deposition of cumulates. Locally in all five lobes of the Complex, remarkable differences in thickness and facies of layers have been noted that point to proximity of magma inflow (Maier & Eales 1994). The cyclic units of the Critical Zone were formed by mixing or mingling of two different magmas, a resident magma of Main Zone type (or T-type) precipitating plagioclase, and fresh inflows of Critical Zone type (U-type) contributing orthopyroxene (Naldrett et al. 2009). Based on trace element data, Barnes et al. (2010) suggest that three different high-Mg tholeiitic basalt magmas B-1 to B-3 formed the Rustenburg Suite; the liquids probably resulted from the interaction of a rising mantle plume with metasomatized subcontinental lithospheric mantle. The uniquely high PGE concentration of Bushveld magma (19 ppb Pt) remains unexplained; one hypothesis is the involvement of a component from the Earth's core (Maier & Groves 2011). Apart from chemical processes, pressure fluctuations are thought to have controlled rhythmic layering and ore deposition in the Bushveld melt chamber (Cawthorn 2005b).

A partly hypothetical holistic path of Bushveld metallogeny was sketched by Maier et al. (2013): In the Mesoarchean, extraction of komatiites and formation of the Kapvaal subcontinental lithospheric mantle (SCLM) caused depletion in Pd but retained ~4 ppb Pt. In the Neoarchean and early Proterozoic, subduction metasomatized the refractory residue, introducing sulfur and volatiles, and thus fertilized and oxidized the SCLM. At 2.05 Ga, a mantle plume impacted, induced heat and added primitive melts, and caused partial melting of the Kapvaal SCLM resulting in formation of the Bushveld B1 siliceous high-Mg basaltic liquid, which extracted most of the Pt and Pd of the affected mantle and consequently displays concentrations of 33 ppb Pt+Pd at a ratio of Pt/Pd=1.5. Along its rise into the shallow crust, it acquired a strong crustal signature. After intrusion, progressive fractional crystallization precipitated

olivine, chromite, orthopyroxene, clinopyroxene, plagioclase and sulfide droplets. Reversals of the expected sequence are explained by major replenishments. Lopolithic subsidence caused increasingly inward-dipping layering. This resulted in liquefaction and slumping of relatively liquid-rich, semi-consolidated cumulate layers towards the center, causing features such as potholes, gaps, pipes (including the iron-rich ultramafic "hortonolites") and numerous smaller deformational patterns. Slurries unmixed under gravity and flow forces into bands of plagioclase, pyroxene, PGE alloys, PGE-rich sulfides, and oxides (cumulate sorting), producing the PGE reefs and the chromite and magnetite seams of the Bushveld. Note that not all proposed genetic models are compatible with each other.

The Bushveld contains the world's largest exploitable resources of chromium, platinum metals and vanadium. New discoveries continue to be made (e.g. the PGE-rich Waterberg Project north of the Northern Lobe: Huthmann et al. 2018). For the future, large masses of titaniferous magnetite and apatite are available that presently, have no economic value. The thermal influence around the Bushveld Complex produced contact metamorphic deposits of industrial minerals (e.g. andalusite, asbestos).

Layered mafic intrusions occur in several geodynamic settings:

- Archean greenstone belts;
- intracratonic regions (the Bushveld);
- at passive margins of continents; and
- in active orogenic belts.

Intracratonic regions that experienced tensional tectonics can also exhibit unstratified, complex mafic-ultramafic intrusions with Cu-Ni-PGE ores. The most important district of this kind is Noril'sk-Talnakh in Siberia, which originated at the Permo-Triassic transition in a feeder system related to the giant Siberian trap basalt province (Li et al. 2009, Yabkubchuk & Nikishin 2004). Ultramafic complexes of the Urals-Alaska type are concentrically zoned intrusions in orogenic and platform settings (Taylor 1967). In the dunite core of the ring complexes, important chromium and platinum ore can be concentrated (e.g. at Inagli: Svetlitskaya et al. 2018). Orthomagmatic concentrations of minerals and metals are also part of the economic significance of carbonatites.

Impact magma bodies with orthomagmatic ore deposits

Mineralized impact structures are very rare. A giant example is the *Sudbury Igneous Complex* (SIC) of Ontario, Canada (Lightfoot 2016). It may be the second-largest source of nickel (plus Cu and PGE) in the world after Noril'sk in Russia. The SIC is the remnant of a voluminous melt body that has been produced by the impact of a meteorite into continental crust 1.85 Ga ago (Dietz 1964). The surrounding rocks comprise Archean granites and gneisses, and metamorphic Paleoproterozoic volcano-sedimentary suites. The elliptic outline of the intrusion is thought to be due to later orogenic deformation. Hydrothermally altered suevitic breccias, shales and turbidites (Whitewater Group) cover part of the intrusive complex, forming a central basin. Ore deposits occur mainly in embayments of the footwall contact of the intrusion, in radiating dykes ("offsets", Fig. 1.7) and within intensely brecciated footwall rocks up to 2 km from the contact. Orthomagmatic PGE assemblages are characterized by native Pt metals, Pt-Fe alloys and PGE sulfides. Footwall ore is in part hydrothermal, driven by the heat of the SIC (Tuba et al. 2014). There is a lithologic zonation from the footwall upward and towards the centre of the intrusion. Marginal norite, gabbro and quartzdiorite with dunite inclusions and the Ni-Cu-sulfides form the "Sublayer Norite" and the offsets, followed by norite of the "Lower Zone", quartz-gabbro of the transitional "Middle Zone" and granophyre of the "Upper Zone". The rocks are clearly the product of crustal melting but are very different from layered intrusions (e.g. there is no rhythmic banding). At Sudbury, lithologic zonation is interpreted to be due to gravity separation of mafic and felsic liquids that formed an emulsion immediately after the impact, and subsequent vigorous thermal convection within the norite and granophyre layers (Zieg & Marsh 2005). The ore-bearing sublayer displays typical features of mafic cumulates and gravity segregation of sulfide liquids. Offset dykes and footwall deposits host an important part of metal resources. Total

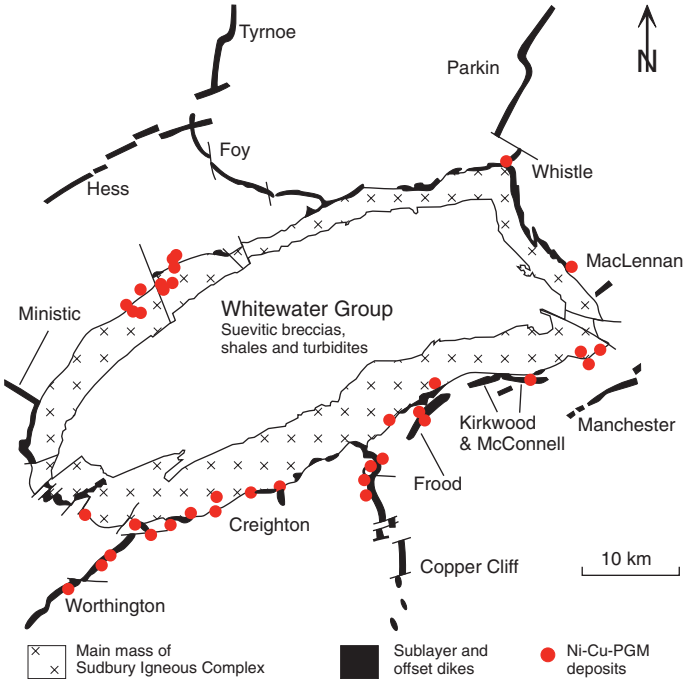

Fig. 1.7. Overview map of the Sudbury impact structure, Canada, one of the super giant nickel-copper mining districts of the world. Of close to 90 single deposits known (Lightfoot 2016), a selection is shown here.

past production and remaining resources of the Sudbury District are estimated at >1700 Mt of Ni, Cu, Co, Pt, Pd, Au and Ag ore (Ames et al. 2008). Among ~90 known Ni-Cu-PGE deposits five are currently worked.

Anorthosite-hosted titanium deposits

Mineralized anorthosite plutons are restricted to Mesoproterozoic and early Neoproterozoic ages (1.8–0.9 Ga) and have an outstanding role as sources of titanium (Charlier et al. 2014, Ashwal 1993). The origin of their mafic parental melts is not fully understood; late to postorogenic partial melting of tongues of lower crust in the mantle (Duchèsne et al. 1999), crustal contamination of mantle melts or a depleted upper mantle source are considered (Gleißner et al. 2011). The formation of anorthosites involves a first stage of accumulation of plagioclase at the top of deep-seated magma chambers that is followed by the intrusion of buoyant plagioclase mushes into mid-crustal levels. The diapiric intrusions may be guided by weak crustal structures. Final emplacement is marked by large contact metamorphic halos that formed at 3–6 kbar. The tectonic setting of emplacement was probably in continental arc environments during a post-collisional regime. The 1.06 Ga Lac Allard anorthosite hosting the giant Lac Tio deposit (Canada), for example, occurs in the central Grenville Orogen, a collisional belt formed at ca. 1100–980 Ma during the amalgamation of Supercontinent Rodinia. In this province, as elsewhere on the Earth, anorthosites are associated with coeval intrusions of mangerite, charnockite and rapakivi granite (the AMCG magmatic suite). Host anorthosites are commonly coarsely crystalline, massive rather than layered and consist of >90% andesine to labradorite.

Key processes of ilmenite ore formation are an early saturation in ilmenite, the segregation of immiscible Fe–Ti–(P)-(V) rich liquid, or fractional crystallization with settling of solid Fe-Ti oxide, possibly accompanied by plagioclase flotation and gravity enrichment forming cumulates. Common shapes of orebodies include tabular intrusives, lenses, stocks, sills or dykes in massive anorthosites but also stratified accumulations in layered segments of anorthosite massifs or in layered intrusions. Orebodies are massive or disseminated as at Lac Tio in Quebec, Canada. Ore

consists of ilmenite, hematite (magnetite), apatite and a gangue of silicates. Nelsonites of the same ore mineral composition are devoid of silicates. Exceptionally, ore may be hydrothermal as at Damiao, China (Li et al. 2014).

Fe-rich liquids, solids and fluids segregated from intermediate to felsic magmas: the Kiruna-type iron oxide-apatite (IOA) deposits, and their relation to iron oxide-copper-gold (IOCG) deposits

The metallogenetic role of Fe-rich liquids, solid-vapour foams and fluids segregated from intermediate to felsic magmas is a more contentious case of orthomagmatic ore formation. Magmatic-hydrothermal replacement models for IOA (such as described by Sillitoe & Burrows 2003, 2002) stand against orthomagmatic (± fluid-assisted) interpretations. The second rest on the observation that under conditions of high aH_2O and fO_2 an immiscible FeO_x-Ca-P liquid is in equilibrium with melt of felsic composition (Hou et al. 2018). One of the objections is that the high viscosity of SiO_2-rich liquids should physically inhibit segregation by gravity. Counter-arguments include: i) shearing by slow convection of the melt may concentrate low-viscosity FeO_x liquid; and ii) high contents of fluxing agents may be involved. In fact, high fluorine and chlorine contents of the apatite, and the presence of minerals such as amphibole and scapolite imply a role of magmatic volatiles (H_2O, Cl, F, CO_2, etc.). Volatiles promote segregation and mobility of ore liquid and solid-vapour foams. High fluid and salt contents of melt batches segregating from felsic magmas evoke a likeness to pegmatites and similar to pegmatite systems, the transition to hydrothermal ore formation can be gradual and indistinctive (Borrok et al. 1998). Knipping et al. (2015) report that at the 350 Mt iron Los Colorados deposit in the Cretaceous Chilean iron ore belt, set in a suprasubduction volcanic arc, Fe-isotopes and magnetite geochemistry suggest the magmatic origin of magnetite cores, which are mantled by hydrothermal growth zones. The authors' interpretation involves crystallization of magnetite microlites from high fO_2 andesitic liquid, followed by flotation and uplift by attached bubbles of hypersaline low-density magmatic fluid. At higher levels, the system gradually acquires a magmatic-hydrothermal character, where magnetite may continue to be precipitated and conditions approach iron-only IOCG systems. Knipping's et al. (2015) flotation hypothesis is contested by Broughm et al. (2017), based on a broader assessment of magnetite geochemistry; according to these authors, common magnetite discrimination diagrams fail to reveal the genetic setting. Yet, Rojas et al. (2018) reconfirm the flotation model based on multiple data, for El Romeral and the Chilean Iron Ore belt.

The unusual chemical composition of parental magmas and fluids may be due to assimilation of evaporitic and phosphatic upper crustal rocks as in the Mesozoic Zhonggu iron ore field in China (Hou et al. 2010), or of seawater (Knipping et al. 2015), or of saline basinal brines (Riehl & Cabral 2018, Barton & Johnson 1996). After the discovery of giant Olympic Dam in southern Australia, numerous iron oxide-rich deposits were subsumed in a new class, the *iron oxide-copper-gold (U-REE) deposits (IOCG)* (Groves et al. 2010, Cox & Singer 2007, Pollard 2006, Sillitoe 2003, Hitzman et al. 1992). Although a magmatic-hydrothermal origin of IOCG mineralization is generally accepted, the broader group displays a considerable variety of geological setting, of the ratio of orthomagmatic and magmatic-hydrothermal mineralization, the nature of hydrothermal alteration systems and mineralizing fluid compositions.

Box 1.3 Orthomagmatic iron oxide – apatite ore at Kiruna, Sweden, the eponymous IOA type deposit

Kiruna in northern Sweden (Fig. 1.8), the largest iron ore field in Western Europe, is traditionally considered as the type-deposit of orthomagmatic iron ore formation related to felsic melts because the ore is cogenetic with Paleoproterozoic (1.89 Ga) igneous host rocks formed during the Svecokarelian orogeny at an active continental margin. Lower Ti concentrations distinguish this type from massive iron oxides (e.g. nelsonite) segregated from mafic magmatic melts. Because of the volcanic host rocks, and of ore with vesicular portions that resemble lava flows, finely banded ore that might have originated by ash falls, and brecciated ore from pyroclastic breccias, arguments have been put forward for an orthomagmatic-extrusive ore formation (Nyström & Henriquez 1994). Thin apophyses of the ore extend into both hanging wall pyroclastic rhyodacites and footwall trachyandesitic lavas; this was thought to prove intrusion of an ore melt. Other authors invoke a magmatic-hydrothermal metasomatic origin related to IOCG deposits (Hitzman et al. 1992), but Kiruna is not part of this class because it lacks Cu and Au (Groves et al. 2010).

Yet, host rocks in the Kiruna district display strong alkali metasomatism (albitization). Precise age dating suggests that ore is slightly younger than host rocks but is coeval with a buried granite intrusion, favouring a magmatic-hydrothermal model; oxygen and hafnium isotopes in zircon suggest an involvement of episodic magmatic-hydrothermal fluids in the genesis of the Kiruna iron ore deposits; iron may have been leached from footwall greenstones (Westhues et al. 2016, 2017). However, Broughm et al. (2017) report that magnetite at Kiruna is largely influenced by metamorphism and/or metasomatic alteration that might have affected isotope systems.

The Kiruna region lies in the ~1.9–1.8 Ga Svecofennian Orogen that was formed by subduction and accretion. An evolving continental arc displays numerous different types and styles of Fe-oxide (IOA) and Cu-Au ± Fe oxide (IOCG) mineralization. An exhaustive analysis of the regional metallogeny (Martinsson et al. 2016) concludes that Kiruna type ores did form from an iron-rich magma, although generally displaying a hydrothermal overprint. The authors suggest that at 1.89–1.88 Ga tholeiitic magmas underwent liquid immiscibility during fractionation and interaction with crustal rocks, including meta-evaporites, generating felsic magmatic rocks and Kiruna type iron ore deposits.

Fig. 1.8. Kirunavaara iron ore mountain, northern Sweden. The steeply dipping magnetite orebody was originally mined in an open pit on the left side of the hill. Today, extraction is underground. Reproduced by permission of LKAB.

Extrusive orthomagmatic IOA ore - the surface venting of an IOA system

A magmatic-extrusive origin is well supported for Pliocene-Pleistocene magnetite orebodies at El Laco volcano, Chile (Tornos et al. 2017). At El Laco and at Cerro de Mercado (Durango, Mexico), magnetite or hematite-apatite ores have been described as massive and vesicular lavas, veins, crystal tuffs and pyroclastic agglomerates deposited by volcanoes built of rhyolite and andesite (Lyons 1988; Fig. 1.9). For El Laco, Tornos et al. (2017) summarize observations that textures of massive ore are strikingly similar to those of vesicular low viscosity basalt and provide O-isotopic data suggesting that basalt-like iron oxide ore blankets are in fact solidified melts; plagioclase phenocrysts in andesite, for example, contain melt inclusions with two immiscible melts, one of silicates, the second rich in iron and with small tenors of Ca, Mg, Si, Ti, and P, demonstrating the segregation of an ore melt. During quenching, the iron

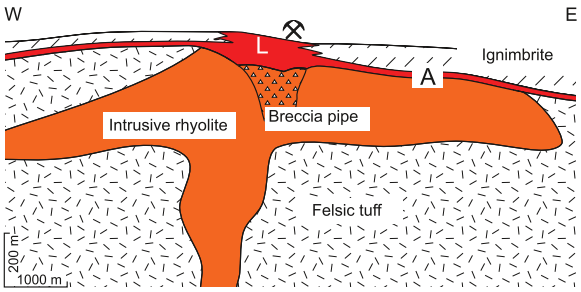

Fig. 1.9. Schematic profile of the volcanogenic iron ore deposit at 30 Ma old Cerro de Mercado, Mexico (modified from Swanson et al. 1978). Magnetite lavas (L) above an eruptive center pass laterally into hematite tuff (A).

Fig. 1.10 (Plate 1.10). Natural outcrops of orthomagmatic-extrusive to pyroclastic magnetite ore bodies (black) at El Laco volcano, Chile. White patches are andesites altered by steam heating to cristobalite, alunite and opal. Steam heating occurs between the paleowater table and through to the paleosurface. The alteration results from attack by relatively cool (≤100°C) ground water acidified by oxidation of boiled-off H_2S-bearing steam (Sillitoe & Burrows 2002). Credits to Matthias Benz (Germany, https://world-of-crystals.com/).

oxide melt released large volumes of superhot volatiles (>900°C). Some hydrosaline melt found in pyroxene of El Laco, formed at a temperature of ~800°C. The salt caused magmatic-hydrothermal alkali-calcic alteration of the host andesite, similar to IOCG related alteration, providing the main argument for a possible hydrothermal replacement origin. The vapour produced the white caps of acid-sulfate steam-heated alteration (Fig./Plate 1.10). White rocks are andesites altered by steam heating to cristobalite, alunite and opal. Steam heating occurs between the paleowater table through to the paleosurface. The alteration results from attack by relatively cool (≤100°C) ground water acidified by oxidation of boiled-off, H_2S-bearing steam (Sillitoe & Burrows 2002).

Supported by isotope data such as $^{87}Sr/^{86}Sr$ and $^{143}Nd/^{144}Nd$ on rocks and ore, Tornos et al. (2017) conclude that the magnetite ore crystallized from an iron oxide melt that segregated at 12–22 km depth by mingling between juvenile mafic and crustally derived felsic melt. Likely, oxidized sulfur, phosphorous, and fluorine in the deposit may have been entrained from Late Cretaceous – Paleogene sediments. Nyström & Henriquez (2016) point out that the El Laco deposits are the best preserved examples of apatite iron ore of Kiruna type in the world. They illustrate convincingly features of ore such as vesicles and subvertical tubes that confirm widespread degassing during crystallization. Peculiar spherules of octahedral magnetite in the volcanic ash imply formation

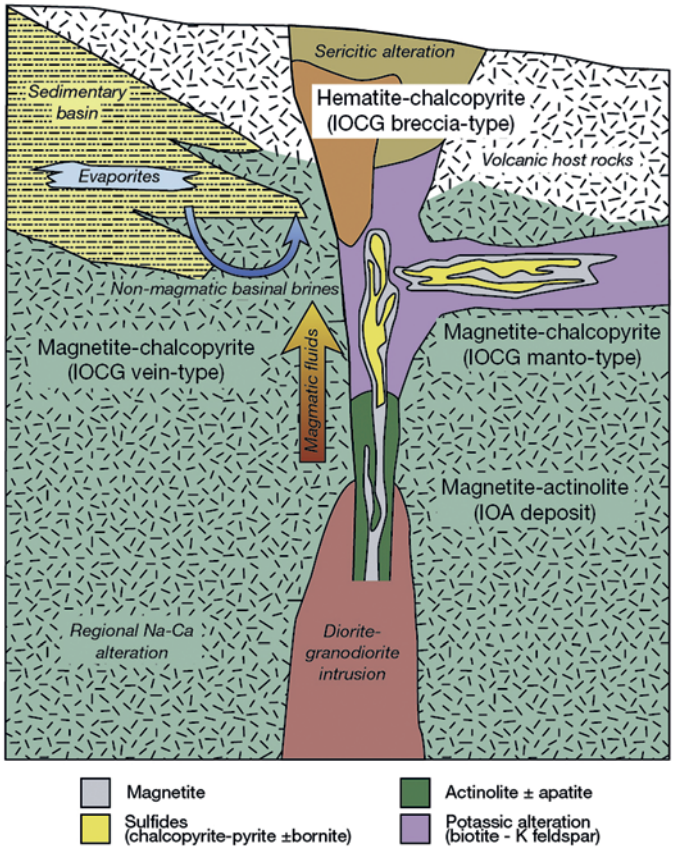

Fig. 1.11 (Plate 1.11). Transitional vertical stacking of deep orthomagmatic IOA evolving upwards into a magmatic-hydrothermal IOCG system, induced by a translithospheric to volcanic column in the Chilean iron ore belt. Modified from Barra et al. (2017).

by rapid crystal growth in a hot volcanic magmatic gas plume saturated in iron during eruption of iron-oxide liquid. Together, Nyström & Henriquez (2016) and Tornos et al. (2017) provide a vivid tableau of orthomagmatic-extrusive and pyroclastic formation of iron ore at El Laco ("the surface venting of an IOA system": Knipping et al. 2015).

In conclusion, orthomagmatic deposits of iron oxides and apatite in intermediate to felsic igneous rocks (intrusive and extrusive styles) share a number of features with IOCG deposits. Both may originate by mixing and mingling of mafic and silicic melt (Clark & Kontak 2004) or by assimilation of crustal material (Tornos et al. 2017). Knipping et al. (2015) deduce from their results that IOA deposits may be the deeper, high-T magmatic section of lower-T magmatic-hydrothermal IOCG systems (Fig./Plate 1.11). Transitional cases between the end-member types are possible.

Lower sections of ophiolites also contain orthomagmatic ore deposits. This includes dunite bodies with streaky or lenticular (podiform) disseminated and massive chromitite. The dunites are mainly sited within deformed refractory harzburgite of tectonized mantle. Tabular chromitite seams are found in the lowermost ultramafic cumulates of gabbroic magma chambers. Both cases are considered to be a consequence of chromite segregation from the melts that rise from the mantle beneath oceanic spreading ridges. The metallogeny of ophiolites is considered in more detail below.

1.1.2 Ore deposits related to ocean floor volcanism (ophiolite hosted Cyprus type Zn-Cu-Au)

Exploration of ocean floors resulted not only in the recognition of plate tectonics but also in the discovery of conspicuous signs of active ore forming systems – the "black smokers". Black smokers are points of discharge of hot metalliferous solutions from the ocean floor. Black smoker fields build accumulations of metal sulfides (seafloor massive sulfides, SMS), some of which are economically exploitable. Comparative investigations revealed that ophiolites, an association of mafic and ultramafic rocks common in orogenic belts, are remnants of oceanic spreading processes that may have been *subduction-unrelated* (continental margin (CM), mid-ocean ridge (MOR) and plume-type (P) ophiolites) or *subduction-related* such as suprasubduction zone (SSZ, e.g. intra-oceanic primitive subduction initiation forearcs, and backarc basins) and volcanic arc (VA) ophiolites (Dilek & Furnes 2014). Ophiolites host ore deposits that display features reminiscent of black smoker fields and sulfide mounds. However, fluid venting on the seafloor may also occur in other tectonic settings, including magmatic arcs above subduction zones, hotspot ocean island volcanoes and dewatering sediments of active and passive continental margins.

Ophiolites

Ophiolites are fragments of oceanic crust and mantle that have been transported (obducted) as thrust sheets (nappes) or schuppen onto continents. The original rock suite is rarely preserved intact. Yet, there exist some exceptionally well conserved ophiolites (e.g. Cyprus, Oman; Dongwanzi in China). Ophiolites display considerable variation (Dilek & Furnes 2014).

Instead of the mid-oceanic model, Dilek & Flower (2003) proposed a slab rollback model of ophiolite formation, from boninitic 'proto-arcs' in oceanic forearc settings; this is often termed the supra-subduction zone (SSZ) model. The Penrose-type ophiolite pseudostratigraphy is compared to mid-oceanic crust and comprises (Anonymus 1972):

- Extrusive (MORB – mid-ocean ridge) basalts of tholeiitic chemical characteristics at the top (tholeiitic magma is reduced and subalkaline i.e. low in Na_2O+K_2O); pillow lavas or lava ponds are remarkable features; ocean floor metamorphism of basalt increases from the zeolite facies at the top to greenschist facies at the bottom; note that many ophiolites display volcanic rocks with geochemical supra-subduction zone (SSZ) signatures such as boninites.
- The sheeted dyke complex, consisting of vertical basalt dykes that strike parallel to the former oceanic graben; greenschist facies metamorphism is dominant but may grade into amphibolite facies near the footwall; contact metamorphism resulting from underlying melt bodies may occur; many ophiolites, however, lack sheeted dykes.
- The plutonic complex, comprising higher intrusive homogeneous gabbro, diorite, tonalite and trondhjemite ("plagiogranite"), and deeper layered gabbro and peridotites, that display properties of cumulate rocks (the "cumulate sequence"); the magmatic rocks are normally not metamorphosed.
- The tectonized and depleted mantle, dominated by large masses of serpentinite (after harzburgite) and characteristic pods of dunite (± chromite).

Various marine sediments may cover the igneous rocks; most frequent are biogenic cherts and pelagic limestones. It is interesting to note that abiogenic exhalite cherts and jasper have only formed before the Middle Cretaceous; since that time, seawater is highly undersaturated with respect to silica because of the emergence of silica-consuming diatoms (Grenne & Slack 2005). An interesting aspect of ophiolite obduction is the climate cooling induced by weathering of large exposed ultramafic masses that abstracts CO_2 from the atmosphere (Macdonald et al. 2019).

Formation of the ophiolite sequence can be modelled by partial melting of primitive fertile mantle under mid-ocean ridges or SSZ, due to heat, upflow and the decompression caused by extension. The liquid rises in numerous melt batches and accumulates to fill large shallow magma chambers. These evolve by fractional crystallization and episodic volcanic processes. Trace geochemistry allows differentiation of C- (contaminated) MORB, N- (normal) MORB, E- (enriched) MORB and P- (plume) MORB basalts (Pearce 2014, 2008). Boninites are high-Mg (> 8 wt. %) basaltic andesites or andesites, often with striking olivine phenocrysts. Oceanic ridges with low spreading rates are composed of sections with high magmatic activity that alternate with sections of tectonic rifting only. The first

produces the typically layered ophiolite sequence ("Penrose Crust"); the second may lead to exposure of mantle rocks (serpentinites and peridotites: "Hess Crust"). Hess Crust is inconspicuous because black smokers are very rare, and has received little attention, but may be a source of metals, for example, in shale-hosted nickel (Jowitt & Keays 2012). Superfast spreading rates produce thin crust and shallow melt bodies.

Economic interest focusses on deep ultramafic rock suites of the Penrose sequence (for chromite and platinum) and the near-surface volcanic hydrothermal systems (for base metals). Tectonized (foliated) harzburgite and the lower cumulates host dunite bodies that may contain massive and disseminated chromite ore. Dunite in harzburgite can be understood as lag segregation formed in conduits from rising basaltic or boninitic melt diapirs. Chromitites (massive chromite rocks) originate from dunite by liquid-liquid immiscibility; ore bodies may also be conduit-controlled. Alternatively, the lenticular pod-like shapes may be due to ductile shearing in the mantle. Chromitites in cumulates occur in seams that lack early deformation.

Black smokers

From the beginning of geological history, newly-formed ocean crust was cooled by convecting seawater. This is at the origin of ocean floor metamorphism and possibly, of earliest life on the Earth (Russell et al. 2005). Processes taking place along the mid-ocean ridges are interconnected with the whole Earth System (Halbach et al. 2003). Rising branches of convection cells transport metals and reduced sulfur leached from mafic and ultramafic rocks towards the ocean floor (Fig. 1.12). Some of the volatiles and metals may be derived from magmatic fluids. More than 150 active submarine vent fields have been discovered over the last decades along the 89,000 km-long worldwide network of oceanic plate boundaries (Hannington et al. 2011). Most vents are basalt-hosted and of the black smoker type.

Submarine black smoker vents are hydrothermal cones or chimneys that may reach a height of ~20 m, often built on outcrops of bare basalt (Fig./Plate 1.13). From an opening at the top, a high-speed jet of hot clear fluid is ejected. The vents are tubes with zoned walls, from pyrite and chalcopyrite inside through sphalerite, marcasite, barite, anhydrite and amorphous SiO_2 to the exterior (Fig. 1.14 and 1.15/Plate 1.15). Oxidation of sulfides by seawater ("seafloor weathering") produces varicoloured ochreous alteration fragments, which

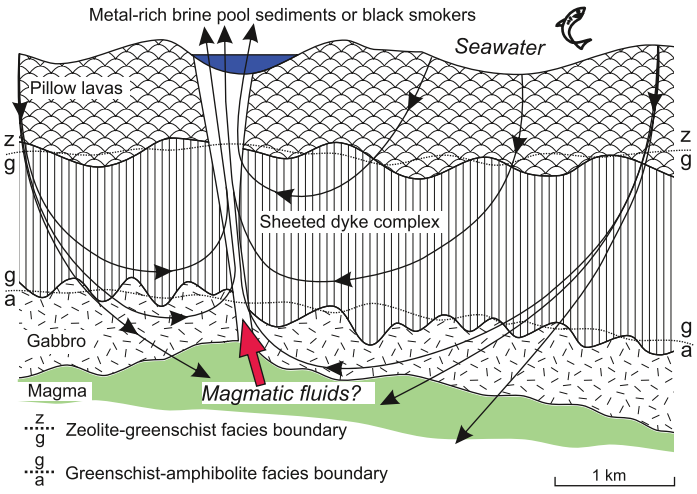

Fig. 1.12. Seawater convection, ocean floor metamorphism and focussing of rising hot fluids by apical parts of a mid-ocean magma chamber and by faults (modified from Gass 1980). By permission of Geological Survey Department, Cyprus.

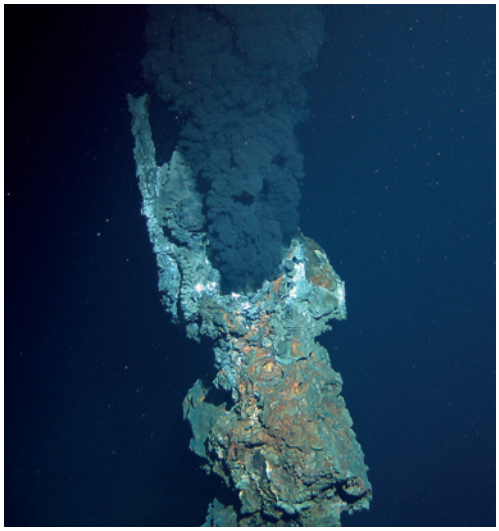

Fig. 1.13 (Plate 1.13). Black smoker in the Mid-Atlantic Ridge graben, (4°48 S, 12°37 W), at a water depth of ~3000 metres. Courtesy P.M. Herzig, IFM-GEOMAR (ROV Kiel 6000, 2009).

mainly consist of iron oxy-hydroxides that assemble on the floor around the vents and build gossan-like mounds. Because the leaky vent tubes draw in cold seawater, an amazing macrofauna of large mussels, bright-red tube-worms, crabs and shrimp finds suitable ecological conditions (Van Dover 2000, Fisher & Girguis 2007). The base of the higher life forms are thermoacidophilic and hyperthermophilic chemotrophic microbes (bacteria and archaea, e.g. *Pyrolobus fumarii*) that inhabit the vent walls at temperatures up to 121°C (read more about *archaea*, the third domain of life, in Friend 2007). Macrofossils similar to some of the fauna living on active vents today were described from the Cretaceous sulfide ore deposits of the Troodos ophiolite on the Mediterranean island of Cyprus (Little et al. 1999). The expulsion temperature of the metalliferous solutions is most often at ~350°C. With 407°C (fluid) and 464°C (vapour), the highest temperatures were measured in the equatorial Atlantic (Koschinsky et al. 2008). Alkaline "white smokers" and diffuse discharges of warm water with little dissolved matter have lower temperatures.

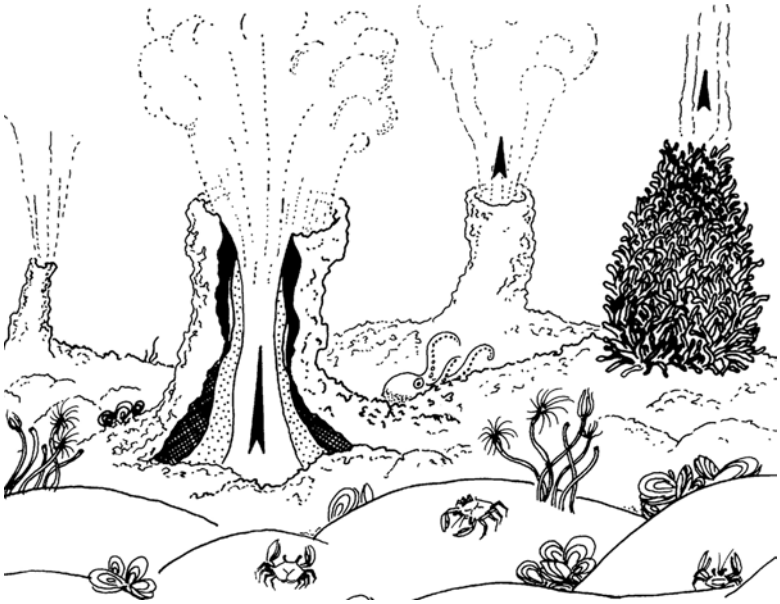

Fig. 1.14. Hydrothermal vents on pillow basalt lava in a mid-ocean rift. Adapted from Haymon (1983). By permission from Macmillan Publishers Ltd. Nature © 1983. In the foreground black smoker vents, white smoker on the right. Section from interior to exterior: Dotted = Cu-Fe-sulfides; hatched = weathered sulfides; white = talc and sulfides; black = anhydrite and sulfides.

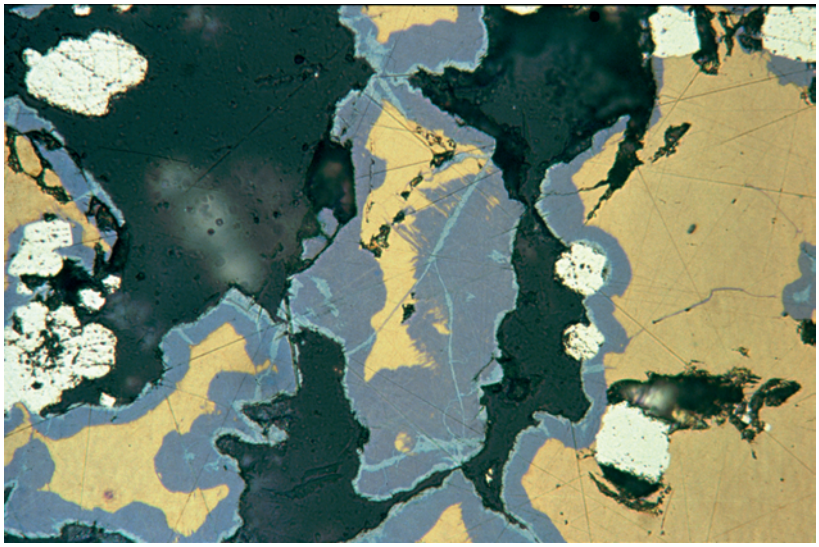

Fig. 1.15 (Plate 1.15). Mid-oceanic copper mineralization in chimney fragments from the inactive Sonne Field in the Central Indian Ocean. Courtesy P. Halbach (©FU Berlin). The polished section shows pyrite (white) as the earliest sulfide phase, followed by chalcopyrite (yellow), and increasing hydrothermal depletion of Fe in bornite (Cu_5FeS_4, blue-brown) and a thin rim of digenite (Cu_9S_5, pale blue). The long side of the image corresponds to 0.6 mm. Pore space filled by casting resin is variably dark.

The hot Na-Ca-Cl fluids of the black smokers are reducing and have pH from 2 to 5.5 (mostly 4–5), salinities from 0.1 to 3 times seawater, contents of iron, copper, zinc, barium and SiO_2, and traces of As, Cd, Li, Be, Cs, Mn, B, Cl, HCl, H_2S, and CH_4. Different solutes are derived from various protoliths including cooling magma, and also reflect different conditions of water-rock reactions. Copper, for example, is enriched relative to iron under moderately oxidizing conditions, whereas low fO_2 results in a high Fe/Cu ratio (Seyfried & Ding 1993). Deep unboiled fluids display higher metal concentrations than vent fluids (e.g. Cu 14–17 ppm, Zn 5–27 ppm: Hardardóttir et al. 2009). Fluid properties change by phase separation, boiling, alteration and mineral precipitation during rise to the seafloor. Manganese, iron and ^3He of the venting fluids disperse in ocean water and form a wide geochemical halo that is a guide to the search for submarine hydrothermal zones. Indications for supercritical unmixing of fluids into a depleted gas phase and a metal-rich brine before discharge were found at several spreading ridges. Supercritical unmixing and normal boiling followed by condensation of vapour and mixing of products are thought to explain the spread of salinities and unusual compositions of vent fluids (Cathles 2011, 1993). Only one site is known were fluids discharge at supercritical conditions (the critical point of seawater is at 298 bar and 407°C: Koschinsky et al. 2008).

Upon discharge on the ocean floor, hot acidic fluids mix with cold alkalic seawater resulting in immediate precipitation of solutes. If iron prevails, black or grey smoke-like plumes of amorphous iron sulfide and iron-manganese oxy-hydroxides can rise several hundred metres upward. Metalliferous sediment proximal to vents is rich in Fe and oxidizes to *ochre*, at some distance Mn prevails in *umber*. Iron from the largest hydrothermal plume yet discovered moves halfway across the Pacific Ocean (Fitzsimmons et al. 2017). Particulate and nano-sized iron is considered essential for life in the oceans. Zinc forms bluish, SiO_2, barite and anhydrite white clouds (white smokers). So-called "snow-blower vents" emit dense clouds of white filaments of native sulfur that is produced from H_2S by sulfur-oxidizing bacteria (Taylor & Wirsen 1997). Particle chemistry and ^3He, CH_4 and H_2S contents of seawater near vents allow predictions of temperature

and composition of vent fluids (Feely et al. 1994). The activity of vents seems to be constant for a long time. Sudden large hydrothermal outbreaks are related to seismic seafloor spreading events, rapid injection of dykes and seafloor extrusion of basalt lavas (event plume, or megaplume; Palmer & Ernst 1998). In common vents, seismic strain causes changing temperature and discharge rate.

White smokers

White smoker vents discharge fluids between ~100° and 300°C (Halbach et al. 2003). They form mainly: i) in the early stage of a newly established hydrothermal system; and ii) by subseafloor mixing of hot black smoker fluid with cooler waters. The second probably leads to precipitation of sulfides below the seafloor. Therefore, white smokers may indicate the presence of hidden stockwork and vein deposits of copper and zinc. Indeed, Cathles (2011) suspects that the larger part of metals leached by mid-ocean hydrothermal systems is enriched in the sub-seafloor. In Figure 1.14, the third vent from the left in the background is a "white smoker" consisting of barite, anhydrite and amorphous silica.

Mid-ocean submarine hydrothermal systems

The origin of mid-ocean hydrothermal systems is mainly seawater convection in hot young oceanic crust, on top or above the flanks (Cathles 1993) of shallow magma bodies 1–3 km below the seafloor (Fig. 1.12). This setting explains the steep geothermal gradient (up to 500°C/km), that is deduced from several observations. The required high permeabilities are provided by intensive tensional fracturing in mid-ocean rifts and around calderas. In the periphery, seawater flows down to >3 km depth. Because of the retrograde solubility of calcium sulfate, anhydrite is precipitated during down-flow at moderate temperature. At higher temperature and deeper levels, seawater reacts with basalts causing ocean floor greenschist facies metamorphism. Oxygen is rapidly consumed by reaction with Fe(II). Newly formed hydrated minerals (e.g. chlorite, amphibole) incorporate OH^- increasing H^+ concentration in the fluid. The reduced state and high acidity favour dissolution of metals and of sulfur.

A shallow low-temperature oxic seawater-derived domain of alteration (a) marked by celadonite and iron oxy-hydroxides that imprint brown and black halos affects the extrusive section (Patten et al. 2016). Deeper down, in the sheeted dykes and the plutonic complex, the hydrothermal alteration domain (b) originated by circulation of high-temperature (300 to >650°C) reduced fluids. At low water/rock mass ratios this induces a pervasive paragenesis of albite, epidote, chlorite and actinolite. The product is greenstone (note the absence of penetrative deformation such as schistosity). Extreme alteration produces epidosites (equigranular epidote-quartz-titanite rocks) and chlorite-quartz rocks (e.g. beneath the Bent Hill deposit: Teagle & Alt 2004). Similar alteration products are known from ophiolite-hosted sulfide deposits. Magmatic fluids may mix with altered seawater and do have a role in mineralization (Yang & Scott 2005) as indicated by high contents of mantle-derived ^3He and CO_2 although stable isotopes imply mainly seawater. Part of the fluids could have a multi-stage history, for example dehydration of hydrated basalts by prograde thermal metamorphism induced by a new magma intrusion. Hydrothermal alteration leaches metals and semi-metals; gold and Pb are the most depleted elements in the sheeted dyke and plutonic complexes, followed by As~Se >S~ Cu~ Zn > Sb > Te (Patten et al. 2016). Hot fluids take the metals up to the seafloor where black smokers or mafic volcanic massive sulfide (VMS) deposits may be formed.

Near transform faults, rocks of the deeper ophiolite sequence may be hydrothermally altered (e.g. formation of Cl-serpentinite from peridotite). Ultramafic-hosted hydrothermal systems produce highly reducing and high-pH vent fluids such as the Lost City hydrothermal field at 30° N on the mid-Atlantic ridge (Seyfried et al. 2007). High-energy, fast-spreading mid-ocean ridges are dotted by submarine volcanoes and intrusions extending to an off-axis distance of 25 km from the graben margin. Hydrothermal fields and large ocean floor orebodies display a similar range. Explored down to 3000 m depth due to geothermal energy development and production since 2006, the Reykjanes field on the emerged Mid-Atlantic Ridge in Iceland is a paradigma of an active mid-oceanic hydrothermal system (Hannington et al. 2016).

Although most of the emitted metals are diluted in ocean water and sediments, about 165 subrecent metalliferous bodies of significant mass and grade have meanwhile been discovered globally (Hannington et al. 2011). One example is a low sulfide mound on the mid-Atlantic rise at 26° N with a diameter of 250 m and a height of 50 m (the TAG hydrothermal mound: (Patten et al. 2016) that contains ~10 Mt of metalliferous sediments, sulfide debris and anhydrite, covered by oxidized sulfides and active as well as inactive chimneys. It is underlain by a sub-seafloor stockwork. This is comparable to ancient volcanic-hosted massive sulfide (VMS) deposits of obducted ophiolites. In the shallow crust beneath vent fields, large Cu, Zn and Au accumulations are possibly formed by precipitation because of boiling and vapour loss during depressurization (Hardardóttir et al. 2009). Consequently, the mass of different metals in VMS deposits on the sea floor requires unequal volumes of the respective hypothetical source cells (Patten et al. 2016).

Metalliferous mud in several depressions of the Red Sea represents the largest known submarine base metal mineralization. Sulfides in the Atlantis II basin, for example, cover 60 km^2 and reach a thickness of 30 metres. Resources comprise nearly 100 Mt (dry) of sulfides (Halbach et al. 2003). In these locations, the causative hydrothermal activity is not spectacular because metal-bearing solutions do not vent but discharge into stratified brine pools (Blanc & Anschutz 1995).

Ore deposits in ophiolites include two major groups: i) Chromite of the "Alpine" type (so called because of the numerous former mines in the Alpine chains of Southeastern Europe), in rare cases with co-precipitated exploitable platinum; and ii) exhalative volcanic massive sulfide (VMS) deposits of iron, copper and zinc sulfides (± Ag and Au, but note the virtual absence of Pb), including possible underlying stockwork ore. Because historically, the ophiolite-hosted VMS Cu-Au deposits on the Mediterranean island of Cyprus have been of great significance, this type is also termed *Cyprus type sulfide deposits*, of which a new style was recently recognized: sheet-like (exhalative?) ore bodies between lava flows (Adamides 2014). However, most ophiolitic VMS sulfides are pyrite-rich and have low base metal grades. In the future, recently formed concentrations of this type that occur on the floor of the world's oceans may become a viable but limited (11 Mt of combined Zn+Cu: Singer 2014; 1 Gt of Cu+Zn: Hannington et al. 2011), or a giant source of metals (530 Gt; Cathles 2011). Ophiolites host other important mineralizations that they have "acquired" during obduction, nappe transport, deformation, metamorphism and finally weathering. These include asbestos, jade, magnesite, gold (epigenetic in listvaenite), talc, and lateritic Ni-(Cr-Co-Fe) ore in deeply weathered soil profiles.

1.1.3 Ore formation related to alkaline igneous rocks, carbonatites and kimberlites

Rocks of these families generally have low SiO_2 and high alkali element contents, especially of sodium, calcium and potassium. Typically, alkaline igneous rocks appear in cratonic, consolidated portions of continents. An anorogenic setting is affirmed by their clustering near continental rifts, in lithospheric distension zones and over heat anomalies of the mantle (hot spots, plumes, superplumes). Occurrences of the "continental" alkaline rocks in association with oceanic intraplate volcanism are very rare. Most melts of this group originate by a low degree of partial melting of enriched mantle. The enrichment ("metasomatism") may stem from subducted oceanic crust and crustal components (Hulett et al. 2016) that introduce metals, fluids and volatiles, or can be derived from a fertile deeper mantle (Pilet et al. 2008). Nephelinite magma is the most common mafic alkaline liquid that crystallizes into a range of igneous rocks (termed the ijolite suite). Nephelinites may be associated with the much rarer carbonatites that have a prominent metallogenetic role. Fractionated members of the family include alkalic ultramafics with PGE. Complex intrusions with felsic rocks (e.g. A-type granite) in addition to the mafic ones are not rare and may be enriched in rare metals, apatite, zircon or rare earths (REE+Y). This is possibly due to secondary melting and assimilation of continental crust.

The present outcrop pattern of alkaline and carbonatite complexes depend on the depth of

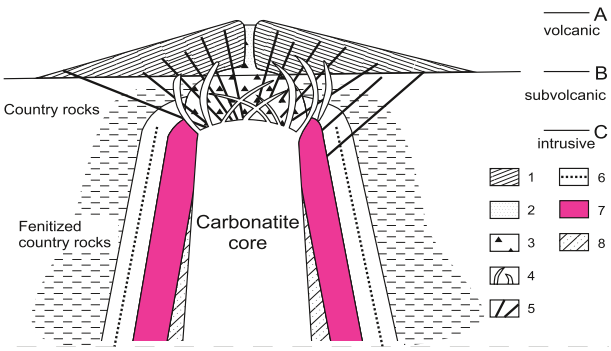

Fig. 1.16. Hypothetical section of a carbonatite complex (modified from Kinnaird & Bowden 1991). With kind permission from Springer Science+Business Media. 1: Phonolitic and nephelinitic lava and tuff; 2: Natrocarbonatite; 3: Breccia; 4: Carbonatite ring dykes; 5: Carbonatite cone dykes; 6: Syenitic fenite; 7: Nepheline syenite; 8: Ijolite.

erosion. By erosion to subvolcanic levels, ring complexes or diatremes are exposed, whereas recent uneroded examples are simple stratovolcanoes (such as the active alkali-carbonatite volcano Oldoinyo Lengai in the East African rift, Tanzania: Bell & Keller 1995; Fig. 1.16). Kimberlite volcanoes form rimmed explosive craters, maar-like circular depressions or maar lakes.

Carbonatites

Carbonatites are igneous rocks with more than 50 wt. % of carbonate minerals. They are further subdivided depending on the nature of the carbonates (Ca-Mg-Fe, rarely Na) and of silicate phases such as biotite, pyroxene, and amphibole (Woolley 1989). Typically, carbonatites are oxidized melts and most dissolved iron crystallizes as magnetite; siderite, ankerite, pyrite and ilmenite are accessory phases. Primary carbonate-rich alkalic melt originates in the mantle from carbonated peridotite by a very low degree of melting at elevated pCO_2. This carbonation is related to subduction of crustal components (Hulett et al. 2016). At about 1000°C, unmixing of nephelinite and carbonatite takes place (Weidendorfer et al. 2017). High temperatures tend to stabilize the rise of Ca-rich carbonatic melts to the low pressure subsurface and in rare cases, to the surface (Hammouda et al. 2014).The formation of alkali-carbonatite complexes is controlled by i) fractional crystallization and ii) unmixing of carbonate and silicate melts (ijolite, pyroxenite, nephelinite and nepheline syenite). At depth, carbonatites are commonly associated with ultramafic rocks. Higher up, pyroxenites and jacupirangites appear, followed by ijolites and nepheline syenites at shallower levels. Intruded silicate country rocks are fenitized. *Fenitization*

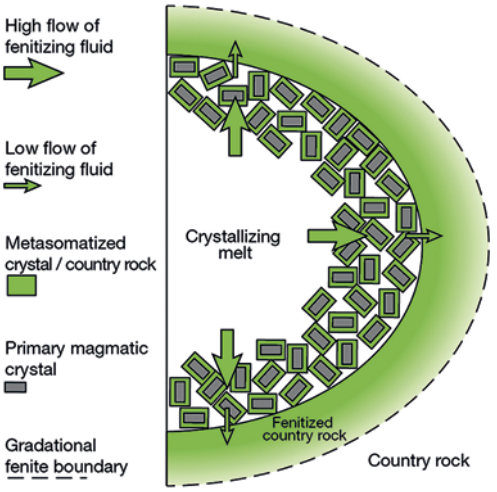

Fig. 1.17. Schematic section of a carbonatite pipe, magmatic-hydrothermal marginal autosomatism and country rock fenitization (Elliott et al. 2018). Fenitization commonly consists of desilication accompanied by addition of Fe^{3+}, Na, K, ± Ca, ± Al to the rock.

denotes alteration into a greenish rock consisting of alkali feldspar, aegirine and alkali hornblende (Fig. 1.17). The alteration is a consequence of the high contents of alkali elements and volatiles in carbonatite melt that are released during solidification (Bühn & Rankin 1999). Anomalous tenors of HFSE (e.g. Nb, Ta, Zr, Hf, Ti, V; Chakhmouradian 2006) and rare earth elements (REE), especially the light members of the lanthanoids, are remarkable features of carbonatites. Half of all known carbonatites occur in Africa

and of those, most are related to the East African Rift System (Woolley & Kjarsgaard 2008). Carbonatite occurrences tend to be location-specific and age-diverse, which is seen as strong evidence for a lithospheric origin of the source magmas (Campbell et al. 2014). Deformed and metamorphosed carbonatites are discerned from metasedimentary marbles by the presence of blue-green Na- and K- amphiboles, perovskite, pyrochlore, columbite-(Fe), and fersmite. In addition, higher Sr, Ba, REE and Y discriminates metacarbonatite from sedimentary carbonates (Simandl & Paradis 2018). Carbonatite ash and tuff are not infrequent but masquerade behind zeolitization (Campbell et al. 2012).

Metals exploited from complex intrusions that often comprise carbonatites, alkali-pyroxenites and nepheline syenites include copper, rare earth elements, niobium (± tantalum), iron-titanium-vanadium, uranium-thorium and zirconium; non-metallic resources are the industrial minerals phlogopite, vermiculite, apatite, fluorite, barite, and limestone (Notholt et al. 1990). In southern Siberia, one mine produces nepheline syenite for Russia's aluminium industry. Four characteristic ore associations occur with carbonatites:

1. Magnetite-apatite carbonatite and nephelinite (e.g. Khibiny, Kola Peninsula) are sources of pyrochlore (a niobium ore), copper (Palabora, South Africa) and zirconium ± hafnium.
2. The carbonatite-associated light REE deposits, formed by REE-rich fluids exsolved from carbonatitic melts, are the most significant sources of critical high-technology metals (Hou et al. 2015). Mineralization styles vary from stockwork or vein systems (Mountain Pass, California), breccia pipe-hosted to disseminated in carbonatite stocks, and strata-bound metasomatic ore in carbonates (Bayan Obo, China). At Bayan Obo, iron ore, light rare earth elements and niobium are exploited (Smith et al. 2015).
3. Carbonatite complexes with multi-element mineralization such as Fe-F-Ba-Sr-REE in the Tuva Republic in southern Siberia, Russia (Prokopyev et al. 2016).
4. Worldwide, the industrial minerals calcite (limestone) and apatite are extracted from carbonatites.

Among the >500 known carbonatitic complexes of the Earth, petrogenesis of carbonatites is varied and complex (Chakhmouradian et al. 2016; Woolley & Kjarsgaard 2008). Likewise, carbonatite-related mineralization may be orthomagmatic, either disseminated or concentrated in aplitic and pegmatitic segregations, transitional, or magmatic-hydrothermal, including metasomatic to hydrothermal vein ore bodies. Hou et al. (2015) provide a remarkably comprehensive geochemical-metallogenetic model of LREE mineralization related to carbonatites proposing that mantle enriched by subducted marine sediments is the source of the elements (cf. Chapter 2.5.8). Nearly 10% of the above number host active or inactive mines, or contain a formal mineral resource (Simandl & Paradis 2018).

Kimberlites

Similar to carbonatite, parental liquids of kimberlites originate by low-degree partial melting from enriched parts of the Earth's mantle (carbonate-bearing garnet lherzolite), and ponding at continental roots, acquire their kimberlitic character by resorption of lithospheric peridotite. At depths underneath the low-pressure stability limit of diamonds (~140 km), the accumulating melts may either crystallize diamond or extract diamonds that formed previously at the lithosphere-asthenosphere boundary (LAB) at high pressure and relatively low mantle temperatures (in the "diamond window"). All North American diamondiferous kimberlites erupted from slopes 160 to 200 km deep that rise from flat Archean mantle keels (Faure et al. 2011). Kimberlites are petrographically variable volcanic rocks and typically occur as strongly altered breccias and tuffs. Basically, they are porphyric, SiO_2-undersaturated, K-rich (1–3 wt. % K_2O) peridotites with xenoliths and xenocrysts of diamond, olivine, Mg-ilmenite and chrome-rich pyrope in a carbonated and serpentinized groundmass and with accessory phlogopite, perovskite, Cr-spinel, and magnetite (cf. Chapter 3.8 "Diamond"). Close relatives of kimberlites are the K-Mg rich, ultramafic lamproites that are characterized by leucite, titanium-phlogopite, clinopyroxene, amphibole, olivine and sanidine. Lamproites received little attention until the great diamond deposit Argyle in Western Australia was found to be hosted in this rock. Kimberlites occur most frequently in subvolcanic pipes and occasionally in sills and dykes, whereas lamproite magmas with lower CO_2 contents also form shallow intrusions.

Kimberlites in old cratons are more often diamondiferous than others, because pre-Neoarchean lithosphere is cooler and geochemically more favourable for diamond formation. Age dating revealed that kimberlites and their diamonds may have the same or widely differing ages. This implies that diamond formation is not necessarily connected with the kimberlite liquid that carried it to the surface. Diamonds are exotic xenocrystals that have either been formed by the kimberlite liquids in contact with, or liberated from the enclosing LAB rocks, in many cases long after their crystallization. It is important to remember that most kimberlites and lamproites contain no diamonds. Kimberlites are rarely older than 1 Ga because they are the response of the mantle to modern plate tectonis and consequent subduction and import of a large mass of C and H2O (Stern et al. 2016). This influx of volatiles increased fluid pressures at the base of thick cratonic lithosphere to >6GPa, explaining the high potential energy driving kimberlite eruptions. Exsolution of carbon dioxide further enhances buoyancy (Russell et al. 2012). The process system leading to diamond formation ends with explosive volcanism, but in the mantle, includes orthomagmatic and contact-metasomatic stages.

Economically significant are potassic igneous rock types originating in suprasubduction settings that can be genetically related to or associated with copper-gold mineralization (Müller & Groves 2016; Sillitoe 1995).

1.1.4 Granites – the earth's workhorses of ore formation

Granites are common felsic plutonic rocks that consist of quartz, feldspar and a variety of minor and trace minerals (Le Maitre et al. 2005). Most granites are the result of partial melts rising and coalescing from the lower crust. Granites and the less narrowly defined granitoid rocks are much used as construction aggregates, building material and for the production of feldspar concentrates. Weathered granites are exploited for kaolin and quartz sand. Deep granite bodies are a potential source of geothermal energy extracted with the hot dry rock technology. In Sweden and in Finland, granites were chosen for the underground storage of heat-producing radioactive waste. In this section, however, we study the basics of granite-related metal ore formation.

Typical members of this diverse group are highly differentiated small intrusions hosting tin and tantalum ("tin granites"), and hydrothermal vein and stockwork deposits of tin,

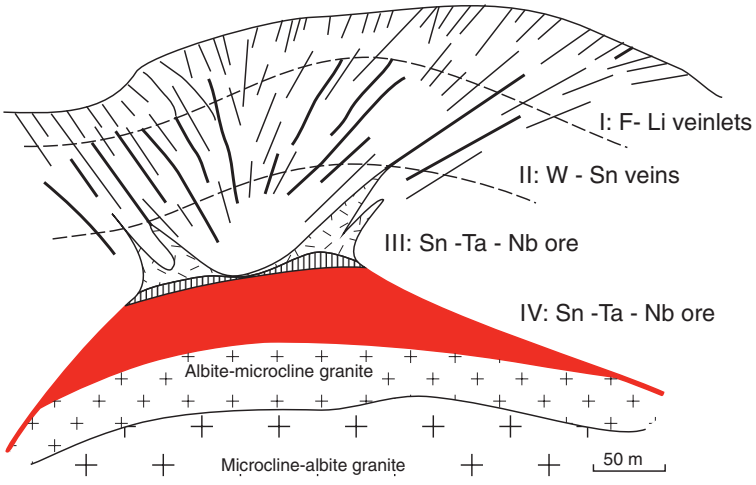

Fig. 1.18. Vertical zonation of the Sn-Ta granite at Shuiximiao in southeastern China (modified from Zhu et al. 2001). With kind permission from Springer Science+Business Media. I – Fluorite-lepidolite veinlets; II – Hydrothermal wolframite-cassiterite-quartz, III – Pegmatite-aplite and stockscheider pegmatite; IV – Albite-topaz-granite. Host rocks are Early Carboniferous limestones and slates.

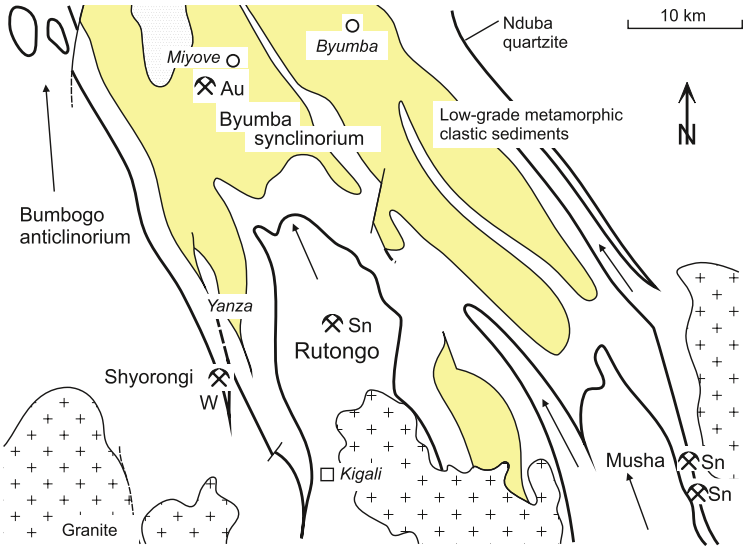

Fig. 1.19. Pegmatitic tin (Musha) and magmatic-hydrothermal vein deposits of tin, tungsten and gold in the sedimentary roof of Early Neoproterozoic granites in the Kibara orogen, Rwanda (Pohl et al. 2013). Thick lines denote a distinct quartzite marker band. Rutongo produced a total of ~50,000 t cassiterite, Shyorongi ca. 2500 t wolframite. Miyove is a small artisanal mine working a gold vein.

tungsten and gold that occur in the roof of granite intrusions (Figs 1.18 and 1.19). Granite-related, stockwork and breccia ores of copper, molybdenum and gold (the porphyry deposits), rare element pegmatites with ores of lithium, tin, tantalum and beryllium, and skarn deposits of iron, copper, lead and zinc, are presented in the following sections. Apart from metals, some industrial minerals (e.g. andalusite, fluorite, talc and wollastonite) can be enriched to exploitable grades within felsic intrusions or in their metamorphic and hydrothermal aureole.

The ore formation potential depends on the origin and evolution of the parental granite. Important controls are the plate tectonic setting, the nature of source rocks, P/T-parameters of melting, contents of water and other volatiles, the depth of intrusion, coeval tectonic deformation, partial pressure of oxygen (redox state) of the melt, and the evolution of the magma from initial partial melting by assimilation, fractionation, cooling and crystallization including fluid segregation. Favourably coinciding factors account for the fertility of a magma. Various fertility indicators are proposed (e.g. Park et al. 2019; Shu et al. 2019). Understanding these and constructing a holistic model assist exploration and rational exploitation of intrusion-related ore bodies.

The deep roots of granites and associated silicic volcanic rocks, i.e. felsic volcanoplutonic centres, consist of complex columns of melting, assimilation, storage and homogenization (MASH), where hot mafic melts from the mantle interact with the continental crust. Consequently, "the source" is not a discrete place or lithology (Hildreth 1981). Processes in the 'fractionation column' determine the melt composition and the entrainment of peritectic minerals (pyroxene, garnet, Fe-Ti oxides) and of accessory minerals such as zircon (Clemens & Stevens 2012). Geochemical analysis of major, minor and trace elements, of oxidation state (Fe_2O_3/FeO) and of isotope systems ($\delta^{18}O$, εHf, εNd, $^{87}Sr/^{86}Sr$ initial ratios, Sr_i) in granitoids provides valuable information on major source components (Fisher et al. 2017; Shaw et al. 2011). It is rare that the actual source of specific granites, commonly granulitic lower crust, is accessible for investigation (Korhonen et al. 2015). Therefore, the proportional contribution of mantle and continental crust is reflected in classifications that designate major 'sources' of granitoids:

1. Peridotites of the Earth's upper mantle (asthenosphere, lithosphere);
2. Intermediate volcanic or intrusive magmatic and metamorphic rocks of the deep continental crust (infracrustal);
3. Clastic sediments and metamorphic equivalents (supracrustal).

Ad 1: **M-type granitoids** are sourced from mantle material. Together with gabbro, they intrude the crustal rocks of the oceanic lithosphere in the form of plagiogranite and quartz diorite, and the thick volcanic piles of primitive oceanic island arcs. Typical ore deposits associated with M-type granitoids are copper-gold porphyries and hydrothermal gold.

A-type, or ferroan granitoids are characterized by iron-rich mafic mineralogy, ferroan, alkali-calcic to alkaline affinities, high LILE + HFSE abundances, dissolved OH-F bearing fluids and crystallization under reduced or oxidized conditions (Bonin 2007). A-type granites are formed under alkali-rich, anhydrous, and anorogenic conditions by melting of source rocks under low-pressure and high-temperature conditions. They occur within plates and at distensive plate boundaries, often exposed at a subvolcanic level in ring complexes together with mafic igneous rocks. The origin of A-type granites was originally sought in extreme differentiation of basaltic melt; currently, derivation from lower crustal or lithospheric mantle is considered more common (Bonin 2007).

Typical A-type granites are the alkali granites of continental rifts, for example the Jurassic W-Sn granites of the Nanling metallogenetic province in China (Li et al. 2018) and the Mesoproterozoic rapakivi granites in Finland with their large red perthitic alkali feldspars mantled by green plagioclase in a fine-grained groundmass. Volcanic equivalents include tin-rich topaz rhyolites in fields of crustal distension (Tertiary volcanics in Mexico). Frost & Frost (2011) suggest to abandon the term A-granite because it is too indiscriminate and to use "ferroan granite" [designating high FeO/(FeO+MgO)] in its place. Different ore associations occur with A-type granitoids: i) Sodium-rich granites, striking because of attached albitite bodies, are related to concentrations of niobium, uranium, thorium, rare earth elements and some tin; and ii) potassium-rich granites with profuse hydrothermal silicification, tourmalinization and acidity produce deposits of molybdenum, tin, tungsten, lead, zinc and fluorspar. The second association may occur within the granite body (endogranitic greisen, pegmatite, and porphyry stockwork ore) or as vein fields in country rocks (exogranitic). A-type granites genetically related to magmatic-hydrothermal iron oxide-copper-gold (IOCG) deposits constitute a third economically important variety (Haapala 1995).

Ad 2: **I-type granitoids** are common intrusive magmatic rocks. Many are metaluminous [$Al_2O_3/(K_2O + Na_2O + Ca_2O) < 1$] and display an abundance of hornblende and higher concentrations of Ca, Na, and Sr compared to S-type granites. Typically, large plutons consist of tonalites and granodiorites, but are often intimately associated with more basic rocks from gabbro to diorite. Some of these melts were undersaturated with water, which enabled them to rise to the surface, forming volcanic rocks. Because of their distinctly crustal isotopic signature, I-type granitoids are attributed to melting of older infracrustal igneous rocks (Blevin & Chappell 1995). Partial mingling of crustal with mantle melts has also been invoked (Kemp et al. 2007); Yanshanian I-type granites related to molybdenum mineralization in SE China may be due to partial melting of Paleoproterozoic basement rock and juvenile material in response to the westward subduction of the Paleopacific Plate (Yang et al. 2017). Often, however, source rocks were not mafic but intermediate crustal volcanic arc rocks such as metamorphic dacites to andesites, characterized by hornblende + biotite assemblages (Clemens & Stevens 2012, Clemens et al. 2011). Accessory minerals of I-type rocks are often magnetite and titanite, prompting their attribution to the class of magnetite-series magmatic rocks (Ishihara 1981, Fig. 1.20). This is due to a commonly higher oxidation degree (Fe_2O_3/FeO) of these magmas, although reduced I-type granitoids are known. The oxidation state controls enrichment or depletion of redox-sensitive trace metals in the melt, and accordingly, the metallogenetic potential. Deposits characteristically related to oxidized granitoids comprise the iron oxide-copper-gold-U-REE (IOCG), porphyry copper-molybdenum, Mo-W-Cu skarn, hydrothermal lead-zinc and certain gold and silver classes.

Ad 3: **S-type granitoids** originate by continental collision or subduction of sediments to depths and temperatures where the transition between metamorphism and significant melting is attained (Clemens et al. 2011, Clemens 2003). Products of partial melting crystallize to mainly leucocratic, SiO_2 rich rocks of a peraluminous [$Al_2O_3/(K_2O + Na_2O + Ca_2O)$ >1] and monzogranitic nature (a granite with alkali feldspar and plagioclase in about equal proportions), often with magmatic muscovite besides biotite. Apart from ubiquitous monazite and zircon, accessory minerals include cordierite, garnet, kyanite, and ilmenite as prevalent opaque minerals. S-type granites are the most common ilmenite-series magmatic rocks. The degree of oxidation of these magmas is low, due to organic carbon in the source sediments. Melting is facilitated by dehydration of muscovite in the metasediments. The resulting liquids are rather "wet" and crystallize at greater depth. Therefore, volcanic rocks are rare in this group. In the Paleozoic Lachlan Fold Belt (Australia) both I- and S-type granites are common. Highly fractionated hydrous and overpressured intrusions ("tin granites") of both suites are clearly associated with tin, tungsten and tantalum ore deposits (Blevin & Chappell 1995). Across larger regions, the chemistry of synchronous granitoids may change from purely crustal sources to admixture of mantle-like end-member components (Korhonen et al. 2015).

Not all granites can be assigned to one of the source categories because of several reasons including complex mixtures of source rocks (Shaw et al. 2011) and extreme fractionation, which leads to increasing convergence of magma chemistry (Taylor & Fallick 1997). Often, the youngest granites in orogenic provinces geochemically approach those that occur in anorogenic settings such as continental rifts, zones of crustal extension and continental "hot spots" (Turner et al. 1992). These observations motivate classification of Phanerozoic (and older) granitoids according to tectonic setting: Island arc, active continental margin, post-orogenic uplift, continental collision and continental rifting granitoids (Pitcher 1997). Newly recognized is the role of slab failure magmas that in North America were derived dominantly from the mantle and are commonly associated with Cu-Au porphyries, as well as Li-Cs-Ta pegmatites (Hildebrand & Whalen 2017).

A time-dependent chemical evolution of intrusions has been noted in many granite-related ore provinces of the world: Early batholitic intrusions (i) are geochemically *ordinary*, whereas later and smaller *precursor* granites are transitional to (ii) small, geochemically *specialized*; and to (iii) very small, *mineralized* granites (iv), which are intimately related to ore formation (Simons et al. 2017). Precise dating of rare metal granites and tin mineralization in the Erzgebirge showed that a short time span (ca. 326–320 Ma) may suffice for this evolution, caused by a subjacent large composite granite batholith system (Zhang et al. 2017).

Compared with ordinary granites, precursor granites display higher contents of K, SiO_2 and granitophile elements, and less Fe, Ti, Ca, Sr and Mg. Precursor intrusions always predate specialized granites although they are genetically related. Specialized and mineralized

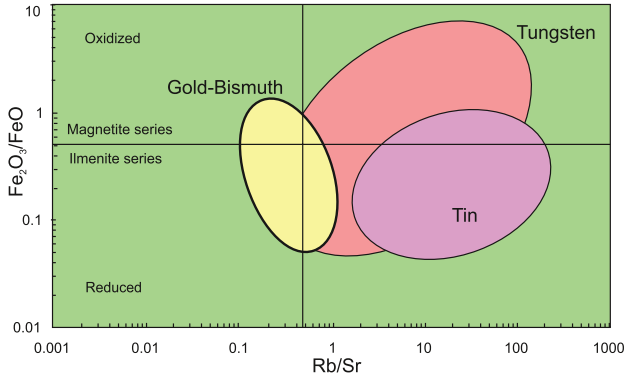

Fig. 1.20. Typical fields of granites that are genetically related to tungsten, tin and gold-bismuth deposits, in a plot of redox-state (vertical axis) versus increasing specialization (horizontal axis). Modified from Baker, T., Pollard, P. J., Mustard, R., Mark, G. and Graham, J. L. (2005) Society of Economic Geologists, *SEG Newsletter*, Figure 4, p. 12.

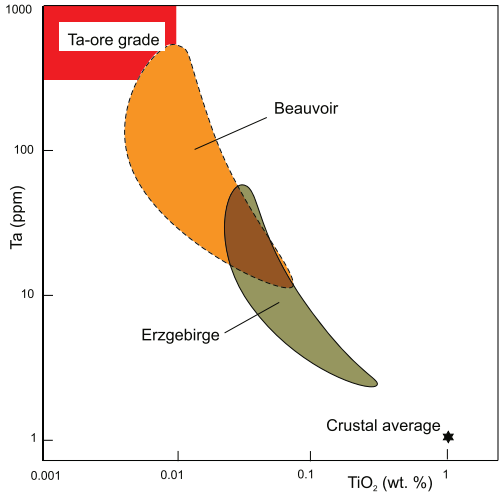

Fig. 1.21. Ta/TiO_2 variation of granites from the northern French Massif Central (Beauvoir) and the Saxo-Bohemian Erzgebirge (modified from Lehmann 1990). With kind permission from Springer Science+Business Media. Tantalum (an incompatible element) is enriched to varying tenors that depend on the degree of fractionation of individual intrusions. Some samples from Beauvoir reach exploitable grades. Concurrently, contents of compatible titanium decrease. Derivation of tantalum from geochemically ordinary crust via partial melting, differentiation and mineral fractionation appears possible.

(parental) granites are distinguished by geochemically elevated contents of Sn, W, Nb, Ta, Mo, U, Th, REE, Rb, Cs, Li, Be, often F (the latter include "topaz granites") and P (Figs 1.20 and 1.21). Petrographically, specialized and mineralized granites are mostly aplitic muscovite-biotite rocks, alaskites and leucogranites that intruded at shallow crustal levels. In specialized granites, rare elements are enriched in silicates and accessory minerals. Mineralized rare element (Linnen & Cuney 2005) or parental granites, in contrast, stand out by their intimate association with ore-grade concentrations of rare elements. The geochemical changes from ordinary to mineralized granitoids are mainly caused by a process system that is generally termed "*magmatic differentiation and fractionation*". The degree of fractionation can be measured by various indices. In metallogenetic research dealing with granitoids, increasing Cs concentration in melt, minerals and fluids is a particularly useful tracer of fractionation (Audétat et al. 2008).

In general chemistry, the Periodic Table is employed to illustrate properties and behaviour of elements (e.g. WebElements 2017). In geochemistry, the observation of their distribution in meteorites and in the Earth is used for classification (cf. Table 1.1). Terms that relate element groups to petrogenesis and ore formation include:

- *Granitophile elements* (such as fluid-mobile Li, Cs, Rb, W, Sn and fluid-immobile Ta);
- *high field strength elements* (HFSE; forming cations with a high charge from +3 to +6, such as Hf, Mo, Nb, P, REE, Sn, Ta, Th, U, W, Y, Zr and Ti. These elements are commonly abstracted from the melt by incorporation into crystallizing biotite, amphibole, apatite, zircon, monazite and magnetite. This process is inhibited by high activity of complexing volatile compounds, which cause the HFS to collect in late peralkaline liquid and fluid phases. Because mobility is limited to special systems such as pegmatites, HFS elements are generally immobile and useful petrogenetic indicators (e.g. Pearce 2008, 1982; Pearce et al. 1984);
- *large ion lithophile elements* (LILE) including Cs, Rb, Sr, K, Ba, Zr, Th, U and light REE are preferentially enriched in late, extremely differentiated melts or fluids derived from restites because these elements are less prone to partition into early water-rich melt;
- *rare* are all elements with a crustal average below 0.01%; in this chapter, granite-related rare elements such as Sn, Li, Be, W, Zr, Hf, Nb and Ta (Linnen & Cuney 2005) are of special economic interest;
- elements that partition preferentially into the solid phase during fractional crystallization are referred to as *compatible* because they are included in nascent rock-forming silicate minerals, e.g. Eu^{+2} substituting for Ca^{2+} in plagioclase. *Incompatible* elements remain in the liquid (melt) phase.

Granites and related pegmatites with extreme fractionation are the source (and often the hosts) of deposits of rare elements. *Rare element granites* are enriched in large ion lithophile elements (LILE) such as Rb and Cs, and high field strength elements (HFSE) such as P, Y, Zr, Hf, Nb, Ta, W, Th and U (Linnen & Cuney 2005, Linnen & Samson 2005). If ordinary and precursor granites are present, the enrichment may be traced back to common, geochemically not anomalous crustal rocks (Lehmann et al. 2000b, Černý 1991a).

Figure 1.21 illustrates this principle and shows how tantalum (an incompatible element) is continuously enriched by differentiation of successively more fractionated (and younger) granite melt batches and finally reaches exploitable grades. Concurrently, concentrations of the compatible element titanium decrease. Derivation of tantalum from geochemically ordinary crust appears possible.

Differentiation (formation of different rock types from one melt body) and *fractionation* (separation of crystals from magma or of melt from source solids) of granitic magmas are commonly attributed to fractional crystallization, early crystal settling and/or removal of liquid from solids either at the source, along the flow paths or in the magma chamber (Weinberg 2006). Alternative explanations include partial melting at very low degrees (Robb 2005) pulsed by different temperatures. Extreme fractionation producing fertile granites and pegmatites involves melt and fluid migration late in the crystallization history of a pluton (Clemens & Stevens 2012). Upwardly differentiated zoned sequences of rare metal granites (Fig. 1.18) may be the result of a series of magmatic injections, with the most fractionated melt having been emplaced at the highest level (Linnen & Cuney 2005); at the comparable Yichun deposit, the zoned sequence in the cupola is attributed to continuous fractional crystallization of the granitic magma (Li et al. 2017). Both variants are possible; the second is more likely if change is gradual and unconformity surfaces are absent.

In some cases, melting of geochemically anomalous source rocks is considered to account for metal enrichment. An example are magmas with high contents of the chalcophile elements Au, Ag, Bi, Sb, Hg and Tl, which are supposedly inherited from a pre-enriched source (Tomkins & Mavrogenes 2003).

Plutons form by incremental assembly of melt batches in the upper crust at injection rates between 0.001 and 0.1 $km^3\ yr^{-1}$ and final volumes ranging from 100 to 10,000 km^3. The respective volume is a first-order control on the mass of volatiles and metals that is available for ore deposit formation (Chelle-Michou et al. 2017). The petrological evolution of mineralized granites can be schematically subdivided into two steps: The first comprises the fractionation of elements between melt and solid phases that crystallize during cooling, and a second step of partitioning of trace elements between the remaining melt fraction and exsolving fluids that concentrate volatiles and metals.

The fertility of granitoids is closely related to fractionation and the formation of residual liquids that are traced in melt inclusions (Thomas & Davidson 2013; cf. 1.1.5 Pegmatites); at about the same time, *magmatic volatile phases* are exsolved. The composition of magmatic volatiles is investigated by sampling volcanic exhalations, melt and fluid inclusions in minerals (especially from miarolitic cavities) and volatiles included in volcanic glass. Miaroles are crystallined cavities in granitoids that are thought to have formed from fluid pockets during the solidification of magma. Fluid and melt inclusions preserved in miarolitic minerals reveal details about segregation, composition and evolution of mineralizing fluids (Audétat et al. 2008).

Water is the most common substance in magmatic volatiles. In cooling silicate melts at intermediate pressure, water dissolved in melt occurs at ~8 wt. %. There are, however, wide variations; pressure (P) being the dominant control on maximum water solubility, whereas the minimum amount of H_2O in granitic melts is strongly dependent on T° (Fig. 1.22). Above critical T/P, water and liquid merge into a hydrous supercritical fluid/melt phase and are completely miscible (Fig. 1.23).

Suprasubduction arc magmas are more hydrous (and commonly more oxidized) than those of other tectonic settings. Water is followed in decreasing order by CO_2, H_2S or SO_2 (Keppler 1999), HCl and HF, and small amounts of N_2, H_2, CO, P, B, Br and CH_4. Trace elements in volcanic emanations include the metals Pb, Bi, Cd, Cu, Zn, Hg, Sb, Te and As, rare alkalis such as Li and Be, and major rock-forming elements such as Al, Mg, Na and K. At the high-silica Chaitén rhyolite volcano, Chile, integrated vapour-melt distribution ratios for Cl are ~200, and exceed 1000 for Li, F, and Be (Lowenstern et al. 2012). Sulfur always partitions into the hydrous fluid with a partion cofficient from 47 (SO_2) to 468 (H_2S) (Keppler 1999). The annual exhalative emissions of Etna volcano, Sicily, include ~2.5 t lead and 250 t potassium. Metal fluxes in vapour from White Island volcano, New Zealand, are estimated to >106 t Cu and 100 t Au in 10,000 years of volcanic activity (Hedenquist et al. 1993). Different volcanoes have ratios of SO_2/HCl and SO_2/HF between 1 and >100. Ratios from 1 to 10 are typical for volcanoes above convergent plate

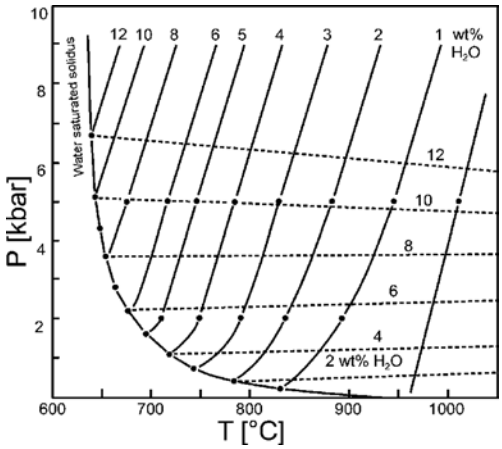

Fig. 1.22. Maximum solubility of H_2O (dashed lines) and minimum H_2O content (solid lines) in simple granitic melt (quartz-albite-orthoclase-water system). Modified from Holtz & Johannes (1994). Remember that 1 kbar equals ca. 3.85 km rock (of density 2.6) or a 10 km water column.

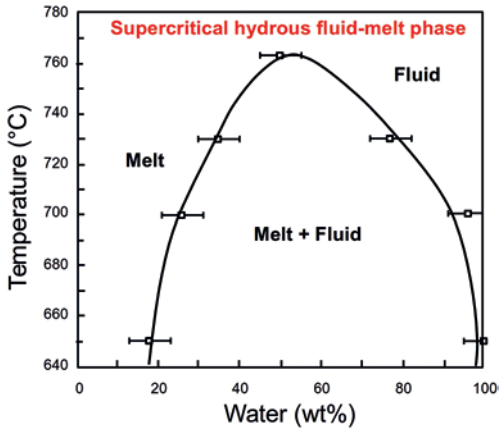

Fig. 1.23. Miscibility of water and a simple silicate melt (albite $NaAlSi_3O_8$) at 14.5 kbar. Modified from Shen & Keppler (1997). Note that in this system, there is complete miscibility >763°C, i.e. one supercritical ± hydrous fluid-melt phase.

boundaries and discharge is high in HCl. Gas released in explosive mode by Stromboli volcano (Italy), for example, consists of 64% H_2O, 33% CO_2, 1.8% SO_2 and 0.33% HCl (Burton et al. 2007). Note, however, that molecular HCl is only stable at very low pressure or in the absence of water. Above 200 bar, chlorine occurs as an ion or is dissolved in magmatic water complexing Na, K and Fe.

Fertile granitoid magmas are distinguished by high contents of volatiles. Volatiles collect common (e.g. iron, Bell & Simon 2011) and rare ore elements, reduce density, viscosity and solidus temperature of a melt, and increase its mobility (Baker & Vaillancourt 1995). Low magmatic temperatures and high salt concentrations favour the fractionation of metals into the fluid phase (Audétat & Pettke 2003). *Oxygen fugacity or redox state* of the melt is an important control (Fig. 1.20). High oxidation state in granitic magma may cause depletion of tin and tungsten in late liquids and fluids because the metals tend to be abstracted by inclusion in dispersed accessory minerals such as magnetite and titanite already during main-stage crystallization. This is due to high *mineral-melt partition coefficients* (Linnen & Cuney 2005). Behaviour of copper and uranium is the opposite. Oxidized magmas (of the magnetite series) dissolve more sulfur (SO and SO_2 as an "anhydrite component", compare Streck & Dilles 1998) and related fluids may produce large Cu-Au deposits. In "reduced" granitic magmas (ilmenite series), early saturation of sulfur in S^{2-} state may result in formation of dispersed sulfide melt droplets that collect copper and gold. Late fluids tend to be barren.

Solidus temperatures of common granites (T of granitic mineral assemblages crystallizing entirely) are believed to range from 650–700°C but may be 100–200°C lower (Ackerson et al. 2018). This can affect fluid segregation. For the genesis of *magmatic-hydrothermal ore deposits*, exsolution of a volatile phase that collects metals is the first critical step (degassing or fluid extraction from melt). Causes may be two end member processes: (1) decreasing pressure; and (2) crystallization of solids, or any combination of both. The first occurs during the ascent of silicate magmas through the crust ("first boiling"), or by sudden decompression in the case of roof fracturing. Physical models of magma degassing assume that melt loses volatiles monotonically during ascent-driven decompression (Fig. 1.22), but volatile regassing, a complex decompression path or volatile resorption may intervene (Watkins et al. 2017).

Supersaturation leads first to formation of dense supercritical fluid bubbles that expand with further ascent until the density reaches that of gas. As a function of the total water

content in melt (commonly 3–5 wt. %) and the chlorine concentration, felsic magmas start to segregate an aqueous fluid phase at a pressure of ~260 MPa (9 km, but more often around 4 km below surface). Commonly at this stage, the melt freezes. Kinetic factors may, however, allow further ascent of the magma. In that case, expansion of fluid bubbles will produce a frothy liquid that is able to convect vigorously. Rare elements are effectively scavenged from the melt, and as the fluids move upwards, ore formation can take place either in the apex of the intrusion or in its roof. The remaining melt solidifies rapidly.

After final emplacement, when ascent is stopped and *first boiling* ceases, the intensive formation of solid phases from melt causes renewed concentration of volatiles. If the concentration is higher than the mass that can be included in minerals (e.g. OH^- in mica) a free volatile phase will form once more (*second* or *resurgent boiling*: Philpotts & Ague 2009). In epizonal shallow intrusions, fluid pressures may cause fracturing of the roof and sudden injection of mineralizing fluids. Commonly, the catastrophic brecciation of porphyry stocks is attributed to second boiling; fragmentation propagates upwards from a narrow focus toward areas of reduced effective mean stress (Tosdal & Richards 2001). In this case, fluid-induced stress is larger than the sum of rock mass strength and the minimum ambient principal stress (Brady & Brown 2004). Unmixing of a fluid phase from mesozonal intrusions (at pressures >2 kbar) is restricted to a narrow temperature interval. Often in this environment, volatiles form small batches of water-rich (20–30 wt. % H_2O: Thomas & Davidson 2016) overpressured silicate melt that solidifies into coarsely crystalline pegmatites. Shallow epizonal intrusions degas over a wide temperature interval (Fournier 1999), producing miarolitic and hydrothermally altered granites, but foremost the many variegated magmatic-hydrothermal ore deposits.

In the past, a *pneumatogenic or pneumatolytic phase* of ore formation was distinguished between pegmatitic and hydrothermal conditions. The assumption was that certain ores were formed by precipitation from a magmatic gas phase of extreme mobility and with high concentrations of rare metals. Greisen orebodies of tin and many skarn ores were thus explained. More recently, the term is rarely used and often explicitly dismissed. Counter arguments include that water vapour (below the critical density of 0.32 g/cm^3) cannot carry more than traces of dissolved matter and supercritical fluids with densities that reach 2 g/cm^3 can hardly be called a gas (Roedder 1984; remember that *pneuma* in classical Greek is "air" or "breath"). Furthermore, the distinction is thought to be difficult, because supercritical fluids may pass into subcritical solutions or gases without any discontinuity (condensation). The limit between pneumatogenic and hydrothermal conditions had been assumed at the critical point of pure water, which occurs at 647 k (374°C) and 22 MPa (220 bar) but rises as a function of increasing pressure and solute concentration.

> Even if there may be no need for the term 'pneumatogenic', attention must be drawn to the fact that supercritical fluids and water-rich liquids (the *fluid/melt phase* of Thomas & Davidson 2016, or Holtz & Johannes 1994) do have properties that differ from subcritical state: The density of supercritical fluids varies widely with changing pressure and temperature, they have higher pH (Ding & Seyfried 1996), are able to dissolve many organic substances, and exhibit extreme dissociation of water and diffusion coefficients. Geologically most important are probably the variable density (from dense fluid to gas), reaction rates and equilibrium constants that control transport and precipitation.

Of course, there is no doubt that magmatic vapour, gas and fluids of low density can transport metals (e.g. Etna, see above) and precipitate ore. Cassiterite-quartz veins in the Mole granite, New South Wales (Australia), contain two types of inclusions: A saline brine (a solution) with elevated trace contents of Mn, Fe, Zn, Pb and Sn, whereas the other is "gas" with ~1% Cu. Observations suggest that both are cogenetic and segregated from magma. Copper was concentrated in the 'pneumatolytic' gas phase (Heinrich et al. 1992). A broader investigation of magmatic-hydrothermal ore deposits revealed that boiling of magmatic fluids concentrates Cu, As, Au and B preferentially into the vapour phase whereas Na, K, Fe, Mn, Zn, Rb, Cs, Ag, W, Sn, Pb and Tl are enriched in the

residual saline brine (Williams-Jones & Heinrich 2005, Heinrich et al. 1999). The most important controls on this behaviour appear to be fluid density (Pokrovski et al. 2005) and sulfur contents (Nagaseki & Hayashi 2008).

Exsolution of magmatic fluids and hydrothermal ore formation are an integral part of ascent and crystallization of a fertile intrusion. Cooling down to environmental temperatures drives meteoric, convective hydrothermal systems that are often called "geothermal". In these systems, magmatic fluids and volatiles typically mix with meteoric or with basinal water. Age determinations, model calculations and observation in nature reveal that an isolated single upper crustal intrusion may sustain a hydrothermal system for ~100,000 years (Cathles et al. 1997). Magmatic-hydrothermal processes can be prolonged to millions of years in the case of incremental growth of a pluton by multiple intrusions, regional deep magmatism and autonomous heating due to radioactive decay that retards cooling.

The last mentioned setting is the home of HHP (high heat production) granites, which are rich in the heat-producing elements (HPE) U-Th-K. These intrusions attract attention where they seem parental to hydrothermal deposits formed much later (posthumous) than the granite. With the most frequent value at ~2.4 μW/m³ the heat production of granites is higher than the average of continental crust (0.9 to 1.2 μW/m³); HHP may be derived from HPE-rich sources (Bea 2012).

The Early Devonian Weardale granite in Northern England, for example, was suspected to have produced the hydrothermal Cu-Pb-Zn-fluorite-barite ore deposits of the North Pennines in the Permian. A geothermal exploration borehole to 995 metres below surface exposed about 700 m of fractured, highly permeable, brine-filled and mineralized granite with radiothermal heat production averaging 4.1 μW/m³ and a mean geothermal gradient of 38°C/km (Manning et al. 2007). The formation of pregnant fluids is related to retrograde-metamorphic convection and leaching.

The explanation for 'posthumous' mineralization is long-lasting heat production due to elevated tenors of HPE (Plant et al. 1985), which produce heat by radioactive decay. Latent heat is one element of HHP ore-forming systems. The second is sufficient permeability that allows deep circulation of down-flowing, usually meteoric water. Crustal permeability is commonly created by tensional tectonic fracturing. Heated water at depth can dissolve substances that are precipitated during ascent. Note that HHP-stocks must be large with a minimal diameter of 15 km and a considerable depth extension because the heat of small granites is rapidly dissipated. Typical HHP-granites include the post-orogenic Variscan tin granites of Cornwall (Simons et al. 2017), which are related to important polymetallic mineralization and are explored for the production of hot-dry-rock geothermal energy.

The often-used term *granite (or granitoid) related* in contrast to "orthomagmatic" or "magmatic-hydrothermal" mineralization reflects the lessons drawn from the observations described above. It is not rare, however, that even complex investigations are unable to solve dubious cases, justifying the non-genetic term.

1.1.5 Ore deposits in pegmatites: sources of high-technology rare and "green" metals

Pegmatites crystallize from highly fractionated hydrous residual melt batches of magma bodies that are enriched in volatiles and incompatible trace elements, or more rarely, from anatectic melts. Pegmatites are characterized by coarsely crystalline textures, occasionally by giant crystals, graphic intergrowths, miarolitic (crystal lined) cavities and by minerals of rare elements. Most pegmatites are related to granites and have a paragenesis of orthoclase (perthite), microcline, albite, mica and quartz. Common minor minerals include tourmaline, topaz, beryl, cassiterite and lithium minerals. Paragenesis and geochemical characteristics distinguish the LCT (lithium-caesium-tantalum) family of pegmatites, which may be derived from both peraluminous S- and from I-type granites or related source rocks, and the less abundant NYF (niobium-yttrium-fluorine) pegmatites with amazonitic K-feldspar, nepheline, apatite, Nb, Be, Ti, Sc, Zr and heavy rare earth elements that are related to anorogenic, within-plate, alkaline granites of the syenite-carbonatite family. Characteristically, LCT pegmatites mark collision, supercontinent formation and the onset of cratonization (Bradley et al. 2017). Pegmatitic ore formation is orthomagmatic to magmatic hydrothermal.

Felsic pegmatite melts intruding ultramafic rocks suffer desilication resulting in plumasites that are characterized by corundum, kyanite and anorthite. A copper-gold mineralized syenitic pegmatite (K-feldspar, clinopyroxene, magnetite) is part of a porphyry deposit at Dinkidi (Luzon, Philippines; Wolfe & Cooke 2011). Gabbro pegmatites are derived from mafic magmas and are composed of anorthite, pyroxene, amphibole, biotite and titanomagnetite, occasionally including carbonates and sulfides (similar to the Merensky Reef "pegmatoid" of the Bushveld Complex, and to parts of the Roby Zone Pd ore body of the Archean Lac des Iles intrusion: Hanley & Gladney 2011). Iron-rich ultramafic pegmatites composed of olivine (intrude the cumulates of the upper Critical Zone of the Bushveld Complex 'dunite intrusions' Fig. 1.6). Certain diamonds are thought to have crystallized from kimberlitic pegmatite melt deep in the mantle (Moore 2009). Anatectic pegmatites (metamorphic segregations) that are formed in the upper amphibolite facies are rarely mineralized. Yet, some mineralized pegmatites may have originated by partial melting at great depth and not from large magma bodies (Shaw et al. 2016). Examples include electronic-grade quartz pegmatites in Southern Norway (Müller et al. 2015) and uranium-molybdenum-rare earth pegmatites of the Grenville orogen in Canada (Lentz 1996). Also, the giant Greenbushes tin, tantalum and lithium pegmatite is not related to a known parental granite but intruded a large Archean shear zone at T between 550–650°C and P of 4–5 kbar (Partington 2017).

The majority of pegmatites crystallized at intermediate crustal levels, at fluid pressures of ~200–400 MPa (2–4 kbar). The most reliable T-P information on pegmatite formation can be deduced from fluid and melt inclusions (Thomas & Davidson 2016) or from lithium aluminosilicates (London 2008). Pegmatites are commonly found in low-grade metamorphic country rocks. Volcanic equivalents of highly differentiated pegmatitic melts are extremely rare.

Classifying granitic pegmatites by emplacement T/P leads to differentiation of the following types (Fig. 1.24):

- Abyssal pegmatites are anatectic stringers in migmatites of amphibolite and granulite facies metamorphic zones.
- Muscovite pegmatites occur in amphibolite facies kyanite-mica schists and are commonly related to ordinary granites; they exhibit little fractionation.
- Highly fractionated rare element pegmatites are derived from strongly differentiated fertile peraluminous granites; country rocks typically contain cordierite and andalusite.
- Miarolitic pegmatites form at low pressure and are mainly derived from A-type granites. They may contain quartz of optical quality, various gemstones and valuable crystals of many rare minerals.

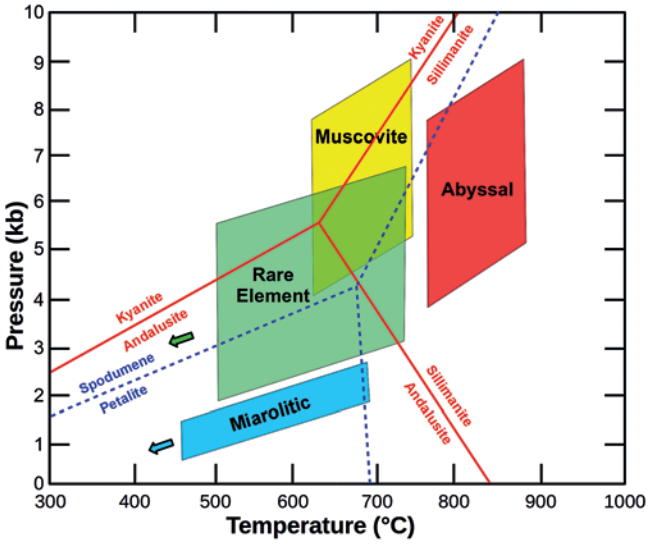

Fig. 1.24. Aluminium silicate phase diagram showing pegmatite classes in P/T space, and stability fields of Li ore minerals. Source: Bradley et al. (2017) based on Černý (1991b).

Granitic pegmatites occur as dykes or lenticular and irregular bodies. Most pegmatites are relatively small with a thickness that rarely surpasses tens of metres and a length of a few hundred metres. Some pegmatites occur at the roof of granite cupolas and form a thin shell between the intrusion and the roof rock (Fig. 1.18; *stockscheider*, i.e. "border pegmatite" in the German Erzgebirge). Giant pegmatites of this type are rare but economically significant (e.g. the tin-tantalum and spodumene pegmatite at Manono, D.R. Congo, that extends over ~6 km^2; Pohl et al. 2013). Granitic pegmatites may be homogeneous (without a change of mineralogy or texture from wall to wall) and isotropic, or strikingly inhomogeneous and anisotropic ("zoned" or "complex" pegmatites). In contrast to the zonation of the interior of a pegmatite body, an external zonation can also be observed. This term designates the occurrence of closely related pegmatite types in one district, with a map-scale zonation, ideally around a central parental granite (Fig. 1.25 depicts characteristics of the pegmatite field classification by Varlamoff 1972).

The internal zonation of complex pegmatites (Fig. 1.26) reflects crystallization from the walls to the centre of a pegmatite body where the last melt solidified. The following zones are distinguished (London 2014):

- *Border zone*: chilled margin, but not representative of bulk composition; often fine-grained, aplitic, and very thin;
- *Wall zone*: marked by abrupt coarsening, ordinary granitic composition, in some deposits with exploitable muscovite and beryl;
- *Intermediate zones*: oscillating proportions of sodic plagioclase, quartz, K-felspar and muscovite, culminating with late albite and lithian minerals; the intermediate zones contain most of the valuable rare minerals (cassiterite, columbite, spodumene, beryl, etc.);
- *Core*: commonly a solid mass of barren grey or white quartz, but may also contain feldspar, tourmaline and spodumen.

The quartz core is possibly formed from a silica liquid unmixing from salt melt and typically, is last to reach solidus, passing through a sol-gel state (Thomas & Davidson 2015). In many LCT and NYF pegmatites, albite with lepidolite or spodumene and other rare minerals is the last igneous unit. Subhorizontal pegmatite sheets may display asymmetric and bottom-to-top differentiation (e.g. Kenticha in Ethiopia: Küster 2009) and zoning, in contrast to the concentric symmetry that characterizes most steeply-dipping bodies. Some cases of internal zonation are so complicated as to appear chaotic. Post-solidus cross-cutting fracture fillings, irregular, commonly sodic or micaceous ("greisen") metasomatic masses and hydrothermal quartz veins (± coarse-grained ore such as cassiterite) can further disarrange the internal structure. Because of crystallization from the wall to the centre, exsolving aqueous fluids will act from the centre outwards. Therefore, post-solidification hydrothermal alteration of magmatic minerals is not rare (e.g. muscovitization, kaolinization).

In contrast to granites, pegmatites frequently exhibit strikingly anisotropic textures. Most obvious examples are the giant crystals of amblygonite-montebrasite, spodumene, beryl, topaz, tourmaline and other minerals that grow radially inward from the cooling surface

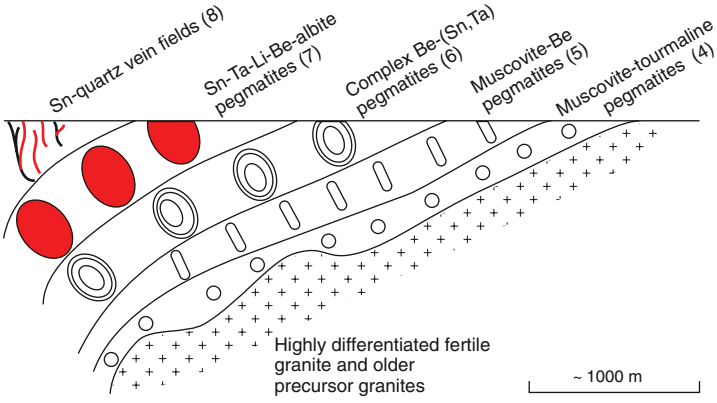

Fig. 1.25. External zonation of rare element LCT (lithium-caesium-tantalum) pegmatites and cassiterite-quartz veins near fertile granites in Central Africa (adapted from Varlamoff 1972; cf. Fig. 1.19). With permission from Springer Science+Business Media.

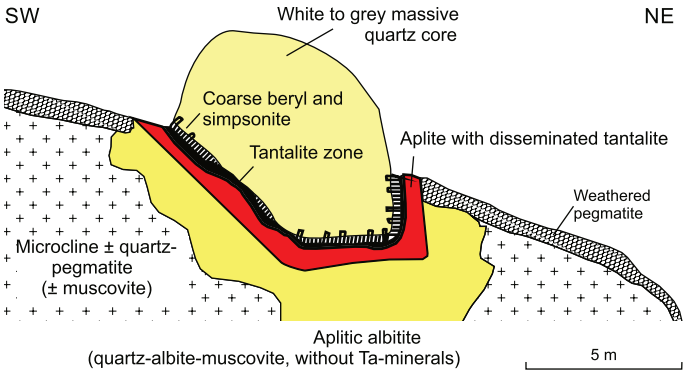

Fig. 1.26. Section of the Mesoarchean tantalum-tin-beryllium pegmatite at Tabba Tabba near Port Hedland, NW-Australia, with a simple internal zonation. Simpsonite is $Al_4(Ta,Nb)_3(O,OH,F)_{14}$ indicating extreme fractionation. After Sweetapple, M.T. & Collins, P.L.F., 2002, Society of Economic Geologists, *Economic Geology* 97, Fig. 5, p. 882.

("unidirectional solidification textures": Shannon et al. 1982). Related features are banding in sugary albitites, and graphic, skeletal or radial crystal growth.

Alteration of host rocks at the contact with pegmatite is often observed. However, the nature of this alteration is not of high-temperature contact-metamorphic type but hydrothermal, for example tourmalinization, silicification, biotitization and propylitization (cf. "Hydrothermal Host Rock Alteration"). Oxygen isotopes and concentrations of rare alkalis in minerals such as mica clearly show that they are derived from the last solidifying fluid-rich melt (London 2014, 2008). A chemical exchange directed from enclosing rocks to the pegmatite is also possible, as shown by garnet appearing in the wall zone, the plumasite formation mentioned above, or the occurrence of a tourmaline border zone that is due to reaction of iron and magnesium mobilized from the host rocks with boron from the volatile phase of the pegmatite.

At emplacement, pegmatite-formation starts in the high temperature range (~800–700°C) as an overpressured volatile-rich *supercritical fluid/melt (SCMF) phase* that is forcefully injected into host rocks. It is characterized by complete miscibility between H_2O and silicate liquid (Thomas et al. 2019, Thomas & Davidson 2016). This supercritical phase is marked by extremely low density, viscosity and surface tension, and high diffusivity, reactivity and mobility. At water concentrations between 20 and 30 wt. % the solubility of some elements such as Be, Sn, As, P, Cl and Ta in the supercritical fluid/melt phase is extraordinarily high. Also, the oxidation potential is elevated and Sn, for example, typically occurs as Sn^{4+} in complexes such as (Na, K)[Sn(OH, Cl, F)$_3$CO$_3$].

Cooling and the onset of crystallization induces the segregation of immiscible liquid phases, which may include (1) peraluminous (type-A) melt containing less water; (2) a carbonate and water-rich peralkaline (type-B) melt; and (3) an Na-CO_2 rich fluid (type-C) as observed in the Li-Ta pegmatites of the Borborema province in Brazil (Thomas & Davidson 2016; Thomas & Davidson 2015, Thomas et al. 2011). The nature of the unmixed melt can be described as a colloid or emulsion of type-A droplets (dispersed phase) in a type-B liquid (continuous phase); with increasing crystallization, the first is depleted and the second is enriched, together with rare elements. Other phases such as hydrosaline melt (a highly concentrated aqueous fluid), saline fluids and vapour may appear at certain stages. Inclusions of coexisting melts and hydrothermal fluid in quartz, feldspar, topaz, tantalite and spodumene confirm this model (Thomas et al. 2012, 2011, Rickers et al. 2006, Thomas & Webster 2000, Thomas et al. 2000).

Ordinary (~haplogranitic) unmineralized pegmatites crystallize at temperatures between 690–540°C, whereas the solidus of fractionated melts with elevated contents of fluxes such as boron, fluorine, phosphorous and chlorine may occur at ~450°C. Thomas et al. (2012) point out that apart from the viscosity-reducing fluxes mentioned, many more compounds modify the melt structure, including H_2O, OH^-, CO_2, HCO^{3-}, CO_3^{2-}, SO_4^{2-}, PO_4^{3-}, H_3BO_3, as well as the elements Li, Na, K, Rb, Cs and Be. This increases the solubility of water (from an average of 20 wt. % to 50%) but inhibits its

vaporization. The most fractionated liquid to crystallize last is flux-rich, hydrous, sodic, enriched in alkali carbonates and bicarbonates, lithium and other rare elements. After solidification, aqueous fluids dominate the system. In some instances, the released aqueous fluids may form classical hydrothermal mineralization such as cassiterite-quartz veins in Rwanda (Fig. 1.19). Ore bodies within pegmatites are notoriously irregular and unpredictable: "*the enrichment of Be (and other rare metals) is the result of fractional crystallization and further enrichment in melt batches of pegmatite bodies due to melt–melt immiscibility at fluid saturation*" (Thomas & Davidson 2015, 2016).

According to London (2014, 2008), liquidus undercooling of the melt injected into cool host rocks is the principle driver in the formation of pegmatite textures and zoning, and is the main difference to systems where crystallization closely tracks the equilibrium surface of the liquidus. Undercooled melt in contact with country rock is semisolid. The development of giant crystals seems to contradict this concept, but a low density of nucleation sites, water-like viscosity of the flux-rich peralkaline and hydrosaline melts adjacent to the growing crystals, and high diffusion rates are proposed to explain its feasibility. The amount of fluxes in pegmatite melt is moderate but they are concentrated in boundary layers at crystallization fronts by "constitutional zone refining" (CZR: fluxing components excluded from solids accumulate in the boundary zone where they promote diffusion). Based on a large body of inclusions research, however, Thomas & Davidson (2013, 2015) and Thomas et al. (2012) refute London's undercooling and boundary layer model. The authors propose that Ostwald ripening (the preferential dissolution of small crystals, diffusion and precipitation onto larger crystals in seeking a state of lowest surface energy) better explains the formation of large and giant crystals; also, the formation of irregularly dispersed cloud-like ore bodies of cassiterite or columbite-Ta appears to confirm their hypothesis.

The internal zonation in complex pegmatites might have two causes: i) fractional crystallization in a closed system; or ii) repeated injection of new melt batches in an open system. The worldwide similarity of zoned pegmatites (and many other data), however, rather supports a closed system. The occurrence of nearly monomineralic rocks such as albitites and part of the enrichment of metals can possibly be explained by zone refining; this concept assumes that pore liquids in outer zones consisting of semi-solid crystal mush take up solutes and move inward.

The external zonation of different pegmatites around parent intrusions is attributed to the increasing mobility of more fractionated melts, because increasing fractionation enriches fluxing compounds and elements, which lower solidus temperature, density and viscosity of melts (Černý 1991b). For the separation of pegmatite liquid from granitic crystal mush, for the migration and for the formation of thin veins at great distances, viscosities of 10–100 Pa·s are typical (Thomas & Davidson 2015) – only 10–100 times more viscous than water at 20°C. This explains why ordinary pegmatites occur near the parent intrusion, whereas specialized, complex pegmatites and hydrothermal ore deposits are found at a greater distance (Figs 1.19 and 1.25). The degree of fractionation of pegmatites can be determined by trace element analyses of whole rock samples (Li, Rb, Cs, Ta), or of mica (Cs, Ta, Nb, Zn, Li, U, Be, Ba) and potassium feldspar (Cs, Rb, Na, Ba) (Morteani et al. 2000, Wise 1995). Some pegmatites display fractionation to <0.05% of the parental melt volume (Evensen & London 2002). Hulsbosch et al. (2014) demonstrate that at Gatumba, a Rayleigh fractional crystallization model explains the evolution of Rb, Cs and REE from parental granite to increasingly fractionated and finally Sn-Ta mineralized pegmatites.

The physical derivation of pegmatite melts from parent intrusions is commonly explained by pulses of increasingly specialized and overpressured melt being ejected while the main magma body crystallizes. Thomas & Davidson (2013) demonstrate that minerals of parental granites contain two principal types of melt inclusions (MI): i) "Ordinary" type 1 represents the equilibrium bulk-rock composition of the intrusion, whereas ii) type 2 "anomalous" pegmatite-like MIs have elevated concentrations of water, F, B, P, alkali carbonates and bicarbonates. The chemistry of type 2 MIs provides a clear link to the pegmatites that occur

around the intrusion. The ability of very low viscosity (<1Pa.s) pegmatite-forming melts to percolate large solidifying granite bodies is the key to their efficient scavenging incompatible trace elements. At high temperatures, a supercritical pegmatitic melt/fluid (SCMF) phase dissolves metals in the percent-range and behaves like water or supercritical fluid but is neither (Thomas & Davidson 2016, 2013; Thomas et al. 2012). Not all pegmatites, however, need to be derived from a parental intrusion. At high metamorphic T and P, partial melting may result in pegmatitic melt batches that may fractionate and crystallize nearly *in situ* (Thomas et al. 2018) or rise directly from the source region without involving "parental" granite (Shearer et al. 1992).

Pegmatites host many useful raw materials (Bradley et al. 2017, Sweetapple & Collins 2002, Morteani et al. 2000, Martin & Černý 1992). Magmatic, transitional and hydrothermal metal ores include Be, Li, Rb, Cs, Ta>Nb, U, Th, REE, Mo, Bi, Sn and W, the industrial minerals muscovite, feldspar, kaolin, quartz, spodumene, petalite and fluorite, and gemstones as well as rare mineral specimens (emerald, topaz, tourmaline, ruby, etc.). The derivation of pegmatites from I-, S- and A-type granites or by anatexis from metasediments and the geochemical character of the source rock body is probably the main control of the availability of specific elements for enrichment. Resource assessment of LCT pegmatites is facilitated by the elaborate "model" of Bradley et al. (2017). The feasibility of pegmatite mining is often limited by the small tonnage and heterogeneous distribution of economic minerals. The determination of mining reserves is notoriously difficult. Therefore, extraction of rare metals and minerals from pegmatites is more common in countries with low labour costs; industrial-scale mining is favoured by large-tonnage deposits.

1.1.6 Hydrothermal ore formation

Nearly each of the preceding chapters contained a reference to the role of aqueous fluids, although relations between igneous rocks and ore deposits were the main subject. In the following, aspects of ore formation by hot aqueous fluids and hydrothermal mineral systems (Pirajno 2009) are presented.

Fig. 1.27. Geothermal hot springs and siliceous sinter mound at Sempaya in northwestern Uganda. The convective system is related to the large border fault of the Ruwenzori Mts. with a vertical displacement of more than 10 km between the petroliferous Tertiary Albert Rift in the West and the Paleoproterozoic crystalline horst in the East.

The term "hydrothermal water" applies to subsurface water with a temperature that makes it an agent of geological processes, including hydrothermal ore formation. "Geothermal waters" are a subgroup of hydrothermal solutions that occur near the Earth's surface and are mainly used as an energy source, but also for balneology. Hot springs (Fig. 1.27) are common indicators of geothermal reservoirs at depth. Many hot springs and geysers currently precipite minerals. However, most hydrothermal ore deposits were formed at depth, at temperatures of ~700–50°C and pressures of a few hundred to >3000 bar. In the past, the term hydrothermal was mainly understood to imply condensed magmatic vapours below ca. 400°C, based on observations in volcanic geothermal districts. Meanwhile, isotopic investigations revealed that many geothermal and hydrothermal waters are not of magmatic but of meteoric derivation (i.e. from local precipitation). Similarly, hot water in mud volcanoes of oilfields is not magmatic but formation or connate water (diagenetically altered seawater enclosed in sediments). Many other observations confirm that "hydrothermal water" has no unique but many possible sources.

Much has been learnt by studying natural thermal springs and geothermal water tapped by drilling. Most hot waters are dilute solutions

of chloride, carbonate and sulfate, but dissolved silica, boron and sulfide are also common (Gallup 1998). At high temperatures and pressures, the S_3^- radical is a dominant, thermodynamically stable aqueous sulfur form (Pokrovski & Dubrovinsky 2011). Examples of thoroughly investigated hydrothermal systems include the mid-oceanic black smokers, gold-rich hot waters of deep geothermal boreholes in New Zealand (Simmons & Brown 2007, Simmons & Browne 2000) and base metal-bearing brines of the geothermal field at Salton Sea in Southern California.

Salton Sea is a saline lake in the Colorado River delta of the Imperial Valley graben. It is the latest of several previous lakes that formed and disappeared during dry and wet climate cycles in a transtensional pull-apart basin formed atop the Pacific-North America plate boundary near the transition of the spreading Gulf of California to the San Andreas transform fault zone. The basin fill comprises 5–6 km of Tertiary and Quaternary sediments and basaltic sills. Mud volcanoes and seeps of hot water and gas (CO_2, methane) are widespread (Svenson et al. 2007). Very high heat flow caused by shallow intrusions supports geothermal electricity production in four fields, one of which is Salton Sea. Up to 10 Mm3/month of brine is produced from ~2 km depth with a temperature exceeding 320°C (Brodsky & Lajoie 2013). The fluid is flashed to steam that drives generators. Spent brine (~80%) is re-injected via separate wells into the reservoir. Fluids contain 506 ppm Zn, 95 ppm Pb and 6 ppm Cu, as well as Na, K, Ca, Cl, S and many other elements (McKibben et al. 1990). Total salinity reaches 27 wt. % (weight percent). Zinc is precipitated from the brine after its passage through the turbines; production attains ~30,000 t/year. Isotope data reveal that the geothermal water is of meteoric origin and closely resembles Colorado River water. Apparently, river water infiltrates along faults down into the basin sediments where it is heated and acquires solutes from the rocks. Metal-rich scales in the well casing (Cu, Ag, Au) substantiate the hypothesis that focused upflow of such waters is a way of ore deposit formation.

Fluids in the Rotokawa and Mokai geothermal fields of the Quaternary Taupo Volcanic Zone (TVZ) in New Zealand have exceptionally high contents of precious metals (gold and silver) and of arsenic, antimony and mercury (Simmons & Brown 2006, 2007). Ore deposits, however, have not been found until now, although the Late Miocene epithermal Hauraki goldfield (Mauk et al. 2011) is less than 200 km to the North. The TVZ systems are only used for the production of electric energy. More than 50 drillholes have been sunk to explore and develop the fields, some of them to >2600 m depth. Very few surface signs of the vast geothermal zone had existed before. One famous site is the Ohaaki pool with siliceous sinter and ochreous muds that contain 85 ppm gold, 500 ppm silver and 10 wt. % antimony as well as high trace contents of As, Hg and Tl. This material would be gold ore if the total mass were not so tiny. The geothermal zone is an excellent natural laboratory for investigating hydrothermal ore formation of the epithermal low sulfidation type (Simmons & Browne 2000). Note that high contents of solutes are rather a nuisance for geothermal energy production. The precious metals, for example, precipitate from the ascending fluids because of boiling and gas loss, so that tubes are clogged.

Hydrothermal convection

Hydrothermal convection cells, such as the ones at Salton Sea are established where heat sources below the surface coincide with permeable flow paths, often provided by extensional tectonic deformation (Fig. 1.12). Cold infiltrating surface and groundwater is drawn to the "heat exchanger" at depth. The lower density of hot compared to cold water causes upflow of hydrothermal solutions and establishes hydrothermal convection.

Chemical composition

The chemical composition of hydrothermal solutions is extremely variable. Generally, chlorine and sulfur are the most important anions. Salinity ranges from very low to >50% and its source (e.g. halite dissolution, evaporation of seawater, etc.) can be identified by determination of halogens and electrolytes (Botrell et al. 1988). Metals are to some extent dissolved as simple ions or ion pairs, but more commonly in the form of complex ions that combine chlorine, dissociated OH^- groups and bisulfides, as well as NH_3, H_2S and CO_3^{2-}. The fraction of dissolved matter in hydrothermal solutions varies from less than 1 to over 50 wt. %. Metal concentrations range from <1 to several 1000 ppm (ppm = parts per million, equal

to gram/tonne). Even higher concentrations in solution are possible when metals are part of complex ions. This reduces the mass of water needed to produce an ore deposit compared to transport in the form of simple ions. Hydrothermal solutions transport metals not only in dissolved form but also as colloidal particles. Colloids are tiny particles (1–1000 nm), which are common in many natural waters, usually at low concentrations (Ranville & Schmiermund 1999). High concentrations of dispersed colloids in water are called hydrosols. In many cases, hydrosols are the precursors of gels. Hydrosols and gels may form by local supersaturation of a substance, for example because of a sudden change of pH, T, P or Eh.

Essentially, the chemistry of hydrothermal solutions is the result of interaction between rocks and hot water, in space and time (Barnes 1998). Most important variables controlling these interactions are the initial state of rock and water, the water/rock mass ratio, temperature, chloride concentration, pressure, pH and redox state (Yardley 2005). Sulfur solubility in water, for example, increases by about five orders of magnitude over the hydrothermal temperature range (20° to 500°C); silica solubility rises from 10 ppm to 1%. Geochemical thermodynamic modelling of hydrothermal systems is a tool that provides both a deeper scientific understanding (Moore et al. 2000) and solutions to very practical problems, foremost in geothermal reservoir and production management.

Possible phase states of hydrothermal waters are liquid, gaseous (vapour) and at sufficient pressure, fluid (supercritical "gas" or "liquid"). In fact, many hydrothermal deposits were formed by supercritical fluids. Water reaches its supercritical state at T >374°C and P >220 bar (647 K and 22 MPa). Beyond this critical point, coexisting vapour and liquid of pure water converge to form a fluid. Increasing salinity moves the critical point to higher T and P (Haas 1971), for example, 298 bar and 407°C for seawater. Similar to gas, supercritical fluids are more compressible than subcritical aqueous solutions and have a smaller kinematic viscosity; they are highly mobile (Eckert et al. 1996). At the molecular level, hydrogen bonds greatly decrease with increasing T and P (Sahle et al. 2013). A fluid comprising CO_2 or CH_4 in addition to water has a high carrying capacity for solutes that depends on pressure and density variations. Very small variations cause either dissolution or precipitation of solids. Highly concentrated supercritical fluids have a texture similar to molten salt with polynuclear ion clusters such as $CuNa_2Cl_2^+$ or $FeNa_2Cl_3^+$. These clusters reach the size of megacomplexes with over six constituent ions that can transport metals efficiently at very low concentrations (Oelkers & Helgeson 1993). In contrast to subcritical solutions, which form a gas-rich vapour with low contents of dissolved matter when pressure is released (true boiling), supercritical fluids segregate into a brine and a dense vapour, which is capable of effective metal transport (Pokrovski et al. 2005).

Hydrogen ion activity (pH) of hydrothermal solutions varies from moderately acidic to moderately alkalic. Exceptions occur, of course, and can be recognized by formation of indicative alteration minerals. Acidic conditions, for example, cause formation of kaolinite, alunite or topaz from feldspar. In the Athabasca district, Canada, concentrations of uranium in fluid inclusions are exceptionally high; experiments suggest that this requires pH 2.5 to 4.5 (Richard et al. 2012).

Deep hydrothermal water is normally reduced; oxygen contents may increase near the surface by mixing with fresh meteoric water. Bituminous substances are a common accessory in hydrothermal deposits, e.g. pyrobitumen in the silver veins at Kongsberg, Norway and oil in the Pb-Zn deposit at Pine Point, Canada. This may be evidence that the hydrothermal solutions were sourced in basinal sediments (e.g. diagenetic formation water mixed with hydrocarbon fluids). Present-day examples are submarine seeps of hot solutions in the Guaymas Basin (Gulf of California) that contain big drops of petroleum (1–2 cm diameter); the vents are mainly built of barite. Organic-chemical investigations (of biomarkers etc.) allow a very detailed reconstruction of causative processes, covering both hydrotherms and hydrocarbon genesis (Svenson et al. 2007, Jochum 2000).

Biological processes

Biological processes at depth influence many hydrothermal solutions. Hyperthermophilic

bacteria and archaea are known from hot springs at the Earth's surface to black smoker vents on the ocean floor. With descending branches of convection systems, microbes can be swept deep into crustal rocks. At ~100°C and in the presence of sulfate (from seawater) and organic matter (oil or gas, kerogen) the anaerobes reduce the SO_4 ion to H_2S. This has been observed in oil reservoirs where flooding with seawater was employed in order to boost production. High H_2S contents favour dissolution and transport of a number of metals. At falling temperature, however, H_2S contributes to precipitation of metals.

Precipitation of ore and gangue minerals

Many causes may induce the precipitation of ore and gangue minerals from solutions. Their understanding is an important element of the search for ore. In the first place, decreasing temperature and pressure reduce solubility even in the case of steady-state hydrothermal upflow. The resulting adiabatic (that is, without exchange of heat with wall-rocks) decompression causes a corresponding drop in temperature. Precipitation is a function of the relative stability of metal complexes. Decreasing temperature often results in the common sulfide precipitation sequence from early Cu to Zn, Pb, Ag and finally Hg. Sudden pressure drops may cause fluid immiscibility, i.e. the formation of two fluids (e.g. aqueous and carbonic) from an originally homogeneous fluid (aqueous-carbonic). This can drastically change pH, fO_2 and temperature, thus inducing mineral deposition. Rapid pressure fluctuations are typically caused by tectonic events ("seismic pumping" Sibson 1990). Falling pressure is especially effective if common *boiling* takes place in the two-phase field of liquid plus vapour. *Flashing* is an extreme form of boiling, where most of the hydrothermal fluid is suddenly converted to vapour. Trapped vapour inclusions may be almost empty (of very low density). In epithermal gold deposits, this causes supersaturation and precipitation of colloidal silica gels and metals such as Au, Ag and Cu, Pb and Zn (Bozkaya & Banks 2015). Boiling and flashing change several chemical properties of a hydrothermal solution (concentration, pH, Eh, stability of complex ions), which reduce the solubility of dissolved matter. The term "effervescence" is preferably used in place of "boiling" when gas bubbles form that are not vapour of the host liquid (e.g. carbon dioxide gas bubbles in water). Yet like boiling, effervescence may induce rapid precipitation of minerals.

Relatively simple systems of this type can be investigated in geothermal power plants where production wells are often affected by mineral precipitation on pipe walls. With time, this process diminishes the open diameter of the tubes ("scaling"). Corrosion and the effects of re-injecting cooled and depressurized solutions into the reservoir are equally instructive (Hardardóttir et al. 2010).

Often, mixing of chemically different waters induces deposition of ores and minerals. A common example is the formation of barite. Barite ($BaSO_4$) is precipitated when ascending chloride solutions with dissolved barium ions encounter sulfate-ion bearing water (e.g. seawater). Furthermore, the reaction of hydrothermal solutions with host rocks or with previously deposited ore minerals is a very efficient means of immobilizing dissolved elements. When metal-bearing solutions encounter sulfide minerals, more noble metals are precipitated whereas less noble elements pass into solution (eq. 1.2). This is a function of properties such as electronegativity, ionization potential, electron affinity, redox potential and the energy of chemical bond formation.

Selective precipitation of more noble metals from solution by exchange with less valuable elements:

$$CuFeS_2 + Cu^{2+}{}_{aq} \rightarrow 2CuS + Fe^{2+}{}_{aq} \qquad (1.2)$$

Gold (electronegativity 2.54 Pauling's) is more noble than silver (1.93), which is followed by Cu (1.90) and Fe (1.83), explaining common replacement relations. Note that in physical terms, only copper, silver and gold are noble metals. In chemistry, the electric ionization potential of elements is used to define relative nobility. Host rocks exert a strong control on noble metal enrichment. Silver ore veins at Kongsberg (Norway) were fabulously rich in native silver and argentite (Fig. 1.28) where they crossed pyrite-rich layers ("fahlband") in host rock gneisses (Kotková et al. 2018). At the giant Golden Mile deposit, Kalgoorlie, Western Australia, deposition of gold is explained

Fig. 1.28. Hydrothermal native silver crystals (isometric, malformed) from Kongsberg in Norway. Gangue includes calcite, barite, zeolite, fluorite and quartz. Courtesy Wolfhart Pohl, Washington.

by reaction of sulfide solutions with reduced iron of doleritic host rocks, forming pyrite ("sulfidation"). This triggered a radical decrease of reduced sulfur in the hydrothermal solutions causing the breakdown of sulfide complexes and gold precipitation.

Organic substances (coal, kerogen, oil, gas) also provoke immobilization of many metals by adsorption or reduction. Gold ore veins at Ballarat, Australia, and the metasomatic gold orebodies of Carlin, USA, are enriched where host rocks contain kerogen-rich layers. Part of the carbon associated with gold ore is, however, derived from CO, CO_2 and CH_4 dissolved in the hydrothermal solutions (Hu et al. 2017). Hydrothermal base metal fluids encountering natural gas, especially methane with H_2S, precipitate sulfides (cf. Central African Copper Belt). In Mississippi Valley deposits, for example, sulfide precipitation is often caused by reaction between solutions and the organic substance of host rock carbonates (Spirakis & Heyl 1995). Incompletely oxidized sulfur (e.g. thiosulfate $S_2O_3^{2-}$, polysulfides S_nS^{2-}, or colloidal sulfur S^0) supports high metal contents in solution. These compounds, however, are easily reduced by contact with organic matter so that metals are instantly immobilized as sulfides. An indirect consequence is the precipitation of gangue such as barite and fluorite.

Although reduction is a frequent means of ore mineral deposition, oxidation can have a similar role, often concerning iron and manganese. Hydrothermal solutions transport these metals in reduced form (Fe^{2+}, Mn^{2+}) and precipitation of hematite, magnetite or pyrolusite requires oxidation to Fe^{3+} or Mn^{4+}.

Contact of metal-bearing solutions with carbonate rocks is a frequent factor of precipitation. Individual agents include the "pH-shock" upon contact with alkaline rocks and formation fluids, a larger permeability compared with pelitic country rocks, a higher solubility of carbonates in acidic or CO_2-rich solutions (which may result in the formation of "hydrothermal karst"), and mixing with formation water in carbonate rocks. Orebodies in carbonates take the form of veins, breccia and karst pipes. They can also occur as stratiform orebodies with irregular outlines ("mantos") and as cross-cutting cloudy masses. When the replacing masses consist of sulfides it is obvious that dissolution of the original carbonate rock and replacement ("metasomatism") by ore must have taken place. The same process term is used for cases where only cations are exchanged (e.g. siderite in limestone). Systems of delicately balanced dissolution of one component and precipitation of another are best investigated by geochemical modelling based on thermodynamic principles (Anderson 1996; Bethke 1996).

Source and origin of hydrothermal fluids and solutions

Source and origin of hydrothermal fluids and solutions may be related to different geological process systems:

- Magmatism (exsolution of an aqueous fluid phase from silicate magma);
- heating of meteoric, oceanic or formation water by convection within or near cooling intrusions, in HHP granites and other heat anomalies including rifts, large faults or uplifted hot metamorphic complexes;
- diagenesis (mainly physical dehydration of sediments by increasing pressure (pore space reduction) and temperature because of increasing overburden, thrust sheet superposition, or accretion on active continental margins);
- metamorphism (mainly chemical dehydration of minerals that include OH-groups in their crystal lattice, caused by prograde metamorphic reactions);

- mixing of two or more of the mentioned source systems.

"Juvenile water" is more a concept than reality. The term implies water that originates from degassing of the mantle and has never before been at the Earth's surface. The first statement is undoubted but the second cannot be proven with present scientific methods. Casual usage of the word wrongly implies any magmatic water. Note that "geothermal water" does not refer to a specific origin but to any hot water that occurs near the surface. Usually, the term is employed in the context with production of geothermal energy. "Primordial water" (unchanged since formation of the Earth) may occur in the deep mantle (Hallis et al. 2015) but so far, has no role in economic geology.

Increasingly, hydrothermal systems are studied by coupled thermal (T), hydraulic (H), mechanical (M), and chemical (C) simulation models (THMC models: Ingebritsen & Appold 2012). Application is largely limited to geothermal reservoir engineering and nuclear-waste isolation.

In the Earth's crust, hot aqueous solutions and fluids are ubiquitous (Pirajno 2009, Yardley 2005, Fyfe et al. 1978) and therefore, hydrothermal ore deposits occur in a fascinating diversity. This includes veins (e.g. "orogenic gold"), metasomatic bodies in carbonates, breccia ores in magmatic rocks ("porphyry deposits"), stockworks and pipes, volcanogenic terrestrial and submarine exhalations, stratiform base metal ore beds in marine sediments (sedimentary-exhalative ore) and stratabound diagenetic Pb-Zn-Ba-F deposits in marine carbonates. More detailed information on these deposit types and their formation is provided in later sections. Here, it is essential to introduce first the most important methods that provide data, which constitute essential building blocks of genetic models.

Methods of Genetic Investigations (1)

Isotope geochemistry – the origin of water and minerals, and the age determination of mineral deposits (Geochronology and Thermochronology)

The application of isotope geochemical methods provides powerful tools of metallogenetic research (Hoefs 2018, Dickin 2018, Allègre 2008). Isotope systems indicate the source of water, gas, metals and other compounds in hydrothermal solutions, illuminate reactions between solutions and host rocks (including the important water/rock mass ratio), reveal formation temperatures and expose mixing processes between solutions of different origin (for a useful overview cf. Hurai et al. 2016). In addition, isotope systems are invaluable means of geochronology (age determination) and of thermochronology (the temperature-evolution in time) of hydrothermal, magmatic, metamorphic and supergene ore deposits (Reiners et al. 2017). Isotope geochemistry is an essential element of the quest for a full understanding of genetic processes. Recent advances in microanalysis such as laser ablation-split stream (LASS) analyses permit sub-mineral-scale determination of both isotope compositions (isotope mapping) and trace element contents (Fisher et al. 2017). Too often, however, complex relations still limit full reconstruction of past processes.

Unstable (radioactive) isotopes are distinguished from stable (non-radioactive) isotopes. Radiogenic isotopes or daughter elements (nuclides) originate by radioactive decay of unstable parent elements. Isotopes of an element have an identical electron configuration but different mass. In physical, chemical and biological processes, this causes thermodynamic and kinetic effects. Isotopes of light elements that have a high mass difference display isotope fractionation. A simple example is evaporation: Lighter isotopes preferentially enter the vapour phase because of their higher vibration energy. Mass difference also affects reaction rate and bond strength, inducing fractionation between syngenetic minerals, and between a mineral and its parent solution. Because the fractionation is a function of temperature, several isotope systems (e.g. sulfur, oxygen, silicon) are very sensitive geothermometers, although only if full equilibrium was attained.

Isotopic compositions are measured relative to standard using mass spectrometers. The fractionation of stable isotopes is commonly expressed as the deviation (δ, in ‰, *per mil,* of mass) from a standard (eq. 1.3).

Calculation of isotope fractionation as a deviation from a standard:

$$\delta(‰) = 10^3 \left[(R_{Sample} - R_{Standard}) / R_{Standard} \right] \quad (1.3)$$

R is the ratio of an isotope pair, e.g. $^{18}O/^{16}O$, D/H etc. Negative δ values indicate an enrichment of the light isotope relative to the standard whereas the heavy isotope is enriched if the sign is positive.

Geochronology and thermochronology

Isotope age dating of minerals that originated as a consequence of ore formation processes is based on the time dependence of the production of a stable daughter nuclide (*D*) by radioactive decay of an unstable parent element (*P*). The age expressed in unit "annum" (a, ka, Ma) is calculated by equation 1.4.

Determination of geological ages by radioactive decay:

$$t = 1/\lambda . \ln (1 + D/P) \quad (1.4)$$

Time (*t*) is the date before present when radioactive decay started, *D* is the number of atoms of the daughter element, *P* the number of atoms of the parent element, and lambda (λ) the decay constant of the parent element (λ = 0.693 divided by its half-life). Resulting age data or model ages can only be considered as real ages if the analysed system was closed for both parent and daughter element during the whole time span (Dickin 2018).

Commonly, gangue silicates or alteration minerals including K-feldspar, white mica (muscovite, sericite), biotite, apatite, monazite, rutile, titanite, xenotime and zircon are used for the age determination of hydrothermal ore deposits. Several isotope systems can be studied, e.g. U-He, U-Pb, Pb-Pb, Rb-Sr, Sm-Nd, K-Ar and $^{40}Ar/^{39}Ar$. Ore minerals such as cassiterite, columbite, sphalerite, several sulfides and scheelite can be dated with these systems. U-He, U-Pb, Th-Pb and K-Ar systems, however, are subject to complications by α-recoil that will damage the "container" with time, allowing partial loss of parent and daughter. Moreover, very careful investigations revealed that many isotope systems are impaired by later thermal events or the passage of migrating fluids, even at relatively low temperature (Selby et al. 2002, Kerrich & Cassidy 1994). Also, alteration and ore minerals may not be strictly coeval. Clearly, the geological significance of age data and model ages must always be critically examined. For *thermochronology,* the concept of closure temperatures (T_c) is essential; at falling T, different minerals and isotope systems enclose (or block) the products of radioactive decay at certain temperatures (Tc). This allows the construction of T/t and, with pressure constraints, depth paths. U/Pb or $^{40}Ar/^{39}Ar$ systems, for example, have relatively high closure temperatures (Tc 350–900°C) whereas zircon and apatite (U-Th)/He can reveal the cooling history between 160 and 200°C and 40 to 85°C, respectively (e.g. Wang et al. 2018). The latter helps to understand cooling, denudation and preservation of ore deposits (Fig. 1.29).

The age of most ore minerals (e.g. sulfides, oxides) cannot precisely be determined with the above mentioned methods because they rarely host lithophile elements in their crystal lattice. One alternative is direct dating of sulfide, oxide and gold ore using the chalcophile and highly siderophile element rhenium. The rhenium-osmium method is based on the β-decay of ^{187}Re to ^{187}Os with a half-life of 41.6 Ga. Initially, most studies targeted magmatic sulfide, molybdenite and gold deposits (Morelli et al. 2007, Stein et al. 2001) but many other deposit types can now be dated (e.g. Irish Ag-Pb-Zn: Hnatyshin et al. 2015). Similar to lead

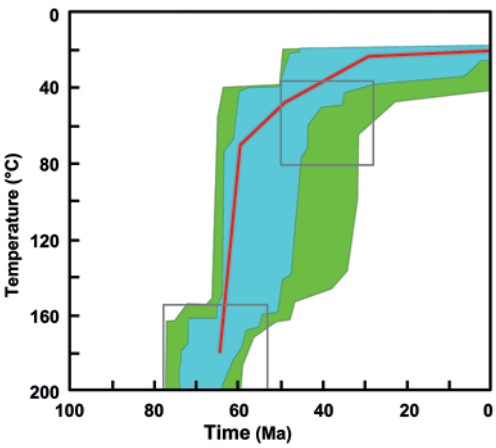

Fig. 1.29. (U-Th)/He thermochronology of Early Cretaceous hydrothermal Wulong gold deposit in the Liaodong Peninsula, NE China. Modified from Wang et al. (2018). Gray squares represent the temperature-time constraints given by zircon and apatite age data. The shaded fields include acceptable evolutionary paths or a higher confidence, and the curve the best-fit evolution. Depth constraints are based on fluid inclusions.

isotopes and other systems, the Re-Os system allows deductions concerning the source of metals apart from dating (e.g. Andean IOCG and IOA deposits in northern Chile: Barra et al. 2017). Also, seawater Re-Os derived from continental weathering, for example, can be distinguished from hydrothermal and cosmic dust sources.

Improvements of the precision of dating techniques, for example by LA-MC-ICPMS and by secondary-ion mass spectrometry (SIMS) and sensitive high-resolution ion microprobes (SHRIMP: Sajeev et al. 2010), allow increasing resolution of ages and with that, reliable measurement of the duration of ore deposit formation. Results show that many hydrothermal ore deposits have been formed in geologically very short time (several thousands to a few ten thousands of years), which is just about the error margin of present methods. Some data imply that other hydrothermal systems may have been surprisingly long-lived (hundred thousand to millions of years).

Stable isotopes of water

Stable isotopes of water, including ^{1}H (hydrogen) and ^{2}H (D, deuterium) as well as ^{16}O and ^{18}O, are exceptionally revealing keys for the comprehension of hydrothermal processes. Average ocean water is employed as a standard (Veizer & Prokoph 2015; SMOW = Standard Mean Ocean Water). Pristine mantle $\delta^{18}O$ varies between 5 and 6‰. During Pleistocene and earlier glacial cycles, $\delta^{18}O_{seawater}$ varied between –0.5 and +1.5‰. The $\delta^{18}O$ of atmospheric oxygen differs from that of the ocean by ~23.5‰. Evaporation of ocean water is the starting point of precipitation/evaporation cycles that produce isotopically "lighter" water vapour (and derived precipitation) as the distance to the sea and to the equator increases. The isotopic composition of precipitation, surface and shallow groundwater forms a band that is termed the meteoric water line (Fig. 1.30). "Meteoric water" is water that has been part of the meteorological cycle of evaporation – condensation – precipitation (excluding seawater). The meteoric water line is in reality a band because of local deviations. Note that "formation water" is not a genetic term but simply designates water of unknown origin and age in sediments; formation waters generally show an increase of $\delta^{18}O$ with increasing burial depth. Brines that form by evaporation from semi-closed marine lagoons are isotopically heavy. Isotope exchange between rocks and ocean or meteoric water produces fluids that retain largely the original hydrogen isotopic composition. Oxygen isotope ratios, however, are considerably altered by partial exchange with oxygen contained in rocks. An equivalent effect is commonly observed in geothermal fields; while the fluids are increasingly enriched in heavy oxygen, the hydrothermally altered rocks are depleted in ^{18}O. The depletion zones allow mapping of fluid passage and can be vectors to ore (Hoefs 2018, Holk et al. 2008).

In the $\delta D/\delta^{18}O$ diagram, waters of magmatic, metamorphic and sedimentary origin occupy partly overlapping fields (Fig. 1.30) so that they cannot always be clearly discerned. Water involved in fossil hydrothermal systems can be sampled from fluid inclusions in minerals, but this is fraught with various limitations

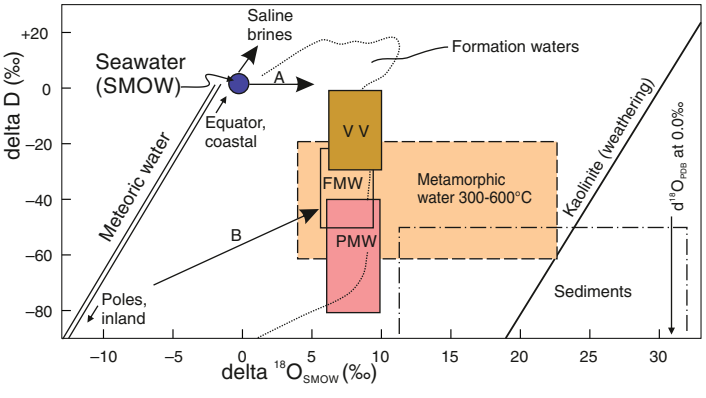

Fig. 1.30. Isotopic composition of waters that participate in hydrothermal ore formation (adapted from Hoefs 2018). With kind permission from Springer Science+Business Media. PMW is primary magmatic water; FMW felsic magmatic water; VV is volcanic vapour. Path A shows evolution of ocean water to formation water. Path B suggests mixing of magmatic with meteoric water.

(Faure 2003). The use of gangue minerals with hydroxyl (OH^-) groups is generally less error-prone. In that case, however, the mineral/fluid fractionation factor must be accounted for. Later isotope exchange with passing fluids (e.g. the common flooding of cooling magmatic bodies and of hydrothermal systems by meteoric and formation waters) needs to be investigated. Ore formation systems involving high pressure fluctuations (e.g. Sibson's "seismic pumping") are characterized by wide variations in D/H fractionation between water and minerals (Horita et al. 1999). This is intensified at conditions above the critical temperature and generally with fluids of very low "gaseous" density (Driesner 1997).

Carbon isotopes

Carbon consists of the stable isotopes ^{12}C and ^{13}C. Because of its short half-life (5730 years), age dating with cosmogenic ^{14}C is limited to geological processes younger than ~50,000 years ago. The ratio $^{14}C/C$ in atmospheric CO_2 ($\Delta^{14}CO_2$) is naturally controlled by CO_2 cycling between atmospheric, oceanic, and terrestrial carbon reservoirs. Common applications in geoscience include dating of organic matter and groundwater, and the reconstruction of solar activity cycles (Solanki & Krivova 2011). Because radiocarbon (^{14}C) content of atmospheric CO_2 varies as a result of nuclear weapons testing and fossil fuel emissions, however, some applications including dating are increasingly compromised (Graven 2015).

The origin of carbonate minerals and rocks is investigated by stable carbon and oxygen isotope fractionation relative to the PDB standard (belemnites found in the Cretaceous Peedee Formation, Carolina, USA). Consequently, marine carbonates have δ_{PDB} values about zero, mantle carbon about –5‰ to –6‰; kerogen between –20 and –30‰. Modern pools of isotopically light organic carbon similar to kerogen include methane hydrates, petroleum and natural gas, soil organic carbon and peat. Deviations of $\delta^{13}C$ in carbonate rocks from PDB illuminate anomalous excursions of the global carbon cycle, for example by large-scale burial of organic carbon or by sudden release of methane from ocean floor gas hydrates (Bijl et al. 2010). Atmospheric $CO_{2(g)}$ displays a $\delta^{13}C$ of –7 to –9‰ and magmatic $CO_{2(g)}$ $\delta^{13}C$ –7 ± 2‰. However, the source signal may be veiled by inorganic isotope fractionation of carbon, which is a function of oxygen partial pressure, temperature, pH, ionic strength and carbon concentration, complicating genetic interpretations. Comparative investigations of the large travertine deposits near Florence (Italy) and warm (29–34°C) springs in the same area that deposit travertine (Guo et al. 1996) provide an instructive example. Recent calcite shows an increase of ^{13}C with higher distance to the spring orifice, due to two factors: i) Simple degassing ($^{12}CO_2$ evaporates preferentially, whereas $^{13}CO_2$ is retained in the solution and collects in the travertine); and ii) bacterial fractionation. Bacteria predominantly abstract ^{12}C from the solution, so that $\delta^{13}C_{Calcite}$ is increased compared to abiotic processes.

Clumped distribution of rare isotopes of cations, C and O in carbonates of Ca, Mg, Fe, etc. allows the determination of the formation temperature. The distribution of clumped carbonate isotopologues in magnesite ($MgCO_3$), for example, comprises $Mg^{13}C^{18}O^{16}O_2$ and $Mg^{12}C^{16}O_3$. The second is the most abundant configuration whereas the first is rare but favoured at lower temperature (Garcia del Real et al. 2016).

Sulfur isotopes

Sulfur isotopes provide genetic information on sulfides and sulfates of ore deposits. Standard is troilite (FeS) from the Cañon Diablo meteorite that is believed to mirror the Earth's mantle with a homogeneous and chondritic composition for $^{34}S/^{32}S$; in fact, however, the mantle is strongly impacted by core differentiation (Labidi et al. 2013). Yet, basalts and other mantle magmas, and sulfide ore deposits derived from them have $\delta^{34}S$ near zero. Deviations are explained by a heterogeneous distribution of sulfur in the mantle, caused by: (i) During the magma ocean stage of the Earth, segregation of about 97% of all sulfur into the core, inducing isotope fractionation; (ii) new chondritic sulfur addition during the Hadean late-veneer phase; and (iii) subduction of sedimentary sulfur and mixing (Labidi et al. 2013). Clearly different is sulfide sulfur produced by organic fractionation with $\delta^{34}S$ from –20 to –30‰ (the so-called "bacteriogenic sulfur"; Canfield & Thamdrup 1994) from sulfate in

seawater and evaporites with +10 to +30‰. The isotopic composition of seawater sulfur is the result of mixing sulfur from several input reservoirs including continental weathering, dissolution of older evaporites and mantle degassing, and by abstraction in pyrite or sulfates (Halevy et al. 2012, Wortmann & Paytan 2012). Magmatic and hydrothermal ore deposits may contain sulfur of mixed origin, veiled by inorganic fractionation. The isotope fractionation between cogenetic sulfide minerals, or sulfides and sulfates can be a useful geothermometer (Zheng 1991). In hydrothermal solutions <250°C, sulfur occurs as sulfate or sulfide. At high temperatures and pressures, >250°C and 0.5 GPa, the S_3^- radical is a dominant, thermodynamically stable aqueous sulfur form (Pokrovski & Dubrovinsky 2011).

Strontium isotopes

Strontium isotopes provide age information as well as evidence of the derivation of ore-forming fluids. The system comprises radiogenic ^{87}Sr, a nuclide from β^- decay of ^{87}Rb (half life 4.75×10^{10} years) and stable ^{86}Sr. It is the base of the widely used Rb/Sr method of age determination. In hydrothermal ore deposits, the ratio $^{87}Sr/^{86}Sr$ is a means of characterizing fluids that formed carbonates (Ca, Mg, Fe), sulfates (Ca, Ba, Sr), fluorite and apatite. Samples used should have extremely small rubidium contents. Rubidium is strongly lithophile, with tenors of ~60 ppm in the crust and 0.06 ppm in depleted mantle (GERM 2018). Therefore, strontium-87 mainly enters the ocean through the breakdown of continental rocks, whereas strontium-86 is sourced from mid-ocean ridges. Consequently, $^{87}Sr/^{86}Sr$ ratios of large source reservoirs such as the Earth's mantle, crust and seawater are different, and display systematic variation in geological time. On that base, analysis of time-dependent processes is possible, especially concerning the Earth's exogenic realm, including oceans, sedimentation and diagenesis (Peters & Gaines 2012, Schreiber & Tabakh 2000). Marine sediments can be readily dated (McArthur et al. 2012) but the method neglects short-time peaks of ^{87}Sr in ocean water that are attributed to submarine brine outflow related to sedex systems (Emsbo 2017). In the Felbertal tungsten deposit, magmatic-hydrothermal and remobilized metamorphic scheelite display clear Sr-isotopic differences (Kozlik et al. 2016).

Lead isotopes

The greatest role of Pb isotopes is in age dating by methods such as U-Pb in zircon using SHRIMP and LA-ICP-MS. Zircon is a "miracle" mineral because of its durability and chemical stability over a wide range of lithospheric pressures, temperatures, and fluid/melt compositions. The closure temperature of zircon is at ~900°C for the U/Pb system, accounting for the widespread use of zircon in high precision thermochronology (e.g. Chelle-Michou et al. 2017, Scoates & Friedman 2008).

Also, lead isotopes are a powerful tool to trace the source of metals in mineral deposits, because their geochemical behaviour in aqueous fluids resembles that of many associated elements (e.g. Zn, Cu, and Ag). Also, traces of lead are ubiquitous in most rocks and in many ore minerals. Terrestrial lead consists of four stable isotopes:

- 1.0–1.6 wt. % ^{204}Pb, primordial (not radiogenic), used as a reference base;
- 20.8–27.4% ^{206}Pb, radiogenic decay product of ^{238}U;
- 17.6–23.6% ^{207}Pb, radiogenic decay product of ^{235}U;
- 51.2–56.2% ^{208}Pb, radiogenic decay product of ^{232}Th.

Due to the minimal mass difference between lead isotopes, fractionation by geological processes is very small. Their inherent useful information rests in formation and mixing of the radiogenic isotopes (Cumming & Richards 1975). Both are controlled by properties of the source rocks, including age, lithology (Chiaradia & Fontboté 2003) and geochemistry (uranium and thorium contents). Uranium concentrations in the source are described by μ-values (the present ratio $^{238}U/^{204}Pb$). Because uranium and thorium are markedly lithophile elements, they are enriched in the continental crust (with high μ) relative to the mantle. The evolution of present-day lead started with the primordial or meteoritic composition ~4550 Ma BP (before present), which is based on troilite of Cañon Diablo meteorite (like sulfur isotopes). Since then, radiogenic lead increased because of uranium and thorium decay in the major geological reservoirs (mantle, lower and upper crust). Without any disturbance, ordinary lead is the result. When ordinary lead is separated from

uranium and thorium, and concentrated in ore deposits (e.g. as galena) its isotopic composition reveals both the age of mineralization and the source reservoir of the lead ("plumbotectonics", Zartman & Doe 1981). This "single stage lead" is derived by single-phase extraction from a very large reservoir, probably continental lower crust or uppermost mantle and is present in a number of large ore deposits (e.g. Mt. Isa, Broken Hill, Australia). Other ore deposits have lead of an anomalous composition, which originated by multi-stage processes. Typically, anomalous lead provides model ages that are different from the geological age (Allègre 2008).

J-type lead: An unusually high radiogenic fraction was found in lead of the Joplin mine (Tri-State mining district, USA). Its source is thought to lie in uraniferous Cambrian sandstones and Precambrian basement rocks that had relatively low contents of ordinary lead. Therefore, the migrating hydrothermal brines took up the easily soluble radiogenic lead from decayed U-Th phases. Lead model ages of galena plot in the geological future, whereas the epigenetic mineralization age is Late Paleozoic (Symons et al. 2005).

Accordingly, lead model ages are very often not "dates" but nevertheless provide constraints on ore genesis. Lead, like rhenium-osmium, lutetium-hafnium and samarium-neodymium isotope systems may indicate the source of magmas or of mineralization, an essential element of genetic models. Lead isotopic maps reveal important metallogenetic features. Parameters used include μ, and the difference between the true age of mineralization and the Cumming & Richards (1975) lead isotope model age of mineralization (Δt). Variations in μ coincide with boundaries at the orogen, subprovince and zone scales (Huston et al. 2017).

Other isotope systems

Many other isotope systems provide deeper insight into ore forming processes. Examples include chlorine (Nahnybida et al. 2009), nitrogen (Jia et al. 2003), iron (Mendes et al. 2017), mercury (Xu et al. 2018) and boron (Fig. 1.31). Based on tenors of Th and U in trace concentrations, and reaching back to several hundreds of thousands of years, the age of calcite precipitates (e.g. in caves) is determined with the uranium-series disequilibrium method. From very small samples, $^{230}Th/^{238}U$ and $^{234}U/^{238}U$ activity ratios provide precise ages (Reich et al. 2009). Traces of noble gases such as $^{3}He/^{4}He$, $^{40}Ar/^{36}Ar$, ^{84}Kr and ^{130}Xe are determined to constrain the source of fluids; the atmosphere, meteoric fluids and seawater, for example, display $^{40}Ar/^{36}Ar$ ratios of ~296 whereas values over 10,000 mark ancient basement and

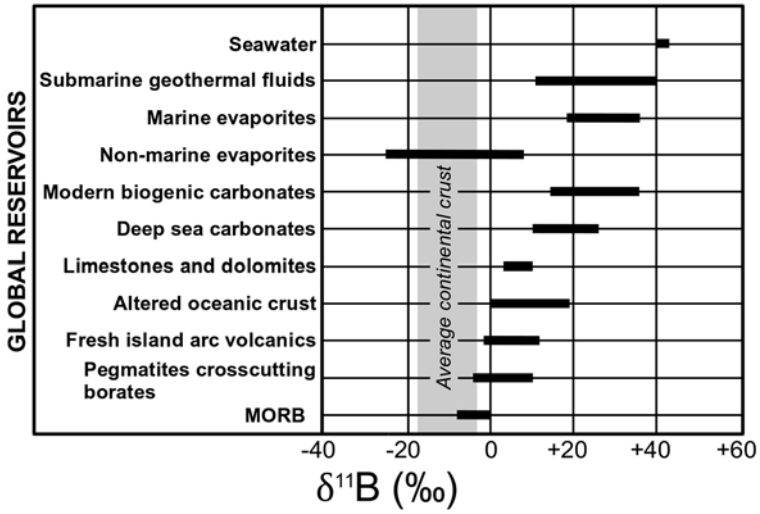

Fig. 1.31. Boron isotopes are sensitive indicators of the source of boron in fluids, minerals and rocks. The diagram shows characteristic $\delta^{11}B$ values of major global reservoirs (adapted from Ranta et al. 2017).

mantle fluids (Fairmaid et al. 2012). Subrecent geological processes (younger than ~20 Ma) such as the age of supergene ore deposits are investigated with cosmogenic nuclides (e.g. ^{10}Be, ^{14}C, ^{26}Al, ^{36}Cl and ^{129}I; Blanckenburg & Willenbrink 2014, Reich et al. 2013, Siame et al. 2006). Typically, results reveal extraordinarily long durations of supergene processes, although hardly at constant rates. Cosmogenic nuclides are formed by the interaction of cosmic rays produced by stellar explosions, with the Earth's atmosphere and its surface. Because the Sun's activity modulates the incidence of cosmic rays, the abundance of these nuclides can also be interpreted as a chronicle of solar activity.

Methods of Genetic Investigations (2)

Energy in hydrothermal ore formation: Temperature and pressure

Apart from geochemical parameters, temperature and pressure of a hydrothermal system are essential physical determinants of its workings. P and T being correlated variables, a third independent measure of either needs to be established (Hurai et al. 2015), such as conventional petrologic geothermometers and geobarometers (Bucher & Grapes 2011, Philpotts & Ague 2009). Investigations of fluid and melt inclusions in minerals are used to calculate P-V-T-X parameters of former fluid systems (Bakker 2012). In magma-related or high-grade metamorphic systems, melt inclusions (MI) preserve the chemical composition of the parental or partial melt, including volatiles and metals. Investigating MIs comprises the determination of minerals and other phases, remelting and homogenization, quenching and analyzing the bulk melt-fluid system (R. Thomas in Hurai et al. 2015).

Frequently employed "geothermometers" of economic geology include:

- Microthermometry of fluid inclusions in minerals;
- cation-exchange geothermometers, indicating the temperature of the last equilibration of fluids with host rocks (e.g. silica: Fournier & Potter 1982; magnesium-lithium: Kharaka & Mariner 1990);
- trace element geothermometers (e.g. Ti-in-zircon for very high temperatures: Watson et al. 2006);
- Titanium-in-quartz thermobarometry (Ackerson 2018);
- different modifications of minerals (e.g. α- versus β-quartz at 573–600°C)
- exsolution or unmixing of phases during cooling (e.g. cubanite lamellae in chalcopyrite that formed >205°C);
- oxygen, silicon, carbon and sulfur isotope fractionation in cogenetic minerals, fluids and gas (stable isotope geothermometry; for a useful overview cf. Hurai et al. 2016);
- the distribution of clumped isotopes (in carbonates: Garcia del Real et al. 2016);
- the distribution of certain elements in cogenetic minerals (e.g. Fe-Zn-S or Au-Ag-S systems; As-contents in arsenopyrite, or Se concentrations in pyrite (Keith et al. 2017);
- chlorite and muscovite mineral geothermometers.

All of the above mentioned geological thermometers are inaccurate due to factors that cannot be precisely determined. It is best practice in economic geology to combine several methods, for example microthermometry of fluid inclusions (Hurai et al. 2016, Roedder 1984, Samson et al. 2003), the arsenopyrite geothermometer (Kretschmar & Scott 1976), and the fractionation of stable isotopes.

Fluid inclusions

Petrographic investigation of fluid inclusions is indispensable (Kerkhof & Hein 2001). Fluid inclusions are commonly very small (below 100 μm) and work is carried out on polished thin or thick sections using a microscope. During formation of minerals from fluids or solutions, irregularities on growth planes often cause inclusion of tiny droplets of the parent liquid *(primary inclusions)*. Quite common are also inclusions that are hosted by microfractures in a mineral *(secondary inclusions)*. At room temperature, many inclusions contain an aqueous liquid with a gas bubble that occupies ~10–40% of the volume (type 1 of Fig. 1.32). Upon heating the sample, the bubble disappears at a determinate temperature that is described as the *homogenization temperature Th*. In the simplest case, T_h is equal to the *formation, or trapping temperature* T_t because the bubble results from cooling and shrinking of the hot inclusion within a volume fixed by the surrounding host mineral. However, T_h is only the minimum temperature of trapping since pressure at the time of formation controls size and density

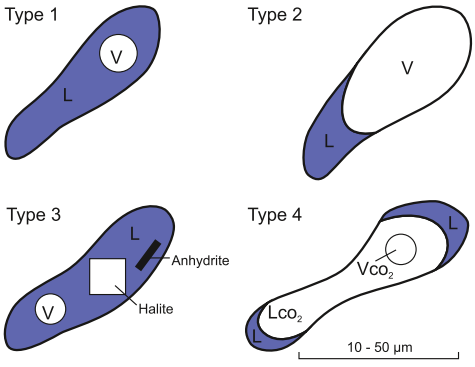

Fig. 1.32. The four most common types of fluid inclusions as they appear under the microscope at room temperature. Note that the term 'liquid' in FI research does not denote liquid melt but the liquid state of a solution or fluid.

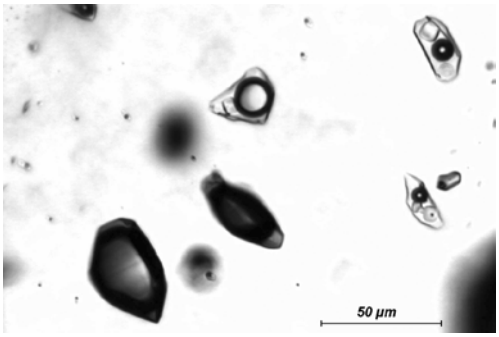

Fig. 1.33. Fluid inclusion assemblage (FIA) formed by subcritical boiling in quartz from miarolic cavities in the barren Torres del Paine granite (Patagonia, Chile). Vapour (dark) concentrated Cu and As, whereas the brine inclusions marked by halite crystals are enriched in metals such as Mn, Fe and Zn (Lüders et al. 2005). Courtesy Volker Lüders, GFZ Potsdam.

of the bubble. An accurate determination of the formation temperature is only possible if the formation pressure is known and the so-called pressure correction can be calculated (actually, this is a correction of temperature as a function of pressure: Roedder 1984). The *density of the inclusion,* its *degree of fill* (liquid versus total volume), the *salinity* of the liquid (mostly due to dissolved NaCl, but Mg, Ca, K etc. may be involved), the presence of *daughter crystals* (common are halite cubes: type 3 in Fig. 1.32), of fluid hydrocarbons and contents of non-aqueous gases (frequently CO_2, followed by CH_4, N_2 etc.) are all needed for a full understanding (Hurai et al. 2015). Isochore T-P diagrams (lines of equal volume and density) assist in fixing T and P (using appropriate software). Investigations must also address the identification of groups of associated inclusions that were trapped from a fluid of the same composition at the same time, temperature and pressure (a "fluid inclusion assemblage" or FIA). Natural minerals typically contain many different FIAs that reveal the evolution of a hydrothermal system.

Most fluid inclusions observed in hydrothermal ore deposits belong to one of four groups (Fig. 1.32):

Type 1: Liquid (L) aqueous inclusions of low to moderate salinity (<26.5 wt. % NaCl that marks saturation at room temperature), a water vapour bubble (V) and a density of ~1 g/cm^3;

Type 2: Water vapour occupies more than 60 % of the inclusion volume, the salinity is similar to type 1; the density is clearly <1 g/cm^3; if types 1 and 2 (or 2 and 3) are cogenetic in the same sample, true boiling (as opposed to effervescence of a dissolved gas like carbon dioxide or methane in water) of the solution below the critical point or at boiling curve conditions is indicated; this gives rise to the term "boiling assemblage" (Fig. 1.33);

Type 3: Highly saline (26.4 to over 50 wt. % salinity) aqueous inclusions with halite daughter crystals and with a high density; fluids of this nature can result from dissolution of evaporites, seawater evaporation, by segregation of brines from melt at magmatic temperatures (supercritical phase separation: Audétat et al. 2008), or by formation of residual brines because of vigorous subcritical boiling (abstraction of vapour causes concentration of salt in the liquid phase: Fig. 1.33);

Type 4: CO_2-rich inclusions, with little water; at room temperature carbon dioxide in the inclusions occurs in both liquid (L_{CO2}) and gaseous phase (V_{CO2}).

Very hot, hypersaline, supercritical magmatic liquids (± vapour) may evolve along path I (Fig. 1.34). Above the phase boundary A, cogenetic type 2 and type 3 fluid inclusions segregate. Path II illustrates the fate of late, less saline and much cooler fluids. Part of these may be derived from vapour that, because of cooling, contracts at higher pressure into the liquid

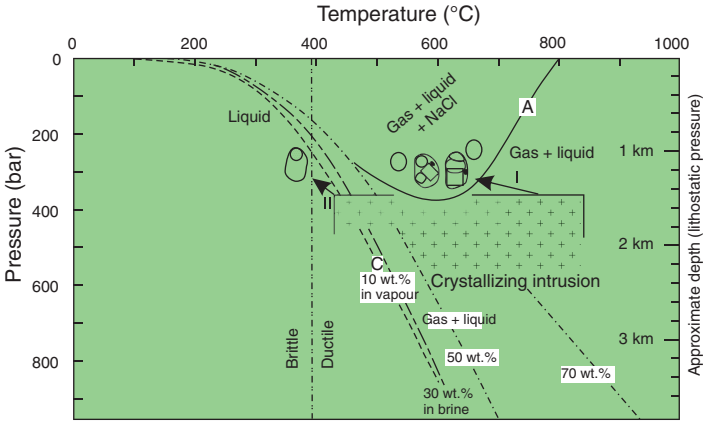

Fig. 1.34. A crystallizing shallow porphyry Cu-Mo-Au intrusion may exsolve (I) early and very hot brines, or (II) later saline fluids of intermediate temperature, resulting in characteristic fluid inclusions (after Brathwaite et al. 2001). With kind permission from Springer Science+Business Media.

phase. Inclusions trapping these fluids are type 1 with low to intermediate salinity (3–20 wt. % NaCl). Phase boundaries between liquid and gas+liquid are shown for different salt contents. Boiling assemblages must have formed at a point along such a phase boundary. C is the critical point for an aqueous solution with 10 wt. % NaCl.

The salinity of 26.4 wt. % separating type 1 and type 3 inclusions is the solubility of NaCl in water at room temperature (20°C). In practice, the presence of other salts such as $CaCl_2$ lowers the NaCl saturation to ~23 wt. %. The salinity of fluid inclusions is determined by freezing with liquid nitrogen and remelting, i.e. the temperature is allowed to rise back to ambient conditions. Because dissolved salts depress the freezing point (Bodnar 1993, Potter et al. 1978), the melting temperature of ice (T_m ice) provides a precise measure of salinity. Results are expressed in the form of equivalent weight percent of NaCl (wt. % NaCl equiv.). The chemical determination of the composition of inclusions is complicated by the tiny mass of individuals. Yet, a number of methods are available; most advanced is the approach with laser ablation (LA) connected to ICP-MS (Sylvester 2008, Audétat et al. 1998). Traces of noble gases such as ^{40}Ar, ^{36}Ar, ^{84}Kr and ^{130}Xe that characterize different Earth reservoirs are measured to constrain the source of fluids (Fairmaid et al. 2012). Merging the data with results from high-resolution investigations of the hydrothermal paragenesis (e.g. SEM-CL, Scanning Electron Microscope-Cathodoluminescence: Rusk & Reed 2002) allows a detailed

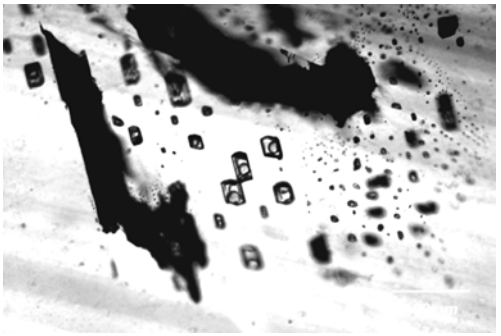

Fig. 1.35. Aqueous fluid inclusions in wolframite of Panasqueira mine, Portugal, studied by near-infrared microscopy. The fluids homogenize between 320 and 325°C and have a salinity of ~12% NaCl (Lüders 1996). Note the large vapour bubbles in inclusions that resemble type 2 of Fig. 1.32. Courtesy Volker Lüders, GFZ Potsdam.

unravelling of the chemical and physical evolution of a hydrothermal system.

The investigation of fluid inclusions is somewhat restricted by the need for samples that are transparent to visible light, thus excluding most ore minerals. Of the opaque oxides, sulfides and sulfosalts, only few such as wolframite, iron-rich sphalerite, and antimonite are transparent for infrared light and can be examined with the methods described above (Lüders 2017; Fig. 1.35). The result is that most fluid inclusion investigations are based on gangue and not on ore minerals. This may introduce severe errors (Wilkinson et al. 2009), e.g. if ore and gangue formed from differing fluids. Different

host minerals affect inclusions, for example by precipitating optically undetectable minerals; especially problematic are carbonate minerals (McKibben 2009) that, however, yield formation temperatures to clumped isotope thermometry (Garcia del Real et al. 2016).

Post-formation changes of inclusions during uplift and cooling, or by renewed equilibration at different P/T-conditions are problematic. Metamorphic shearing and recrystallization often destroy fluid inclusions. Even synmetamorphic inclusions in mobilizates are often decrepitated because of pressure release during uplift (e.g. Joma Mine, Norway: Giles & Marshall 1994). However, in spite of many obstacles, petrographic and microthermometric work on fluid inclusions brought great advances in understanding hydrothermal ore deposit formation. Even eminently practical questions can be solved, such as the differentiation between mineralized and barren veins.

Traditionally, hydrothermal ore deposits were grouped according to assumed formation temperatures into hypo- or katathermal (500–300°C), mesothermal (300–200°C) and epithermal (below 200°C). This classification was quietly abandoned, while a wealth of data has been acquired on real temperatures of hydrothermal processes and resulting deposits. Temperatures vary widely, even during the lifetime of one single hydrothermal system. Accordingly, temperature is a poor criterion for classification, although, of course, an integral part of the genetic description of mineral deposits. In many scientific reports, the terms named above are still used in a very wide sense, indicating rather depth than temperature. In this usage, epithermal deposits are those formed in the shallow crust and below 300°C. "Meso- and hypothermal" describe increasing depth and temperature. However, depth and temperature are not always correlated. Fluids in shallow porphyry copper deposits, for example, may originally have had temperatures approaching 800°C (Fig. 1.34). From the volcanic iron ore at El Laco, Chile, Tornos et al. (2017) report hydrothermal T reaching 900°C. Clearly, depth (or pressure) is a much more useful criterion to describe related groups of hydrothermal deposits. Therefore, Gebre-Mariam et al. (1995) suggested to adopt the terms "epi-, meso- and hypozonal" (Table 1.3), similar to the notations referring to metamorphism or the intrusion depth of granites. The proposal could be advantageously used for all hydrothermal mineral deposits.

Table 1.3 Depth-zone classification of hydrothermal mineral deposits.

Epizonal	150–300°C	0.5–1.5 kbar	<6 km depth
Mesozonal	300–475°C	1.5–3.5 kbar	6–12 km
Hypozonal	475 to >700°C	3–6 kbar	>12 km

Temperature is not a classification criterion. T-values given here apply to epigenetic Archean gold deposits only (Gebre-Mariam et al. 1995).

Formation pressures

Rarely, formation pressures of hydrothermal ore deposits can be precisely measured. Usually, geological estimates are derived from the assumed depth of formation and lithostatic or hydrostatic boundary conditions. Also useful can be modern methods of metamorphic petrology in combination with fluid inclusions data (Philpotts & Ague 2009). Isochores of fluid inclusions (lines of constant volume and density in P-T space) can be intersected with independent data such as the solidus temperature of a parental granite (Ackerson 2018, Audétat et al. 2008). Some fluid systems allow pressure analysis based on experimental data of thermodynamic properties of synthetic fluids similar to natural inclusions; simple systems such as H_2O-NaCl provide a good approximation, but high vapour and gas contents cause large error margins. Unambiguous evidence of boiling still provides the most accurate geobarometry and depth data available (Cruz-Pérez et al. 2015, Roedder 1984).

Methods of Genetic Investigations (3)

Mineral succession, textures and structures of hydrothermal mineral deposits: Paragenesis and paragenetic sequence

The precipitation of minerals from hydrothermal solution is controlled by various boundary conditions, some of which have been discussed earlier. For a reconstruction of the conditions at a point in time and for the whole duration of hydrothermal activity, a *mineral assemblage* formed simultaneously

(a *parageneses)* must be strictly discerned from the sequential order of mineral assemblages (the *paragenetic sequence*). Macroscopic observations of mine exposures and hand specimen, ore microscopy and other mineralogical techniques are combined to resolve the evolution of mineral precipitation through the life of a mineral system.

Because most ore minerals are opaque, microscopic examination is based on polished specimen and reflected light. This allows resolution of the intergrowth of different minerals. The position of minerals in one paragenesis or in the whole paragenetic sequence is revealed by observations that include exsolution, replacement along grain boundaries or microfractures and many other textures and structures. Ore microscopy has attained a level of very high perfection (Craig & Vaughan 1994, Ineson 1989, Ramdohr 1980, Stanton 1972). Methods such as electron probe microanalysis (EPMA), transmission electron microscopy (TEM), scanning electron microscopy – cathodoluminescence (SEM-CL) and other novel methods of mineralogical analysis (e.g. QEM-SCAN, CSIRO, Australia) confirm and refine optical determination. Even greater resolving power is available with one-hundred-nm-resolution secondary ionizing mass spectrometry (nanoSIMS; e.g. Barker et al. 2009).

Macroscopic features that assist in establishing the mineral succession include overgrowths and crusts, symmetric vein fillings and cross-cutting relations of veins. This is supplemented by colour, texture type and grain form or crystal habit of minerals, and by examination of fluorescence and luminescence. Because quartz is an important part of most hydrothermal parageneses, recording its structures and textures is most instructive (Dong et al. 1995). Combined with results of microthermometry, trace and isotope geochemistry and geological investigations, the evolution of an individual hydrothermal ore deposit can be resolved.

Open space filling is a characteristic feature of many hydrothermal ore deposits. The term implies that precipitation of minerals occurred in open fissures, pipes or caves, which acted as flow channels for hydrothermal solutions. Open space filling starts with nucleation of minerals on a solid surface of the channel walls. As the vein walls are receding because of tensional strain, the often observed younging of the mineral succession proceeds towards the centre. In Figure 1.36, different parageneses of a specific phase of vein formation can be read vertically, whereas the horizontal axis reflects evolution in time (from left to right; euhedral crystals in the open space on the right represent the youngest hydrothermal minerals and the vein's symmetry axis). Banding of hydrothermal precipitates results from variations of physical and chemical conditions in time. Tectonic movements during hydrothermal activity cause fracturing of earlier minerals and

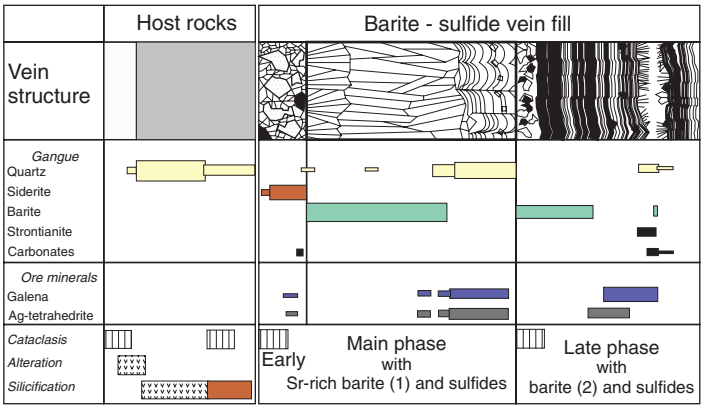

Fig. 1.36. Parageneses and paragenetic sequence of Tertiary rift-related lead-silver-barite veins in the Caroline mine, near Freiburg, Germany (modified from Germann et al. 1994). With kind permission of R. Lang and LGRB Freiburg.

cementation by younger precipitates. Fibrous texture of minerals such as quartz aligned vertically or obliquely to vein margins indicates synchronized opening and mineral growth. In near-surface hydrothermal channels, clastic sediments have been observed that indicate high flow velocity of solutions. Hydrothermal sediments formed in this way include bedded rock flour, clay, sand, solid hydrothermal precipitates and even gravel (pebble dykes). Mainly epizonal features include hydrothermal breccias that may host fabulous orebodies. Many breccias were formed by self-sealing of flow paths and consequent phreatic explosions.

Sedimentary textures of material filling open spaces of hydrothermal veins are not rare. This occurs when solid material is eroded, or when minerals and colloidal particles nucleate in suspension from ascending fluid. Sedimentation of these particles depends on the ratio of the upflow speed of the fluid to gravitational settling of the particles. Stoke's law can be used to calculate the settling velocity (V) of the particles allowing an estimate of the fluids' upflow velocity (eq. 1.5). Suspended minerals nucleating and growing in fluids settle to produce "blocky" vein textures (Okamoto & Tsuchiya 2009).

Settling velocity of particles in a fluid:

$$V = \frac{1}{18} \cdot \frac{(\sigma - \rho)g.D^2}{\mu} \qquad (1.5)$$

V = free-falling velocity (m/s), σ = density of the particle, ρ = density of the fluid, D = particle diameter (m), g = acceleration due to gravity (m/s^2), μ = viscosity of the fluid (m^2/s).

Often, hydrothermal open space deposits are coarsely crystalline. In other deposits, minerals may occur in dense, reniform-botryoidal and banded crusts, in cases with fissures due to shrinkage. Such textures are described as "colloform" and are thought to imply formation from a gel (a hydrosol with a mechanical resistance). These precipitates are amorphous and may gradually mature into phases such as opal, wood tin and garnierite, or crystalline minerals such as chalcedony, reniform sphalerite and malachite. Often, but not necessarily always, the origin of colloform substances may be traced to colloids forming in supersaturated hydrothermal fluids. Sudden supersaturation is induced by boiling or effervescence (Bozkaya & Banks 2015). Coagulated colloids may be are transported with the hydrothermal flow and deposited higher up as a gel. Colloidal particles in water typically have a free negative charge, which leads to electrostatic repulsion and dissipation (Ranville & Schmiermund 1999). While the formation of aggregates may be due to van der Waals forces, neutralization of the charge (by mixing with an electrolyte, pH-change, cooling, etc.) frequently effects aggregation and precipitation as a gel. Some hydrosols form "colloidal crystals" or dendritic structures. Apart from colloids, hydrosols and gels, botryoidal textures may be inherited from microbial mats (Labrenz et al. 2000). Obviously, different ways may lead to formation of a colloform mineralization.

The characteristic banding of many colloform precipitates may be due to external factors, but also to self-organization. Heany & Davis (1995) propose that the banding of agate, which is a rhythmic succession of chalcedony and quartz, is the product of a changing degree of polymerization of the solution at the tips of the growing chalcedony fibres. Polymerization decreases when chalcedony is rapidly deposited, so that the system flips to slow quartz precipitation from a monomeric solution. In this phase, diffusion slowly raises the concentration of the solution until the state of a concentrated polymeric solution is again reached. Colloform SiO_2 can also form from "silicothermal fluids" (Prokofiev et al. 2017, Wilkinson et al. 1996). These are liquids with ~90% SiO_2 that coexist with an aqueous supercritical fluid in a wide temperature field (~400 to >750°C). Silicothermal fluids might be the explanation of the high frequency of amorphous silica phases in epizonal and especially in epithermal ore deposits.

Replacement of earlier solid phases is very common in hydrothermal ore deposits. As one mineral is dissolved, another forms in the same place, often without a change of volume and with conservation of very fine textures (pseudomorphism). Characteristic examples include cassiterite replacing orthoclase (Cornwall, England) or even crinoids (New South Wales, Australia), scheelite after wolframite, and from low-temperature solutions, the silicification and pyritization of entire tree trunks in coal seams. The term "replacement,

or metasomatic ore deposit" is only used if the process produced ore bodies. Carbonates are frequently the subject of replacement because of their chemical reactivity. Advection and evacuation of matter is usually enacted by physical flow but diffusion can also play a role.

The waning stages of hydrothermal systems typically display falling temperature, lower mass flow, pervasive fracturing and cataclasis, and often infiltration of oxidizing meteoric water. This leaves fractures and thin fissures of the hydrothermal vein mass covered by films of goethite, hematite or manganese oxides.

Methods of Genetic Investigations (4)

Hydrothermal host rock alteration: Vectors to ore

Host rocks influence hydrothermal solutions to the point of controlling the site of ore precipitation, but at the same time they are affected by alterations that emanate from the solutions. The resulting changes ("hydrothermal alteration") may extend from only centimetres off the flow channel (Fig. 1.37) to very wide halos in the case of pervasive flow, which may be controlled by rock type (Perrouty et al. 2019). In petrogenetic terms, the latter case may be rightfully called metamorphism and the host rocks would be called 'metamorphic' (cf. ocean floor metamorphism). Fluids and solutes from the metamorphosed host rocks may be essential for ore formation as evidenced by Fe at Panasqueira; the process system comprises magmatic-hydrothermal and metamorphogenic features. The case demonstrates the potential of mixed genetic components in metallogenesis.

Alteration zones are important clues for ore deposit exploration (Lentz 1994). Some alteration halos can be mapped by remote sensing from space. Hydrothermally altered rocks are often so fine-grained that even the microscope may not suffice in revealing the constituent minerals. Portable SWIR (short-wave infrared) spectrometers are routinely used to determine alteration parageneses. Novel tools are spectrometric sensors mounted on drones that can map alteration in pits or natural outcrops (Kruse et al. 2012).

Induced changes concern colour, texture, mineralogical and chemical composition including stable isotopic ratios in different combinations. The end product is a function of the fluid/rock ratio, the nature of both the solutions (pH, Eh, T, P, chemistry) and of the affected rocks (mineralogy, permeability, porosity). Ion

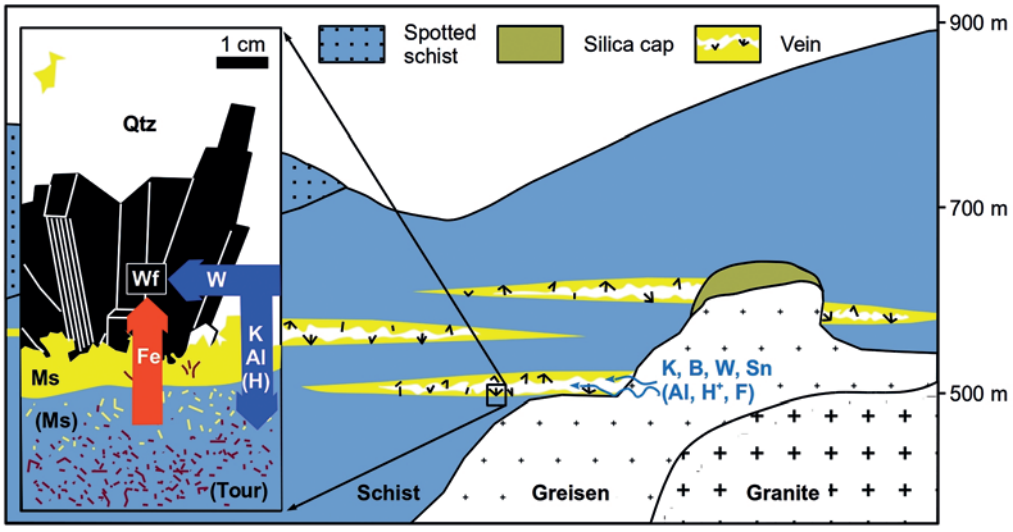

Fig. 1.37 (Plate 1.37). Fluid-rock reactions leading to wolframite ($FeWO_4$) precipitation at Panasqueira (Portugal). Magmatic-hydrothermal fluids delivered K, B, W, and Sn (Al, H^+, F) whereas Fe was leached from the host schists (Lecumberri-Sanchez et al. 2017). Wf – wolframite, Ms – muscovite, Tour – tourmaline, Qtz – quartz. Note that the geological section is simplified.

exchange is ubiquitous, implicating an open system with import and export of matter (e.g. Anthony & Titley 1994). Dissociated water plays an eminent role because of reactions with silicate minerals that include incorporation of OH^- groups and exchange of cations with H^+ (hydrolysis). Frequently, altered rocks display a zebra-like pattern of rhythmic banding that is caused by coupling of diffusion with precipitation reactions (Kapral & Showater 1995). Hydrothermal alterations also affect mass and volume of the altered body, with a positive or negative balance. Calculation of the balance relies on assumed immobility of specific elements (e.g. zirconium, titanium). By comparison of concentrations in unaltered rock and in its altered equivalent, enrichment or dilution can be calculated (cf. 'metasomatism').

In many cases, hydrothermal solutions are weakly acidic because of F or CO_2 contents and dissociation of water. In that case, carbonates, zeolites, feldspathoids and calcium-rich plagioclase are especially prone to alteration. Pyroxene, amphibole and biotite are somewhat more stable, whereas albite, K-feldspar and muscovite are relatively resistant. Quartz is rarely affected.

Alteration of pervaded rocks before the solutions reach the site of ore formation may extract trace metals that can be concentrated in the ore. It is possible that ore deposits are a product of this process (e.g. cassiterite ore produced from aqueous solutions that have passed through tin granite bodies: Lehmann 1990). Examples of trace elements that are incorporated in minerals include copper and zinc in biotite, amphibole, pyroxene and magnetite, lead in K-feldspar and accessory uranium minerals, tin in mica and ilmenite, tungsten in biotite, fluorine in amphibole and mica, and barium in mica and feldspar. Based on appropriate data, genetic ore formation models consider such relations.

Not only ascending hypogene hydrothermal solutions may cause host rock alteration. Some alterations are the product of downward-percolating waters. Examples include solutions formed from magmatic-derived HCl, HF, H_2S and SO_2 steam condensating into, and heating shallow groundwater. Resulting strong acids cause acid-sulfate alteration characterized by alunite (eq. 1.6), typically in near-surface epithermal gold ore-forming systems (Mutlu et al. 2005).

Alunite formation under extremely acidic hydrothermal conditions:

$$\underset{\text{K-feldspar}}{KAlSi_3O_8} + 2Al^{+3} + 2H_2SO_4 + 4H_2O \rightarrow \underset{\text{Alunite}}{KAl_3(SO_4)_2(OH)_6} + 3SiO_2 + 6H^+ \quad (1.6)$$

Hydrothermal host rock alterations include the less visible change of increased maturation of dispersed organic matter (kerogen) under the influence of heat imported by the solutions (Bertrand et al. 1998). Along flow paths and around orebodies, the induced thermal anomaly can be mapped by appropriate methods, for example by measuring the increased reflectance of organic particles (cf. 6.3 "The Coalification Process").

Spatial zonation of alteration types has an outstanding role in ore deposit investigations. Alteration zoning illustrates changing chemistry of the solutions by reactions with wall rocks, and different physico-chemical boundary conditions (temperature, pressure, etc.). Zoning is an extremely useful guide and spatial vector pointing to ore as this is always connected with a certain type of alteration. Zonation is best illustrated by the alteration shells associated with porphyry copper ore deposits (Halley et al. 2015).

There are many different hydrothermal alteration types (Thompson & Thompson 1997). Some characterize certain ore deposits, others are linked to the presence of specific rocks. Propylitization, for example, typically affects andesite and diorite, listwaenitization ultramafic rocks and dolomitization limestone. The names given to alteration types are mainly derived from the most noticeable newly formed mineral, but some have their own traditional rock names (e.g. greisen, propylite). Important examples of hydrothermal wall rock alteration include:

- *Silicification* is the permeation of country rocks with dissolved silica, resulting in increased contents of opal, chalcedony or quartz. The rocks often obtain the aspect of quartzites. Silicification is very frequent around epithermal gold deposits.
- *Albitization* (or sodic alteration) often affects magmatic rocks by replacing more calcic with sodic plagioclase, but albite (± chlorite, epidote, etc.) may be introduced into most rock types. The source of the sodium can be seawater, evap-

orative brines, or dissolution of salt bodies and transport by basinal or metamorphic brines. Also, sodium is enriched in some liquids and fluids segregating at high temperatures from crystallizing magmas.

- *Argillic alteration* is the conversion of rock-forming silicates into clay minerals. Two variants are distinguished, advanced and intermediate argillization. In the first case, the core of the altered rock body typically consists of alunite and quartz, and is surrounded by argillic zone minerals nacrite, dickite, kaolinite and pyrophyllite with variable contents of sericite, pyrite, tourmaline and topaz. The agents are strong acids that impose a nearly total loss of alkali elements and aluminium enrichment. Advanced argillization is often found with gold or tin mineralization. Intermediate argillization is marked by conversion of feldspars to kaolinite (proximal to main flow channels) or montmorillonite (in a distal position). Extending into the distance, a propylitization halo is often developed.
- *Propylitization* may affect large rock masses in the wider vicinity of ore deposits, by imparting a greenish tinge. It is a complex alteration with neoformation of chlorite, epidote, albite and carbonates (calcite, dolomite, ankerite) that was first observed in diorite and andesite near gold deposits. If one of those minerals prevails, terms like chloritization can be applied and mapped as subzones.
- *Sericitization (muscovitization)* is a common alteration of aluminium-rich felsic rocks (granite, gneiss, schists). Fine-grained hydrothermal sericite is either muscovite (formed at higher T) or illite (formed at lower T, typically <300°C). The resulting paragenesis comprises sericite and quartz (± pyrite). The involved solutions were acidic and leached part of iron or alkali element contents (Ca, Na and part of K; eq. 1.7).

Sericitization of K-feldspar:

$$\underset{\text{K-feldspar}}{3KAlSi_3O_8} + 2\,H^+ \Rightarrow \underset{\text{Sericite}}{KAl_2(AlSi_3O_{10})(OH,F)_2} + 2K^+ + 6SiO_2 \quad (1.7a)$$

Sericitization of biotite:

$$\underset{\text{Biotite}}{K\left(Fe^{2+}\right)_3[AlSi_3O_{10})(OH,F)_2} + 2Al^{3+} \Rightarrow 3Fe^{2+} + \underset{\text{Sericite}}{KAl_2(AlSi_3O_{10})(OH,F)_2} \quad (1.7b)$$

- *Greisenization:* High-T, acidic, fluorine-rich fluids reacting with felsic rocks convert feldspar to topaz. Medieval tin miners in the German Erzgebirge called the resulting grey rock *greisen*. Greisen is a massive or vuggy rock that consists of quartz, topaz and light mica (muscovite or lepidolite). Greisen-associated alteration such as mica-quartz and quartz-topaz rocks, and massive mica pockets may be considered as part of the greisen "family" of hydrothermal alteration (Štemprok 1987). Giant kaolin deposits in Cornwall (cf. 3.14 Kaolin) are related to thin greisen veins in granite. Greisen may contain accessory tourmaline, fluorite, rutile, cassiterite and wolframite. Tin and tungsten enriched greisen bodies can be profitable ore.
- *Dolomitization* is the prevalent alteration of limestone adjacent to lead-zinc ore. It is due to import and exchange of magnesium for part of calcium (e.g. Navan/Ireland: Braithwaite & Rizzi 1997).
- *Carbonatization* originates by reaction of silicate rocks with CO_2-rich fluids. Calcite, dolomite and ankerite (more rarely siderite and magnesite) are common alteration products adjacent to gold quartz veins in Archean and Paleoproterozoic greenstones (Eilu et al. 2001). In practice, the distinction of different carbonate minerals can be done with portable or laboratory imaging spectrometers (Greenberger et al. 2015) or by colouring techniques (Hitzman 1999).
- Listwaenitization describes carbonated and silicified ultramafic rocks that may be associated with hydrothermal epigenetic gold mineralization. The altered rocks consist of magnesium-calcium-iron carbonates, chromian muscovite and quartz, with various accessory minerals (Halls & Zhao 1995).
- *Tourmalinization* is common in tin (Lehmann et al. 2000a), tungsten and gold deposits. If it is very intensive, tough black rocks ("tourmalinites") result that resist both surficial alteration and the geologist's hammer. Tourmalinites mark the proximity of orebodies. In more distal position, pervasive growth of dispersed tiny needles of tourmaline in country rock is only revealed by the microscope.

The study of hydrothermally altered wall rocks is an important subject of economic geology. Alteration reveals the nature of the hydrothermal solutions, assists in the search for ore because it presents a much larger and hence more easily detectable target compared to the actual orebodies (Dilles & Tosdal 2015), and allows dating of ore formation because of neogenesis of minerals such as K-feldspar, alunite and mica. Zonation mapping (assisted by geophysical 3D inversion methods; Chopping & van der Wielen 2011) provides a vector pointing to the site of possible ore. In addition,

hydrothermal alteration is always accompanied by the dispersion of trace metals around orebodies. The resulting trace metal halos are excellent lithogeochemical prospecting guides. And last not least, several alteration products are valuable industrial minerals (e.g. alunite, kaolin, sericite and vermiculite).

1.1.7 Hydrothermal vein deposits

For a long time in the past, ore veins were the most important deposit style. Practice and theory of mining and geosciences evolved with the challenges of vein mining, as shown by fundamental books from Agricola (1556) to Lindgren (1933). More recently, the economic relevance of vein mining decreased compared to large-tonnage low-grade operations such as those based on porphyry copper deposits. Yet, many gold and high-grade base metal vein deposits successfully compete with the mechanized giants. Of course, many of these giants, such as porphyry copper ores, are really formed by dense micro-veining of large rock bodies (Tosdal & Richards 2001). Here we study the macro-veins.

Genetic classes of vein fill include magmatic hydrothermal, diagenetic or metamorphogenic systems, as described in other parts of Chapter One. Veins are tabular bodies of hydrothermal precipitates that typically occupy fissures. Less often, veins originate by metasomatic replacement of rock (replacement veins), propagating from a joint or shear plane. Vein walls range from clean parting planes to "frozen" contacts. Many steeply-dipping veins develop upward or along strike into a fan of thinner veins and veinlets (e.g. Fig. 1.18) resembling a branching tree. At district scale, veins tend to occur in groups that form vein systems.

Thickness, vertical extent and horizontal length of veins vary widely. Less than 0.1 m thickness may allow profitable mining of high-grade gold ore veins, whereas tin and tungsten require a width of 1 m, barite and fluorite a minimum of 2 m. The world's longest veins may be those of the Mother Lode system of California, occurring along 190 km strike length. Most individual veins, however, have lengths between a few tens to several thousand metres. The disposition of veins in space ranges from horizontal to vertical; because hydrothermal solutions have a general tendency to flow upward (more precisely towards lower hydraulic potential), steeply dipping veins are in the majority.

Mechanical properties of host rocks and the prevailing stress field are the most important controls of vein formation. Fractures form more readily in competent rocks than in ductile material. Therefore, the cassiterite – quartz (muscovite, arsenopyrite, tourmaline) veins at Rutongo, Rwanda occur preferentially in vitreous quartzites and few cut across low-grade metamorphic schists (Fig. 1.38). Very brittle rocks such as dolomite, rhyolite and quartzite are prone to form a network of short fractures instead of spatially separated longer ones (Fig. 1.39). In that case, hydrothermal activity may result in stockwork ore. "Stockwork orebodies" consist of numerous short veins of three-dimensional orientation, which are so closely spaced (e.g. 10–30 veins/m in the tin deposit of Tongkeng-Changpo, South China) that the whole rock mass can be mined.

Many vein deposits are spatially and genetically associated with brecciated rock bodies (of tectonic or hydraulic fracturing origin) that

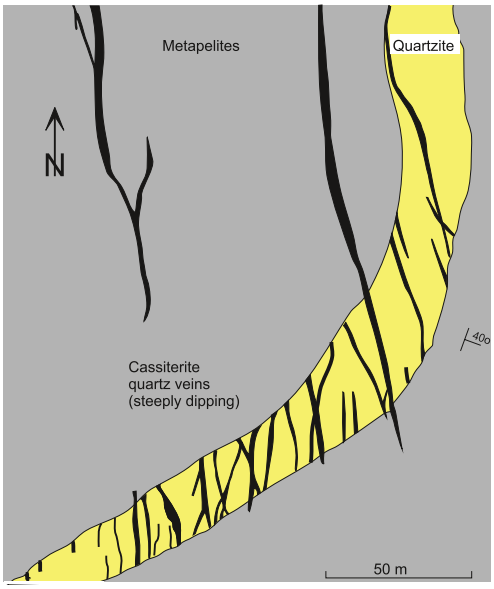

Fig. 1.38. Geological map of a level in Rutongo tin mine, Rwanda, showing closely spaced parallel ("sheeted") quartz-cassiterite veins; structural control is a cross-cutting (F3) east-plunging anticline; lithological control is brittle quartzites (for location cf. Fig. 1.19) (source Pohl et al. 2013).

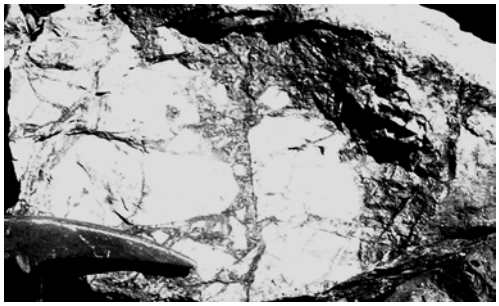

Fig. 1.39. Breccia ore at Mammoth copper mine near Mt. Isa, Queensland. Supergene secondary chalcocite (grey near hammer) replaces primary chalcopyrite and pyrite in veinlets within quartzite (white).

may host rich ore (Jebrak 1997). As a rule, fissures and breccias have a much higher permeability than most consolidated rocks, which are commonly aquitards. Therefore, these structures focus fluid flow at all scales, from single veins to large structures such as the ore shell of porphyry copper deposits, rift faults and crustal shear zones (Weis et al. 2013). Many fissures, for example the Sn-Cu ore veins of Cornwall, England, are surrounded by broad zones of intensive micro-fracturing that provide access to fluids from the main flow channel (Dominy et al. 1996). It is well known in the oil industry that in contrast to common permeable faults, clay and shale gouge can transform faults into very effective barriers to fluid flow (Egholm et al. 2008). Unconsolidated rocks (clay, sand) are unlikely to fracture but deform ductilely. Typically, this reduces their permeability so that such faults restrict flow.

Veins are paths of former fluid flow. Principally, hydraulic mass flow is a function of the connectivity and hydraulic conductivity of flow structures, and of velocity. Flow in a single fissure is controlled by its aperture and secondary properties such as morphology and roughness of the walls. Note that the hydraulic aperture of a vein was rarely equal to its present thickness, because most veins were filled while stepwise opening. For cases of sheeted vein systems (Fig. 1.38) the total cross-sectional permeability can be estimated by incorporating the distance between veins (Lee & Farmer 1993; eq. 1.8). Only in favourable cases, the flow velocity can be measured, e.g. when upflowing water deposited suspended sediment or hydrothermal precipitates (cf. eq. 1.4 in section "Mineral Succession").

Hydraulic permeability (k) of a single vein and of a sheeted vein system:

$$\text{Singlefissure} \quad k_{vein} = (\rho.g/\mu).\left(a^2/12\right)$$

$$\text{Sheetedfissures} \; k_{sum} = (\rho.g/\mu).\left(a^3/12d\right) \quad (1.8)$$

ρ = density of the fluid (g/cm^3), g = gravitational acceleration (m/s^2), μ = dynamic viscosity (m^2/s), a = aperture (m), d = distance between veins (m)

Methods of *fractal analysis* (Mandelbrot 1982) were conceived for studying structures built of many elements. Examples of vein-related topics include the statistical distribution of vein thickness and the spacing of veins, and extrapolation of results into adjacent blocks or to different scales (Roberts et al. 1998, Marrett et al. 1999). In some cases, the fractal distribution of tectonic features and of mineralization, that is their similarity from microscopic to regional scale, can be used for the definition of new exploration targets (Weinberg et al. 2004).

Rock mechanic and tectonic interpretation of vein systems have a central role in vein mining, from creating exploration targets to predicting the shifted position of a vein behind a fault. Mining districts display individual controls that must be identified by careful mapping and structural analysis at all scales (e.g. the Macraes gold mine: Daniels & Mascini 2012). Neogenesis and opening of fissures, shear planes and faults reflect spatial orientation and the ratios of principal stresses during vein formation (Fig. 1.40). A number of geological features can provide information about the former *in-situ* stress field (Fossen 2016, Anderson 1951). The opening of fissures is only possible if normal stress is negative (simple tension) or if fluid pressure (u) is high enough to counteract normal stress (effective stress $\sigma_{eff} = \sigma - u$). This condition is often realized by injection of high-pressured hydrothermal fluids. Many veins display pronounced banding (Fig. 1.36) that indicates a correlation between pressure increase of the fluids, movement of the fissure walls and precipitation of hydrothermal fill. This is called "seismic pumping" or "fault valve cycling" (Sibson 1990); the process may be seen as a self-organized critical system.

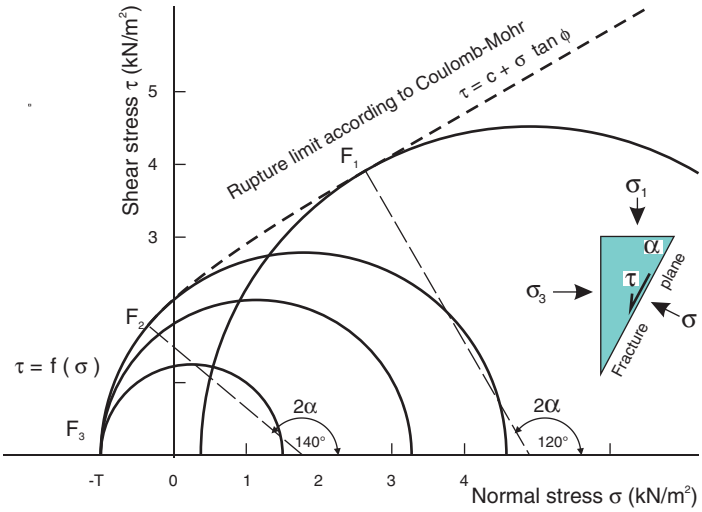

Fig. 1.40. The Mohr-Coulomb failure criterion: Formation of shear fractures (F1), shear fissures (F2) and tensile fissures (F3) with the corresponding angle of fracturing (α), and tectonic stresses $\sigma_1 > \sigma_2 > \sigma_3$ in the Mohr diagram. The inset triangle on the right depicts a section of the upper half of an originally cylindrical sample specimen with the stress geometry of fracture case F1. Fracturing is often assisted by high fluid pressure (u) that reduces strength according to $\sigma_{effective} = \sigma - u$.

Pressure cycles control the nature of fluids and hydrothermal precipitates. At Porgera Mine (Papua New Guinea), exceptionally high-grade magmatic-hydrothermal gold ore (reaching 1000 g/t) deposited by flash boiling during pressure drops is related to pyrite with strongly negative $\delta^{34}S$ and enriched in chalcophile elements (Cu, Ag, Au, Pb, Sb, As). During high pressure stages, fluids and precipitated pyrite are low in metals (Peterson & Mavrogenes 2014).

Very large faults and shear zones are rarely the site of hydrothermal mineralization but locate deposits in a km-wide band parallel to the main break. Orebodies occur rather in clusters of fractured rock near jogs or bends in the large structures. This can be explained by the time-integrated evolution of rock mass permeability after faulting (Sheldon & Mikleswaithe 2007): Main faults that experience a high displacement seismic event enter a healing regime that rapidly reduces permeability. The rock mass at some distance from the fault, however, undergoes a period of weakening that may result in seismic aftershocks. Because this causes elevated permeability for weeks or months after an earthquake, the time-integrated fluid flow will be larger than in the main fault, favouring the formation of ore. The distribution of orogenic gold deposits along major Archean faults in Canada can be described by a log-uniform model that yields a 5.6 km distance (Rabeau et al. 2013); segments that are longer are considered to be prospective exploration targets for hidden deposits.

Tectonic control of ore veins, vein geometry and kinematics

Structures hosting ore veins may be (a) new fractures that formed synchroneously with the fluid event, or (b) opened pre-existing structures. At Panasqueira in Portugal, overpressured fluids hydraulically forced apart older joints that originated as ac-joints of vertical folds during oroclinal buckling of the Ibero-Armorican arc (Jacques et al. 2017). Using structural geology methods (Cardozo & Allmendinger 2013, Fossen 2016), both cases allow an examination of the tectonic processes that were active during vein formation. Not unexpectedly, many veins are associated with large-scale tensional tectonics including rifting (e.g. silver-lead-barite ore veins near the Tertiary Upper Rhine Rift, Fig. 1.36; silver veins at Kongsberg near the Permian Oslo Graben;